Chapter 1

Introduction

Recently, computational methods in sciences have become one of the major tools for conducting research. In many cases, the computed values are so good that they agree with the experimentally measured data so that it is possible to understand the electronic structures of atoms, molecules and solids. The improvement in the technology of processors has lead to the improved speed of computers for solving large matrices. Some of the calculations are so big that they can not be solved by hand. Since the software developers have improved the accuracy of the software, it has become reliable to get results by computation. The density-functional theory (DFT) has gained its place in computational science. The DFT has been used widely to simulate a cluster of atoms, a molecule and a crystalline material. By minimizing the ground state energy of the electron, the Schrödinger equation can be solved. The ground state properties have been described very well by DFT using electron density while the exchange-correlation potential (υ_{xc}) has been introduced which has become a key to DFT in practical applications [1]. The exchange and the correlation energies can also be obtained by DFT. However, by using an approximation like local density approximation (LDA), Generalized Gradient Approximation (GGA) and others, the exchange-correlation potential can be calculated. The effect of the Pauli principle and Coulomb potential has been described appropriately so that the many-body problem can be solved by calculating the exchange-correlation potential [2]. In 1998, Walter Kohn [1] and John A. Pople [3] have been awarded together the Nobel Prize in chemistry. W. Kohn was awarded because of his contribution to the development of DFT while John A. Pople was awarded for using a modern electronic technology to find a solution of the Schrödinger's wave equation . This is the first time the Nobel Prize was awarded to scientists for developing a computational and theoretical method. Walter Kohn's famous equation called Kohn-Sham equation [1,4] developed in 60's with co-researcher, Lu-Sham becomes a core of DFT for solving the Schrödinger's equation. Kohn-Sham equation was an improvement from the Hohenberg-Kohn theorem [2,5] as a core of DFT. The approximations of the equation have been made to increase the accuracy of the calculation and to solve the exchange correlation potential [1,6]. Since the popularity of the DFT has increased, this theory will be use in this thesis.

Chapter 1 gives a brief description of the DFT with local density approximation (LDA). Chapters 2 to chapter 11 describe the results of the calculations using the Amsterdam density functional (ADF) software and DMol^3 software. The calculation of vibrational frequencies in vitreous glasses, graphene and carbon nitride has been done. These calculations include the clusters of materials, the analysis of the data and comparison with experimental results that is obtained from literature review. The conclusion of this thesis explained in Chapter 12 for all of the material that has been calculated using DFT.

All molecules are selected for which the calculation has not been done in the literature but the Raman spectra are available in journals. All the clusters of atoms are new and identified from the Raman spectra of vitreous material for the first time. This calculation is not using the classical calculations which are done by some old articles.

1.1 Hohenberg-Kohn Theory

The basic of the DFT was started in 1927 with developments by Llewellyn Thomas and Enrico Fermi after the introduction of the Schrödinger equation. They used a statistical model to approximate the distribution of electrons in a solid. The Thomas-Fermi model does not treat the exchange correlations. In 1964, the DFT has been put on firm theoretical approach introduced by Pierre Hohenberg and Walter Kohn [5]. There are two theorems that have been proved by Hohenberg and Kohn . The first fundamental mathematical theorem states that the density of the ground state is a unique functional that determines the external potential [1, 2, 5]. There is one-to-one mapping between the ground state wave function and the ground state electron density. The ground state electron density can determines the energy and the wave function of the ground state. The Schrödinger equation can be solved by finding the spatial derivative of the Hamiltonian [7, 8] in the case of non-degenerate ground state.

$$\rho = \langle \psi_o | \rho | \psi_o \rangle = \int dr |\psi_o(r_N)|^2 \tag{1.1}$$

and

$$E_o = \langle \psi_o | H | \psi_o \rangle = \int v_o(r)\rho(r)dr + \langle \psi_o | T + U | \psi_o \rangle \tag{1.2}$$

where ψ_o is a ground state wave function , v_o(r) is an external potential, ρ(r) is the non-degenerate ground state density, E$_o$ is an energy of the ground state, T is the kinetic energy and U is interaction energy. The assumption is the other external potential, v_o'(r) is equal to the potential, v_o(r) plus constant with the ground state of another potential, ψ_o' using same ground state density, ρ(r). The second energy functional for another potential, v_o'(r) is

$$E'_o = \langle \psi'_o | H' | \psi'_o \rangle = \int v'_o(r)\rho(r)dr + \langle \psi'_o | T + U | \psi'_o \rangle \tag{1.3}$$

Because of the inequality of the ground state ψ_o, the trial ground state wave function, ψ_o' for Hamiltonian of first potential, H has been taken.

$$E_o < \langle\psi'_o|H|\psi'_o\rangle = \int v_o(r)\rho(r)dr + \langle\psi'_o|T+U|\psi'_o\rangle \tag{1.4}$$

The equation (1.3) is rearrange so that,

$$\langle\psi'_o|T+U|\psi'_o\rangle = E'_o - \int v'_o(r)\rho(r)dr \tag{1.5}$$

The equation (1.5) is used to replace the last term of equation (1.4) to become,

$$E_o < \langle\psi'_o|H|\psi'_o\rangle = \int v_o(r)\rho(r)dr + E'_o - \int v'_o(r)\rho(r)dr \tag{1.6}$$

so,

$$E_o < \langle\psi'_o|H|\psi'_o\rangle = E'_o + \int \rho(r)[v_o(r) - v'_o(r)]dr \tag{1.7}$$

Using the ground state , ψ_o as a trial of Hamiltonian, H' gives,

$$E'_o < \langle\psi_o|H'|\psi_o\rangle = \int v'_o(r)\rho(r)dr + \langle\psi_o|T+U|\psi_o\rangle \tag{1.8}$$

Similarly,

$$E'_o < \langle\psi_o|H'|\psi_o\rangle = E_o + \int \rho(r)[v'_o(r) - v_o(r)]dr \tag{1.9}$$

Both equation (1.7) and (1.9) will be added (E_o + E_o') to become,

$$E_o + E'_o < E'_o + \int \rho(r)[v_o(r) - v'_o(r)]dr + E_o + \int \rho(r)[v'_o(r) - v_o(r)]dr \tag{1.10}$$

Finally,

$$E_o + E'_o < E'_o + E_o \tag{1.11}$$

The assumption of equal density, ρ(r), for the two potentials, υ_o'(r) $\neq$ υ_o(r) + constant is not justified. This is the case for the non-degenerate ground state.

The second theorem of Hohenberg-Kohn states that the minimum energy of the functional obtained when the electron density ρ(r) is the ground state electron density [1, 2, 5]. This theorem explains the functional of electron density that is in the first theorem. This principle can be used to find a minimum energy of Schrödinger equation while trying to choose a right electron density. The energy can be written as:

$$E[\rho] = \int \upsilon(r)\rho(r)d^3r + F[\rho] \tag{1.12}$$

With E[ρ] minimized through ground state energy and F[ρ] is unknown but universal functional of the density ρ(r) only. The first term on the right for equation (1.12) is the Coulomb interaction between the electrons and nuclei. The functional of F[ρ] is,

$$F[\rho] = \frac{e^2}{2} \int \int \frac{\rho(r)\rho(r')}{r - r'} d^3r d^3r' + T_o[\rho] + E_{xc}[\rho] \tag{1.13}$$

The first term represent the classical approximation of Coulomb interaction energy between pairs of electron. The second term shows the kinetic energy of a system of non-interacting electrons while the third terms represent exchange and correlation energy.

Even though the Hohenberg-Kohn becomes a basis of DFT for density of many electron systems, this equation does not promise that solving it is as easier as others for treating a wave function of Schrödinger equation. The exchange-correlation also does not explain very well. A year after, Kohn proposed an upgrade of DFT with co-researcher, Lu Sham called Kohn-Sham equation.

1.2 Kohn-Sham Self-Consistent Field Theory

The main point of DFT is to use electron density, ρ to replace the many body electronic wave functions. The complexities of the many-body problem make it difficult to find accurate expressions. Walter Kohn and Lu Sham [1, 4] have produced a solution for the Schrödinger equation using electron density functional. The effective potential includes the external potential and the effects of the Coulomb interactions between the electrons. The strength of Kohn-Sham equation is that we are dealing with the electron density functional rather than the position dependent Slater determinant.

$$(-\frac{\nabla^2}{2} + \upsilon_{eff}(r))\psi_j(r) = \varepsilon_i \psi_j(r) \tag{1.14}$$

The electron density,

$$\rho(r) = \sum_{j=1}^{N} |\psi_j(r)|^2. \tag{1.15}$$

The effective external potential is,

$$\upsilon_{eff} = \upsilon(r) + \int \frac{\rho(r')}{|r - r'|} dr' + \upsilon_{xc}(r) \tag{1.16}$$

Here, the first term is the interaction of electrons and nuclei, second term is a Hartree potential (v_H) that Coulomb repulsion between electrons and the last term is the exchange-correlation potential [1,4,10–13]. The exchange-correlation potential in term of electron density in r orbital is,

$$\upsilon_{xc}(r) = \frac{\delta E_{xc}}{\delta \rho(r)} \tag{1.17}$$

The ground state energy is;

$$E = \sum_{j=1} \varepsilon_j + E_{xc}[\rho(r)] - \int \upsilon_{xc}(r)\rho(r)d^3r - \frac{1}{2}\int \frac{\rho(r)\rho(r')}{|r-r'|}drdr'. \quad (1.18)$$

Before the Kohn-Sham equation can be solved, the Hartree potential should be found. But, the Hartree potential can be found when the electron density has been defined. But how to get the electron density while we do not know the single-electron wave functions that solves the Kohn-Sham equation. To break this circle, a trial electron density, ρ(r) should be defined. By using trial electron density, the Kohn-Sham equation can be solved and a single-particle wave function, ψ_j(r) can be found. Single particle wave function can be used to calculate the electron density, ρ'(r). Compare ρ'(r) with trial electron density ρ(r), so the total energy can be calculated when the electron density is same as the trial electron density. The ground state energy can be defined. But, if both electron densities are different, the circle will restart with new trial electron density. This chain of calculations is called self-consistent field (SCF) approach [2, 9].

1.3 Exchange-Correlation Potentials

The explanation of electronic structure through the electron density presented by DFT becomes a breakthrough for scientist like chemists and physicists for understanding the multiparticle quantum systems. While Hohenberg-Kohn-Sham explained the mathematical view of electronic potential, the exchange-correlation function included in that equation needs to be specified for finding the ground state energy. The Hartree equation does not have any exchange-correlation potential, while Hartree-Fock approach shows the existent of exchange potential [2, 9]. The electron density ρ(r) in the homogenous electron gas is constant at all points. This situation has been used for treating the exchange-correlation functional. This approximation shows that the exchange-correlation potential, υ_{xc} is

$$\upsilon_{xc} = \upsilon_{xc}^{electrongas}[\rho(r)] \tag{1.19}$$

and called the local density approximation (LDA) [2, 4, 9]. LDA is the easiest way to treat the exchange-potential by means of local density. The LDA expression for exchange correlation is

$$E_{xc}^{LDA} \equiv \int \varepsilon_{xc}[\rho(r)]\rho(r)dr \tag{1.20}$$

where $\varepsilon_{xc}(\rho)$ is the exchange-correlation energy of a homogenous electron gas of ρ. LDA generally well described the covalent, metallic and ionic bonds but not adequate on hydrogen bond. While LDA is the simplest approximation for the exchange and correlation functionals to define the Kohn-Sham equation, this approximation does not solve the exact Schrödinger equation because it is not using true exchange-correlation functional. Next approach is generalized gradient approximation (GGA) that has more physical information then LDA. The difference between GGA and LDA is that while LDA uses the local density the GGA has the effect of the nearest neighbors by a linear gradient in the electron density. Many functionals have been used for GGA because of many ways to include the gradient of the electron density. The most widely used functional in GGA is produced by Perdew and Wang (PW91) and Perdew-Burke-Ernzerhof (PBE) [6, 14].

$$\upsilon_{xc}^{GGA}(\rho) = \upsilon_{xc}[\rho(r), \nabla\rho(r)] \tag{1.21}$$

The basic concept of GGA is the real electron densities are not uniform. The additional information on the spatial variation of density can be described with greater flexibility in a real material.

1.4 Raman Scattering

Raman scattering has been discovered by Chandrasekhara Venkata Raman together with K. S. Krishnan in 1928 [15] . This great discovery was awarded the Nobel Prize in 1930. The inelastic scattering is important to study properties of glasses and crystals by analyzing the frequency of vibrating molecules. When an incident light with frequency ν_o passes through matter, most of the radiation continue in the original direction that has same wavelength as the incident light. This elastic scattering is called the Rayleigh scattering. Some part of radiation is scattered in other directions with different wavelength than that of the incident light, is called Raman scattering. When ν_o is frequency of an incident light of photon, the emitted photon has frequency;

$$\nu_{emitted} = \nu_o \pm \omega_o/2\pi \tag{1.22}$$

The light with lower frequency compared to the incident light is called Stokes scattering. This down-shifted frequency shows that molecule is absorbing the energy from incident light. Here $\omega_o/2\pi$ is the characteristic frequency of the molecule. Hence, Raman scattering can be used to determine the molecular frequencies. Hence a large number of chemicals can be used to determine their frequencies.

$$\nu_{emitted} = \nu_o - \omega_o/2\pi \tag{1.23}$$

Electrons in this molecule usually found in the ground state level. That is why Stokes scattering is commonly found compared to the anti-Stokes [16,17]. For the high frequency in Raman scattering, the emitted light has a higher energy compared to the incident light due to energy losses from molecules. This is called the anti-Stokes. The shorter wavelength, the up-shifted frequency is usually found because of the molecules being in the excited state.

$$\nu_{emitted} = \nu_o + \omega_o/2\pi \tag{1.24}$$

In Raman effect, the Stokes and anti-Stokes does not count because the difference of energy between vibrational levels is the important thing to understand the properties of materials. At low temperatures the excited state populations are very small so that only the Stokes lines appear in the spectrum. At high temperatures, both the Stokes as well as anti-Stokes lines appear in the spectrum. The Raman scattering occurs because of a change in the polarizability of the molecule upon shining with light and hence it does not show all of the infrared region.

1.5 Objectives

The objective of this thesis is to make the clusters of atoms and calculate it using density functional theory (DFT) to get the vibrational frequency. The calculated vibrational frequencies will be compared to the experimental Raman spectra.

(i) Make the clusters of atoms for which the energy is minimum. The energy of the Schrödinger equation is minimized by varying the geometry of the molecule and bond lengths are determined .

(ii) Calculate the vibrational frequencies of the molecules.

(iii) Compare the calculated values of vibrational frequencies with those experimentally found in the Raman spectra.

(iv) To identify the molecules which exist in the vitreous state or in the glassy state.

Chapter 2

Ab Initio Calculation Of The Vibrational Frequencies Of $\mathbf{Ag}_x$ $\mathbf{Ge}_{x-1}$ $\mathbf{Se}_{2x+1}$ Glass

The vibrational frequencies of Ag_2, Ag_3, Ag_4, Ag_5, Ag_6, AgGe, Ag_2Ge, Ag_3Ge, Ag_4Ge, $AgGe_2$, Ag_2Ge_2, Ag_3Ge_2, Ag_4Ge_2, $AgGe_3$, Ag_2Ge_3, Ag_3Ge_3, Ag_4Ge_3, $AgGe_4$, Ag_2Ge_4, Ag_3Ge_4,Ag_4Ge_4, AgSe, Ag_2Se, Ag_3Se, Ag_4Se, $AgSe_2$, Ag_2Se_2, Ag_3Se_2, Ag_4Se_2, $AgSe_3$, Ag_3Se_3, $AgSe_4$, Ag_2Se_4 and Ag_4Se_4 are theoretically computed from the first principles by using density functional theory. The clusters are built in plane, pyramidal or ring shape configurations. The vibrational frequencies for all of the 47 clusters have been calculated. The bond lengths and bond angles of all of the molecules are calculated. The vibrational frequencies of all of the clusters are calculated using a variety of wave functions. The single zeta wave functions as well as the double zeta wave functions with and without the polarization have been used. The experimental Raman spectra show almost a continuum of small frequencies. In particular below 100 cm^{-1}, the Raman response is due to particle size in the sample, where light scattering is a result of scattering from the edges of the particles. The spectra of glassy $GeSe_2$ are considerably modified by addition of silver. Most of the Raman spectra are weak and occur near 200 cm^{-1}. Clusters of pure silver have been made and the vibrational frequencies in all cases have been calculated. Ag_2 oscillates weakly at 185 cm^{-1}. Due to the metallic character, the intensity of Ag_2 is very small. The Ag_3 oscillates at 117 cm^{-1}. The pyramidal Ag_4 has a vibrational frequency of 107 cm^{-1} whereas the square shaped molecule Ag_4 oscillates at 140 cm^{-1}. The ring of Ag_5 oscillates at 141 cm^{-1}. The pyramidal Ag_5 has oscillations near 178 cm^{-1} and Ag_6 ring oscillates near 132 cm^{-1}. The calculated frequencies of the clusters $AgSe_2$, planar-Ag_3Se, Ag_2Ge_2, Ag_2Ge and planar Ag_3Ge are in the neighborhood of those found experimentally. The bond lengths and angles have been determined for the minimum energy configuration in all cases. These calculated frequencies are usually very near to the measured values.

2.1 Introduction

The effect of Ag doping on the properties of glasses is of considerable interest [18–21]. In particular, in some cases, there are two sublattices in such a way that one sublattice remains a solid whereas the other starts melting. In AgI at some high temperatures, the I atoms remain stationary whereas Ag atoms start moving. This property is known as “superionic conductivity” because the thermal conductivity becomes very large. It will be of interest to find the effect of doping by superionic atoms such as silver. The glasses are also characterized by their long relaxation times [22] due to self-organization and soft modes in which case the frequency of a phonon goes to zero [23]. There is a phase transition in the rigidity [24] as a function of concentration of one of the atoms. Recently, the expertise to optimize the bond distances and angles for the minimum energy of the Schrödinger equation have been developed [25–28]. This program is able to calculate the frequencies of vibrations of clusters of atoms to a very high accuracy. Since these calculated values can be compared with those measured by the Raman spectra for a real glass, it found that these predicted values are very good. In this way, the clusters that actually present in the glass can be identified.

The results of these first principles calculations of the formation of clusters of atoms in a glass, $Ag_xGe_{x-1}Se_{2x+1}$ have been reported. The vibrational frequencies of about 40 clusters of atoms have been calculated and those which are closest to the experimental values obtained from the Raman spectra of AgGeSe glass have been reported. The vibrational frequencies in the pure Ag metal has been found. The Ag_2 molecule oscillates but the number of these molecules is very small. The Ag_3 is also weak but pyramidal Ag_4 is reasonably strong. The formation of molecular clusters in Ag metal has been reported. A detailed study of vibrations in $AgSe_2$, Ag_3Se, Ag_2Ge_2, Ag_2Ge, Ag_3Ge and Ag_3Ge_3 will be report here. It found that the vibrational frequencies of these clusters were in the proximity of the experimental values.

2.2 Silver Clusters

The density functional theory has been used to make clusters of atoms and the geometry for the minimum energy of the Schrödinger equation has been optimized. Since Ag is a metal, the molecule formation is very weak. The Ag_2 molecule is found to stabilize at the bond distance of 262.4 pm (picometer) and its oscillation frequency is 185 cm^{-1} in single zeta wave function (SZ) but the intensity is almost zero, so that it will not be observable as a peak in the vibrational spectrum. The same values are obtained when double zeta wave function (DZ) is used. In the case of double zeta wave function with polarization (DZP), the bond length is reduced to 260.5 pm and the oscillation frequency is reduced to 176.8 cm^{-1} but the intensity continued to be zero. The results obtained with triple zeta wave function with polarization (TZP) are similar to those of DZP. The triple zeta with double polarization (TZ2P) gave 256.4 pm for the bond distance and 181.8 cm^{-1} for the oscillation frequency but the intensity is still zero. Similarly, 4 zeta with four polarizations (QZ4P), results are about the same as that of TZP. This type of wave functions has been applied to methane molecule by Sherrill *et* *al.* [29] and also to water dimmer [30].

In Ag_3 the bond distance of the optimized triangle is 277.1 pm and the vibrational frequency is 117.2 cm^{-1} in the single zeta wave function. These values remain unchanged when double zeta wave function is used. When the double zeta wave function with polarizations is used, the bond length of the triangle is slightly reduced to 276 pm and the frequency also reduces to 111.1 cm^{-1}. When triple zeta wave function is used the bond length is still 276 pm but the frequency is reduced to 110.8 cm^{-1}. As compared with Ag_2, which has almost zero intensity, the Ag_3 is having a strong peak. Hence, Ag_2 is not formed and Ag_3 is the smallest cluster, which vibrates in silver metal.

The clusters of atom Ag_4 are very interesting because one of them is of pyramidal structure but the square shape planar ring structure is also stable. In the case of pyramidal structure bond length is 287.8 pm and the angle is strictly 60 degrees as expected. The vibrational frequency is 107 cm^{-1} when single zeta wave function is used. The double zeta wave function (DZ) gave the same values as those obtained from single zeta (SZ). However, when double zeta wave function with polarization (DZP) is used, the frequency reduced to 100.4 cm^{-1}. The triple zeta with polarization (TZP) gave the same values as DZP. The frequencies as well as the bond lengths in the TZ2P are found to be 273.9 pm and 161.9 cm^{-1}. The QZ4P gave 276 pm and 161.9 cm^{-1} for the pyramidal bond length and the vibrational frequency, respectively. The square shaped Ag_4 clusters has a vibrational frequency of 140.7 cm^{-1} and the length of the square is 273.9 pm when single zeta wave function is used. The double zeta wave function gave almost the same values as the single zeta. The cluster Ag_5 forms a ring as well as a pyramid. In the five sided ring, the bond length is 272.3 pm and the vibrational frequency is 140.9 cm^{-1}. The double zeta wave function gave the same value as the single zeta. In the case of double zeta with polarization, the bond length is 271.6 pm whereas the frequency is 131.4cm^{-1}. The TZP values are 271.7 pm for the five sided bond length and the vibrational frequency is 131.26 cm^{-1}. The TZ2P gave 264.1 pm for the bond length and 147.5 cm^{-1} for the frequency. The QZ4P values are 264.2 pm and 147.3 cm^{-1}, respectively. The clusters Ag$_5$ in the pyramidal form gave two strong bonds. First a square of four atoms is formed with bond distance 286.6 pm. Then on top one more atom is placed which is at a distance of 276.6 pm from each of the four atoms. The vibrational frequencies are 69.2 cm^{-1} (2 values), 87.2 cm^{-1} (one strong value), 146.1 cm^{-1} (2 weak values) and 178.9 cm^{-1} (one strong value). The DZ values are the same as those of SZ. The DZP values are 286.7 pm for the square bond length and 274.8 pm for the on top atom. The frequencies, intensities and degeneracies are given in Table 2.1.

Table 2.1: The vibrational frequencies of the Ag$_5$ (pyramid) by using DZP wave functions and degeneracies

S. No	Frequency cm^{-1}	Intensity	Degeneracy
1	64.6	0.488	2
2	81.8	2.273	1
3	139.7	0.146	2
4	169.8	1.683	1

*S. No is a short form for Serial Number of vibrational frequencies.

The Ag$_6$ ring in single zeta wave function has a bond length of 270.8 pm and a strong vibration at 131.9 cm^{-1} with degeneracy 2 and weak lines at 114.1, 165.7, 167.6 and 172.1 cm^{-1}. In the case of DZP, the bond length changed to 270.1 pm which is only a minor change compared with the unpolarized single zeta function. However, in the case of DZP, the vibrational frequencies (intensities) are changed to 103.6 (0.03), 122.5 (2.8), 124.2 (2.77), 154.1 (0.004), 155.8 (0.004), 160.4 (0.007) cm^{-1}(arb. units). It is clear that there is a strong ring oscillation as about 122.5 cm^{-1}.

2.3 The AgSe Clusters

The $AgSe_2$ has Se - Ag bond length 260.3 pm and Se - Se bond length 237.2 pm when single zeta function is used. The frequencies (intensities) are 146.8 (0.16), 211.3 (6.31), 338.5 (1.18) cm^{-1} (arb. units). The double zeta wave functions give Se - Ag distance 265.4 pm and Se - Se distance 251.8 pm and frequencies (intensities) 129.4 (1.74), 176.8 (8.05), 266.9 (0.73) cm^{-1}(arb. units). The DZP gave Se - Ag distance 262.2 pm, Se - Se distance 240.5 pm and frequencies (intensities) of 139.7 (1.23), 177.5 (7.9), 292.3 (0.24) cm^{-1}(arb. units). The vibrational spectrum of $AgSe_2$ calculated from the first principles is shown in Fig. 2.1.

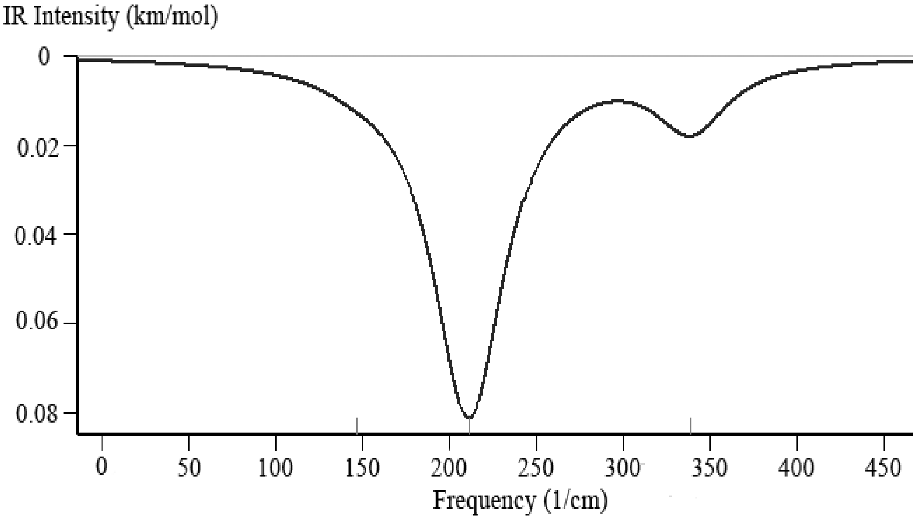

Figure 2.1: The vibrational spectrum of $AgSe_2$ calculated from the first principles showing two strong vibrations.

The Ag_3Se has a single Se in the centre of a triangle, which is built from three Ag atoms. The bond length is 256.0 (picometer) when single zeta (SZ) is used. In the DZP, the bond length changed to 252.2 pm. The vibrational frequencies (intensities) are given in Table 2.2. A picture of the charge density is shown in Fig. 2.2.

Table 2.2: The vibrational frequencies and intensities of Ag_3Se in single zeta(SZ) as well as double zeta with polarization(DZP) wave functions for Ag_3Se

S. No	Frequency cm^{-1}(SZ)	Intensity	Degeneracy	Frequency cm^{-1}(DZP)	Intensity (DZP)
1	28.63	1.85	2	31.2	1.95
2	51.59	10.14	1	56.5	8.71
3	223.71	0.66	2	217.7	0.16

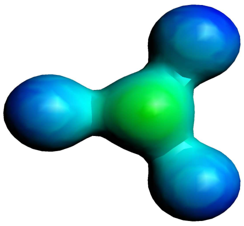

Figure 2.2: A picture of the charge density of Ag_3Se using SZ wave functions.

2.4 The AgGe Clusters

(i) The Ag_2Ge_2 has the Ag - Ge distance of 251.5 pm, Ge - Ag - Ge angle of 88 degrees and Ag - Ge - Ag angle of 92 degrees when single zeta wave function is used. The frequencies (intensities) are 184.4 cm^{-1} (4.75) and 201.9 cm^{-1} (7.48) when double zeta wave function is used, the bond length comes out to be 264.0 pm, Ge - Ag - Ge angle 62.5 degrees and Ag - Ge - Ag angle comes out to be 121.3 degrees. The frequencies (intensities) are 107.2 cm^{-1} (0.135), 201.6 cm^{-1} (8.2). The double zeta with polarization gave Ag - Ge bond length of 261.8 pm, Ge - Ag - Ge angle of 61.1 degree and Ag - Ge - Ag angle of 118.9 degrees. The frequencies (intensities) in the double zeta with polarization are 100.37 (0.25) and 196.3 (6.71).

(ii) The Ag_2Ge has Ag - Ge distance of 258.5 pm and Ag - Ge - Ag angle 71.7 degrees. The vibrational frequencies with SZ are 67.1 (0.005), 168.3 (0.272) and 215.02 (0.227). The DZ values are Ag - Ge distance 258.3 pm and bond angle 71.6 degrees. The frequencies (intensities) are, 67.1 (0.004), 169.05 (0.277) and 215.7 (0.227). The values calculated for DZP wave function are, Ag - Ge bond distance 253.4 pm and bond angle Ag - Ge - Ag is 74.5 degrees. The vibrational frequencies and intensities are 58.2 (0.006), 175.15 (0.255) and 215.2 (0.244). The TZP functions gave Ag - Ge bond distance 254.1 pm and bond angle Ag - Ge - Ag of 74.1 degrees. The vibrational frequencies for the TZP are 59.5 (0.004), 172.45 (0.243), 213.1 (0.253), cm^{-1} (km/mol). A charge density plot of Ag_2Ge is shown in Fig. 2.3.

(iii) The Ag_3Ge with Ag_3 on the corners of a triangle and Ge in the center gives Ge - Ag bond length of 255.2 pm and Ag - Ge - Ag angle of 120 degrees as it should be for the center of an equilateral triangle. The vibrational frequencies (intensities) are 22.6 (1.26) two values, 117.4 (12.9) one value and 227.9 (0.034) two values

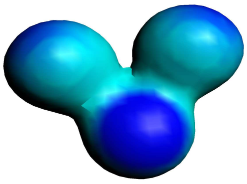

Figure 2.3: A picture of the charge density of Ag_2Ge calculated from single zeta wave functions.

when DZ is used. For DZP, Ge - Ag bond distance is 251.7 pm and Ag - Ge - Ag angle is 120 degrees as it should be for a triangle. The frequencies (intensities) are 38.8 (0.026) two values, 124.2 (0.000001) one value and 226.2 (2.43) two values, cm^{-1} (km/mole).

(iv) The system Ag_3Ge_3 is hexagonal with alternate Ag and Ge atoms with Ge - Ag distance 246.4 pm. The SZ vibrational spectrum is shown in Fig. 2.4. The calculated frequencies (intensities) are 22.4 (1.125) two values, 101.2 (1.87) one value, 202.62 (7.65) two values, 258.8 (0.07) two values when SZ wave functions are used. When DZ wave function is used the bond length Ge - Ag comes out to be 254.0 pm and the frequencies (intensities) (degeneracies) are, 64.1 (0.037) (1), 168.5 (5.22) (2), 224.8 (2.51) (2) cm^{-1} (km/mole). The DZP bond length is 250 pm and the frequencies (intensities) (degeneracies) are 61.2 (0.005) (1), 168.6 (4.331) (2), 222.02 (3.045) (2), cm^{-1} (km/mole). The charge density of Ag_3Ge_3 is shown in Fig. 2.5.

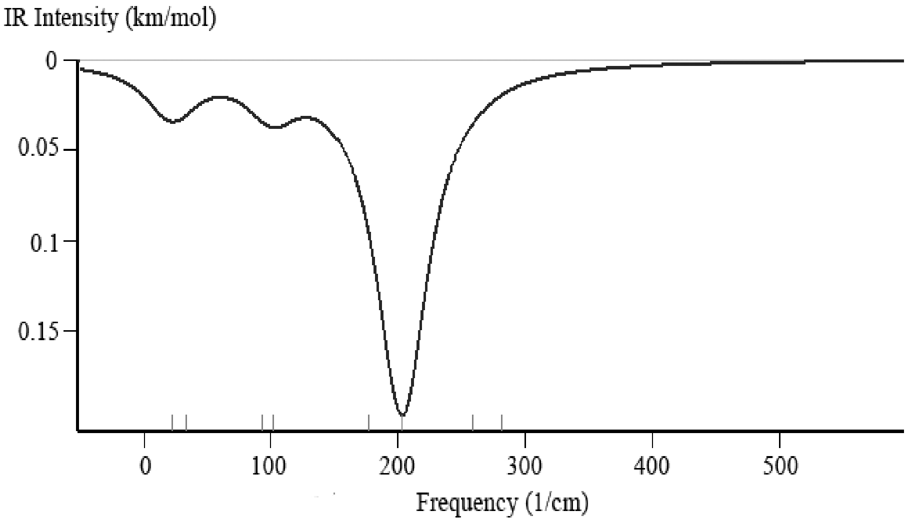

Figure 2.4: The vibrational spectrum of Ag_3Ge_3 hexagon calculated using the first principles with SZ wave functions.

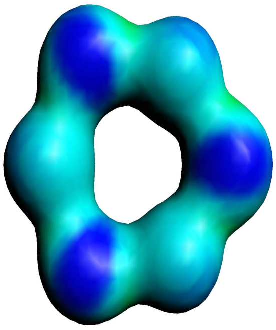

Figure 2.5: The charge density plot of Ag_3Ge_3 using SZ wave functions.

2.5 Comparison of Calculated Values With Experimental Raman Spectra

Fig. 2.6 show the experimental Raman spectra of glassy $GeSe_2$ and glassy $Ag_4Ge_3Se_9$. The experimental work has been done by Dejus *et al.* [31].

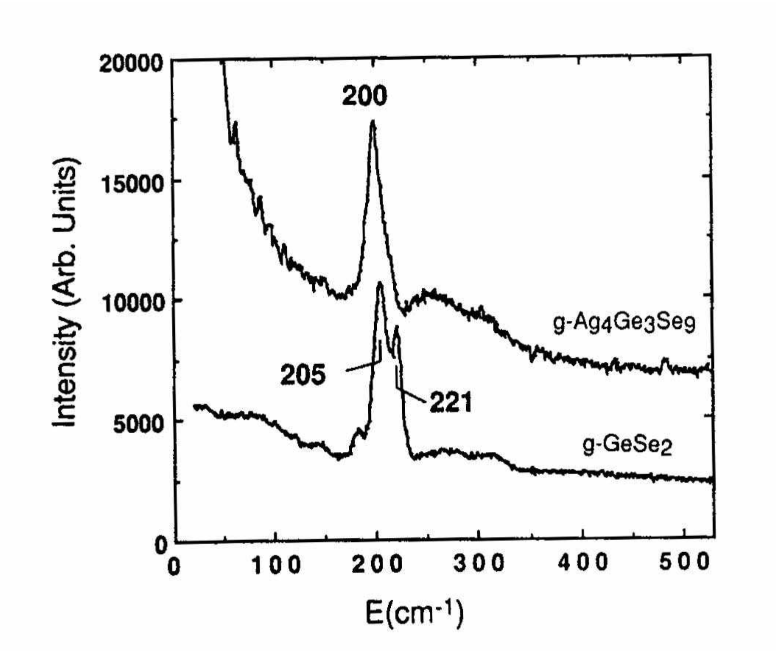

Figure 2.6: The experimental Raman spectra of glassy $GeSe_2$ and $Ag_4Ge_3Se_9$.

The g-$GeSe_2$ has a strong Raman line at 205 cm^{-1} and another at 221 cm^{-1}. There are some weak lines, which are not identified. When silver is added the 221 cm^{-1} goes inside the 200 cm^{-1} line and hence becomes difficult to resolve, but there is a broad line at 200 cm^{-1}. There is a continuum below 100 cm^{-1} and small oscillations are hidden within the noise. In these calculations, it is clear that there is absorption near 215 cm^{-1} in Ag_2Ge (SZ), which is near the experimental value of 221 cm^{-1}. The continuum below 100 cm^{-1} is due to particle size but Ag_2Ge has a mode at 67 cm^{-1}.

2.6 Conclusions

The extensive ab initio calculations of clusters of atoms constituting Ag and Ge atoms have been performed. The calculated values of the vibrational frequencies show that Ag_2Ge is formed in glass. The calculations also show that in Ag metal, Ag_3 is the smallest cluster formed which is of the size of 0.277 nm.

Chapter 3

Vibrational Frequencies in As_xSe_{1-x} Glass

The density functional theory is used to make models of clusters of atoms of arsenic and selenium. The bond lengths and angles are able to determine for which the energy of the Schrödinger equation is minimum. The vibrational spectra of the optimized clusters are computed using several different wave functions. It is found that the double zeta wave functions work the best.By calculating the gradients of the first principles potential, the vibrational frequencies for the optimized clusters in each case have been calculated. The calculated values have been compared with the experimental Raman spectra of As-Se glass. The calculations have been done for many clusters, for example, (i) AsSe (diatomic), (ii) As_2Se (linear), (iii) As_2Se (triangular), (iv) As_3Se (triangular), (v) As_4Se (square), (vi) $AsSe_3$ (triangular), etc. From this study the linear As - Se - As has been identify for which the calculated frequency is 27.6 cm^{-1} is in agreement with the experimental data.

3.1 Introduction

The structure of glasses involves long relaxation times [22] and may exhibit soft modes [23]. There is a rigidity transition as a function of concentration of atoms [24]. In the GeSI, GePS and GeSe glasses, the calculated values of the frequencies of lattice vibrations are close to the experimental values [25,27,32]. The exchange and correlation energies in GaAs [28] have been calculated. The AsSe is interesting from the view point of vibrations in the low frequency regime. Nemanich [33] has studied the Raman spectra in various samples of AsSe which show strong light scattering near 25 ± 12 cm^{-1}. These low frequency modes can arise from the bond vibrations as well as from the particle size which is independent of the constituent atoms. Phillips *et al.* [35] have investigated the Raman scattering by using molecular models. Ahn *et al.* [34] have studied the nuclear quadrupole resonance which is useful for the understanding of the structure of the glass.

In this chapter, the calculations of the vibrational frequencies of several models of AsSe have been reported. It found that As-Se-As linear molecule gives vibrations near 27.6 cm^{-1} which is close to the experimental value of 25 ± 12 cm^{-1}. The particle size can also scatter light in this region. This calculation of several models is also of interest from the view point of structure of the AsSe glass. It found that linear modes exist in the glassy state.

3.2 Clusters

The density functional theory has been used to simulate atoms. The bond lengths are determined by finding the structure for which the energy is a minimum. The nuclear motion separates out from that of the electronic motion so that the vibrational frequencies can be determined. The calculated clusters are given below. The double zeta wave functions are used in all of the computations. The bond lengths are measured in picometer.

(i) AsSe (diatomic): The optimized bond length is 226.8 pm. There is a wide frequency mode at 344.05 cm^{-1} (2.13 km/mol). The intensity, given in small brackets, indicates that the vibration is moderately strong.

(ii) As_2Se (linear): In this cluster, the two As atoms are at the ends and Se is in the center. The As-Se bond length is found to be 228.5 pm and the vibrational frequencies (intensities) [degeneracies] are given in Table 3.1. The vibrational spectrum calculated from the first principles for As_2Se (linear) shown in Fig. 3.1.

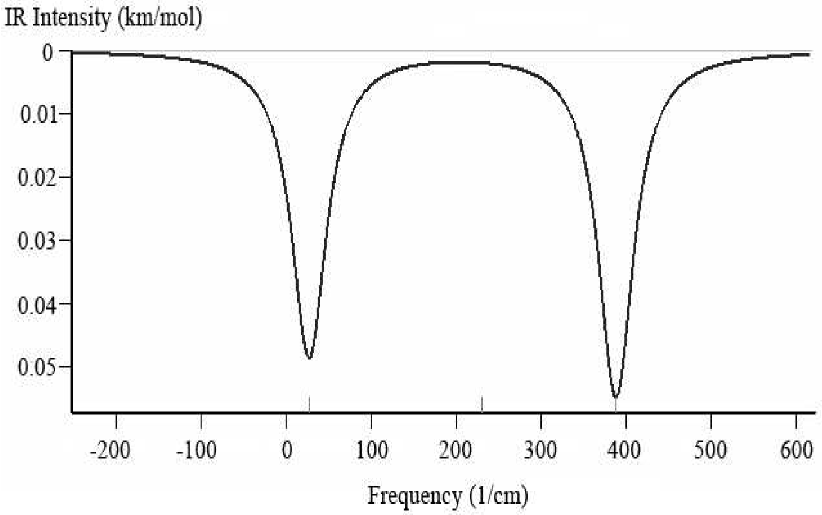

Figure 3.1: The vibrational spectrum of As_2Se (linear) calculated from the first principles.

(iii) As_2Se (triangle): This cluster is in the form of a triangle with As-Se bond length 259.6 pm and As-As distance 233.4 pm. The vibrational frequencies (intensities) are given in Table 3.1. The vibrational spectrum calculated from the first principles for As_2Se (triangle) shown in Fig. 3.2.

(iv) As_3Se (triangle): The three As atoms form a triangle with one Se in the centre. The As-Se bond length is 238.4 pm. The vibrational frequencies (intensities)

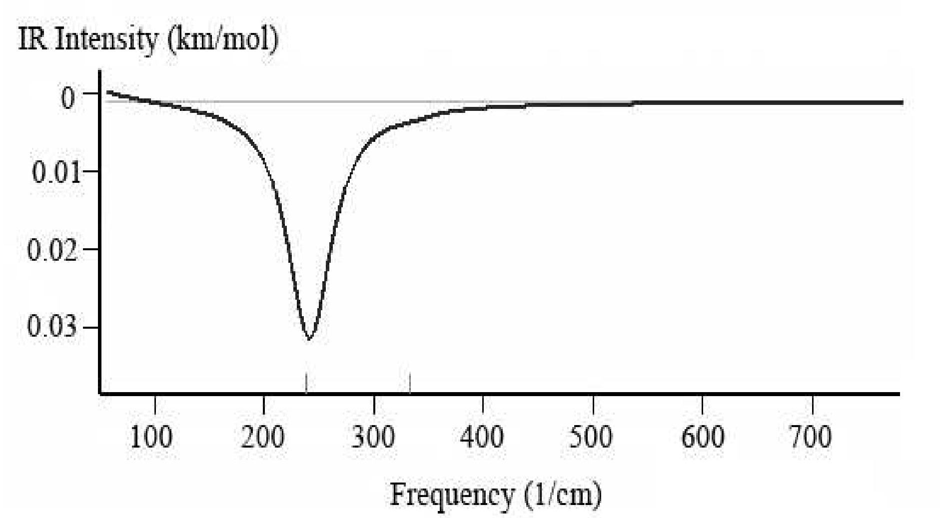

Figure 3.2: The vibrational spectrum of As_2Se (triangle) calculated from the first principles.

[degeneracies] are given in Table 3.1. The vibrational spectrum calculated from the first principles for As_3Se (triangle) shown in Fig. 3.3.

(v) As_4Se (square): The four As atoms form a square with one Se in the centre. The As-Se bond length is 250.2 pm. The frequencies (intensities) [degeneracies] are given in Table 3.1.

(vi) As_4Se (pyramid): The four As atoms form a square with one Se on top position, forming a pyramid. The As - Se distance is 252.1 pm and As-As distance is 253.4 pm. The spectral data is given in Table 3.1. The vibrational spectrum calculated from the first principles for As_4Se (pyramid) shown in Fig. 3.4.

(vii) $AsSe_2$ (linear): In this cluster, the atoms are in a straight line with As-Se distance is 235.5 pm. The strong linear vibration occurs at 330.6 cm^{-1}.

(viii) $AsSe_2$ (triangle): The $AsSe_2$ arranged in a triangle have As-Se distance of 250.1 pm and Se - Se bond length is 258.1 pm. There are three vibrational frequencies (intensities) as given in Table 3.1. The vibrational spectrum calculated from the

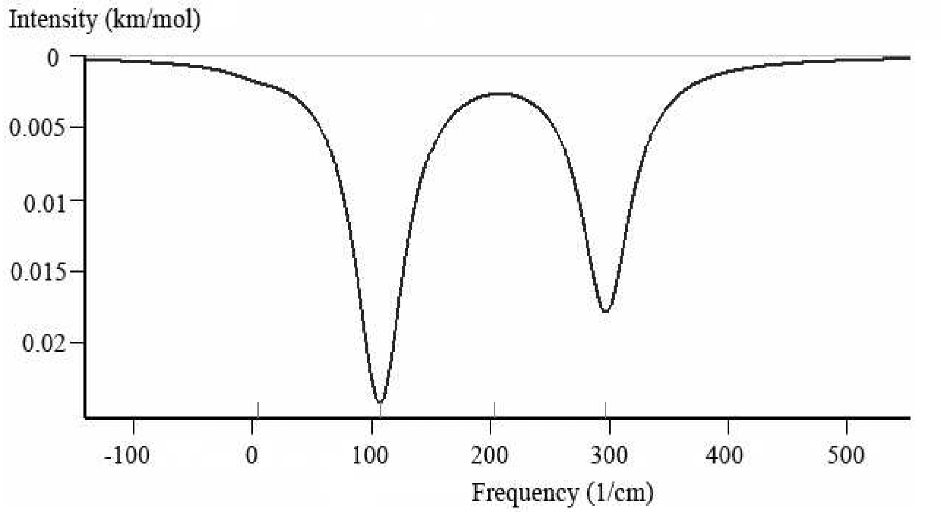

Figure 3.3: The vibrational spectrum of As_3Se (triangle) calculated from the first principles.

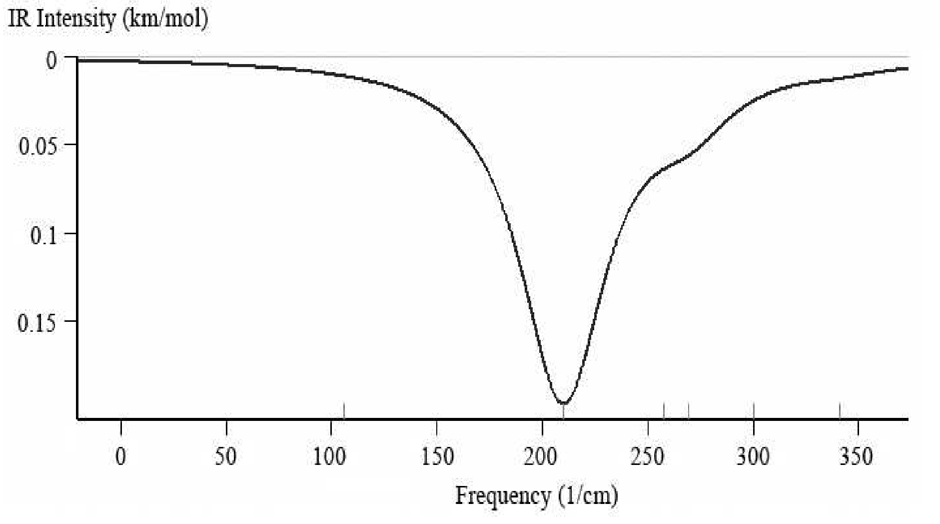

Figure 3.4: The vibrational spectrum of As_4Se (pyramid) calculated from the first principles.

first principles for $AsSe_2$ (triangle) shown in Fig. 3.5.

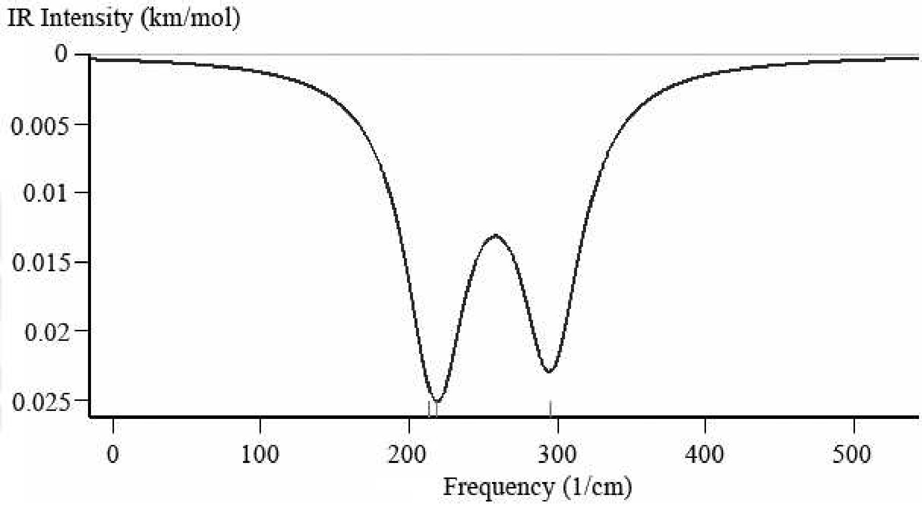

Figure 3.5: The vibrational spectrum of $AsSe_2$ (triangle) calculated from the first principles.

(ix) As_2Se_2 (linear): The alternate atoms As-Se-As-Se in a straight line give the bond length as 228.1 pm. The frequencies (intensities) are given in Table 3.1. The vibrational spectrum calculated from the first principles for As_2Se_2 (linear) shown in Fig. 3.6.

(x) As_2Se_2 (ring): All four atoms have been arranged alternately to form a square. The bond length is found to be 248.4 pm. The vibrational data is given in Table 3.2.

(xi) As_3Se_2 (linear): The bond distance between As-Se atoms is 229.1 pm and 248.4 pm. The frequencies in this linear mode are given in Table 3.2.

(xii) As_4Se_2 (bipyramid): The 4 atoms of As make a square with As-As distance 275.4 pm and one Se is on top and another Se on bottom to make a double pyramid. The vibrational data of this double pyramidal molecule is given in Table 3.2. The

Table 3.1: The frequencies, intensities and degeneracies calculated from the first principles for various clusters of arsenic selenide.

S. No	Cluster	Frequency cm^{-1}	Intensity	Degeneracy
1	As_2Se (linear)	27.6	1.900	2
2		387.6	4.300	1
3	As_2Se (triangle)	237.4	2.400	1
4		332.5	0.050	1
5	As_3Se (triangle)	107.5	1.870	1
6		296.6	0.680	2
7	As_4Se (square)	58.6	0.040	2
8		241.3	5.870	2
9	As_4Se (pyramid)	209.6	7.540	2
10		257.8	0.020	1
11		269.1	1.050	2
12		340.7	0.241	1
13	$AsSe_2$ (triangle)	213.7	0.010	1
14		218.6	1.800	1
15		294.8	1.620	1
16	As_2Se_2 (linear)	69.4	0.025	2
17		82.4	0.003	1
18		124.6	1.900	2
19		331.6	37.360	1
20		342.9	21.420	1

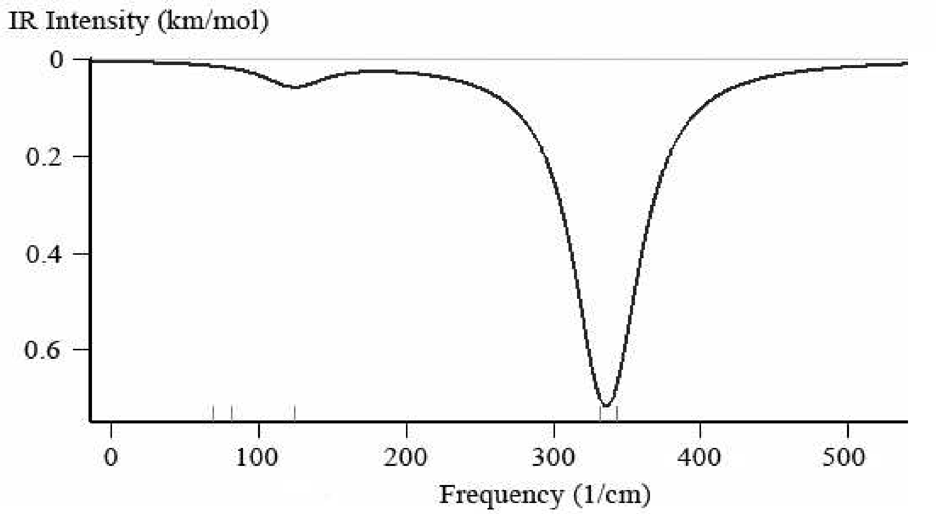

Figure 3.6: The vibrational spectrum of As_2Se_2 (linear) calculated from the first principles.

vibrational spectrum calculated from the first principles for As_4Se_2 (bipyramid) shown in Fig. 3.7.

(xiii) $AsSe_3$ (triangle): The three Se atoms form a triangle and one As is in the centre. The As-Se bond length is 231.2 pm and the vibrational data is given in Table 3.2. The vibrational spectrum calculated from the first principles for $AsSe_3$ (triangle) shown in Fig. 3.8.

(xiv) $AsSe_3$ (pyramid): The three Se atoms form a triangle with Se-Se distance 325.0 pm and one As is put on top with As-Se distance 251.0 pm. In this case, the vibrational frequencies (intensities) [degeneracies] are given in Table 3.2. The As atom apparently can go through the triangle of Se_3 atoms. Therefore, the triangle has become bigger.

(xv) As_2Se_3 (linear): The linear arrangement has bond lengths 219.0 and 235.8 pm. The frequencies are given in Table 3.2. The symmetries in the linear molecule are quite different from that of the bipyramidal structure. The vibrational spectrum

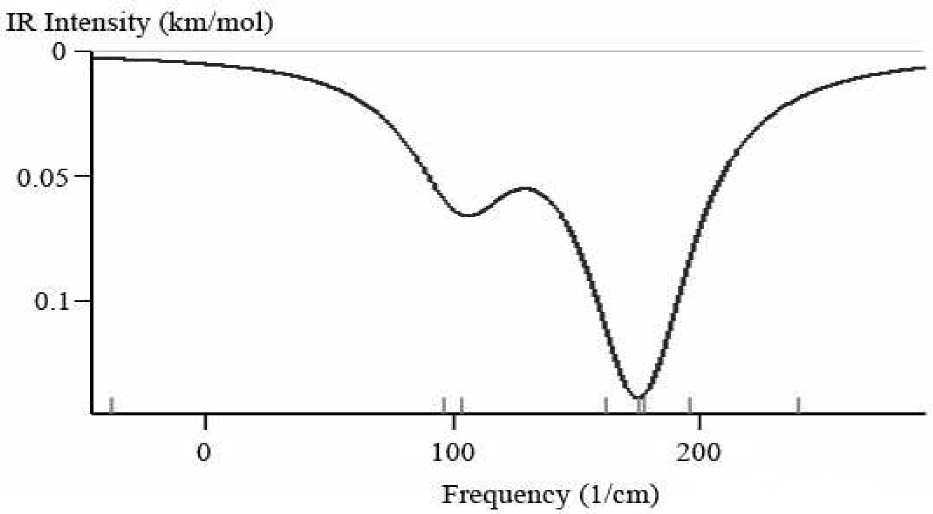

Figure 3.7: The vibrational spectrum of As_4Se_2 (bipyramid) calculated from the first principles.

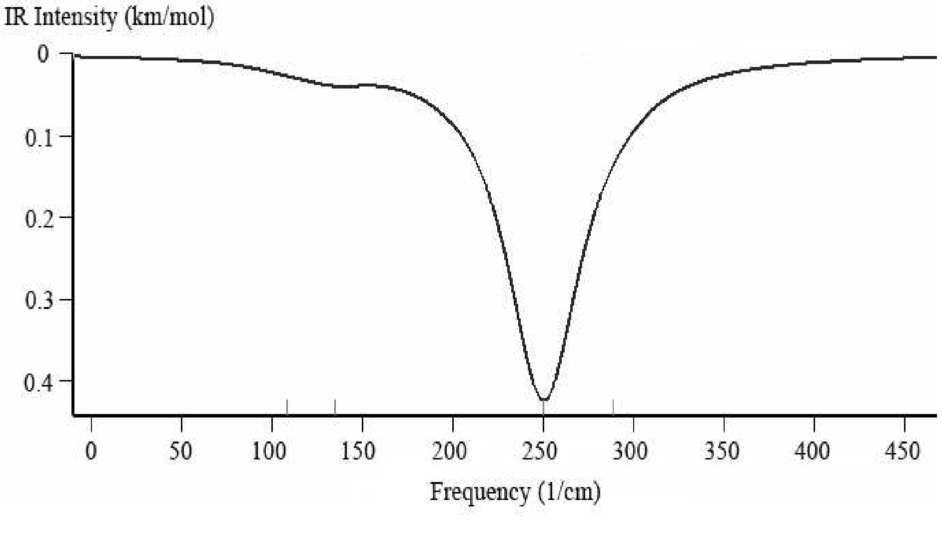

Figure 3.8: The vibrational spectrum of $AsSe_3$ (triangle) calculated from the first principles.

calculated from the first principles for As_2Se_3 (linear) shown in Fig. 3.9.

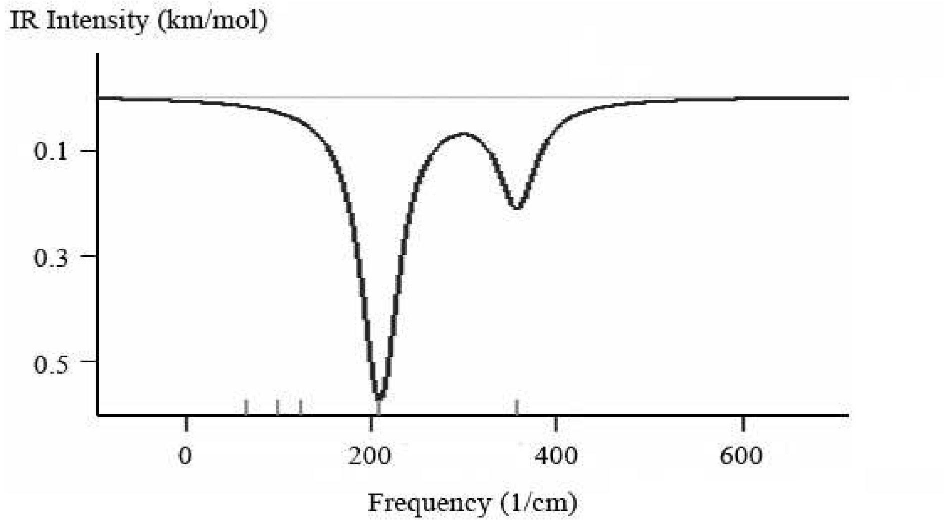

Figure 3.9: The vibrational spectrum of As_2Se_3 (linear) calculated from the first principles.

3.3 AsSe Raman Data

The AsSe Raman scattering has been studied by Nemanich [33]. There is a broad band near 25 ± 12 cm^{-1}. In this computation, the theoretical value for As_2Se is 27.6 cm^{-1}. Therefore, it is clear that linear molecules are present in the glass. This kind of linear bonds give strength to the glass. The theoretical modelling has also been done by Phillips [35]. This work shows that small clusters of atoms are randomly distributed in the glass and tend to self-organize in the solid state. The sample preparation is not good as to resolve the vibrational frequencies in arsenic selenide glass. A lot of scattering is due to particle size. For a particle of diameter d, the Raman frequency is:

$$\nu = \frac{\upsilon}{2d} \tag{3.1}$$

For the sound velocity, $\upsilon = 3 \text{ x } 10^5$ cms^{-1} and $\nu = 50$ cm^{-1}, the light is scattered by a

Table 3.2: The frequencies, intensities and degeneracies calculated from the first principles.

S.No	Cluster	Frequency cm^{-1}	Intensity	Degeneracy
1	As_2Se_2 (ring)	91.04	1.24	1
2		232.04	5.44	1
3		237.04	0.43	1
4	As_3Se_2 (linear)	62.20	1.65	2
5		76.06	2.32	2
6		217.94	44.35	1
7		349.56	0.91	1
8	As_4Se_2 (bipyramid)	103.36	2.02	2
9		175.24	10.34	1
10		177.62	0.08	2
11	$AsSe_3$ (triangle)	75.90	0.003	1
12		103.50	1.26	2
13		350.80	33.26	2
14	$AsSe_3$ (pyramid)	108.20	0.27	2
15		134.80	1.43	1
16		249.80	16.42	2
17		288.50	0.97	1
18	As_2Se_3 (linear)	66.30	0.001	2
19		252.36	16.09	1
20		433.73	3.17	1

particle of size, $d = \frac{v}{2\nu} = 10$ Å. When particles of a few nm sizes are present in the film of the glass, there is considerable scattering due to particles. In fact, the measurement of the Raman frequency as a function of particle size can be used to measure the sound velocity. The vibrational modes occur as given in Tables 3.1 and 3.2.

3.4 Conclusions

The ab initio calculations of vibrational frequencies of several clusters containing As and Se atoms have been performed. The values calculated for a linear system are in accord with the experimental values. In this way, the linear bonds As-Se-As can be identify that is present in the AsSe glass. These bonds are important for the strength of the glassy state.

Chapter 4

Ab initio Calculation of Vibrational Frequencies in As_xS_{1-x} Glass and The Raman Spectra

Many different models have been made to understand the structure of AsS glass. In particular, the models of AsS_3 (triangular), AsS_3 (pyramid), AsS_4 (3S on one side, one on the other side of As, S_3-As-S), AsS_4 (pyramid), AsS_4 (tetrahedral), AsS_7, As_2S_6 (dumb bell), As_2S_3 (bipyramid), As_2S_3 (zig-zag), As_3S_2 (bipyramid), As_3S_2 (linear), As_4S_4 (cubic), As_4S_4 (ring), As_4S (tetrahedral), As_4S (pyramid), As_4S_3 (linear) and As_4S_2 (dumb bell) have been made using the density functional theory which solves the Schrödinger equation for the given number of atoms in a cluster in the local density approximation. The models are optimized for the minimum energy which determines the structures, bond lengths and angles. By calculating the gradients of the first principles potential, the vibrational frequencies for the optimized clusters in each case have been calculated. The experimentally observed Raman frequencies have been compared with those of calculated so that the cluster can be identify whether it is present in the glass. It found that AsS_4 (S_3-As-S), As_4S_4 (ring), As_2S_3 (bipyramid), As_4S_4 (cubic),

As_4S_3 (linear), As_2S_3 (zig-zag), AsS_4 (T_d), As_2S_6 (dumb bell), AsS_3 (triangle) and AsS_3 (pyramid) structures are present in the actual glass.

4.1 Introduction

In recent years, there has been considerable progress in the understanding of glass phase of a solid [43]. The glass phase is often composed of molecules or clusters of atoms. In the formation of a molecule only a single valency is present, for example in AsS, arsenic is divalent. If the relative concentration of As and S be disturbed by mixing more or less of As than S in As_xS_{1-x}, there is a phase transition at a particular value of x from the single crystal to a glass. AsS is called realgar. It is sensitive to light which changes the valency of As from 2 to 3. In the compound As_2S_3 arsenic is trivalent. In this state As_2S_3 is called orpiment. Actually several other forms are also well known, e.g., As_4S (duranusite), As_4S_3 (dimorphite) and As_4S_5 (uzonite). The Raman spectra are poorly resolved so that there is hope to identify new molecular compositions. There has been considerable effort to resolve the Raman spectra in AsS glass [36]. The fractional valency of As is also found, 1.5 in As_4S_3 and 2.5 in As_4S_5 which indicates that there is a strong sharing of orbits between As and S atoms. Yang *et al.* [37] have calculated the force constants in both AsS as well as As_2S_3 from which they determine that As-S bond is much stronger than the As-As bond. Ohsaka and Ihara [38] have analyzed the low frequency region where the phonon frequency is determined by the size of the grains in the sample,

$$\nu = \frac{v}{2d}, \tag{4.1}$$

where v is the velocity of sound, d is the diameter of the particle and ν is the phonon frequency. The Raman spectra of As_2S_3 have been reported by Kawazoe *et al.* [39]. There is a strong peak at 340 cm^{-1} and comparatively weaker peaks at 230 and 490

cm^{-1}. There is a poorly resolved band at 700-800 cm^{-1}. Tanaka [40] has also discussed the Raman peak at 350 cm^{-1} and humps at 230 and 500 cm^{-1}. There is also a peak at about 30 cm^{-1} which is due to scattering related to particle size. In recent years, the density functional theory calculations have successfully performed which predict the vibrational frequency in reasonable agreement with the experimental values [25–27, 41, 42]. The first principles calculations [44–46] have also been useful for the understanding of solids. The detailed theory of relaxation with stretched exponential has been given by Phillips [22] and Thorpe [23] has introduced the concept of soft modes in glasses. Wang *et al.* [24] have found that there is a phase transition in glasses as a function of concentration in which rigidity is the order parameter. Since the calculations of vibrational frequencies in the glasses [25, 27], GePI and GePS are in reasonable agreement with those measured by the Raman spectra, the calculations extend to AsS as report below.

In this chapter, the calculations of vibrational frequencies in clusters of arsenic sulphide have been reported. This calculated value has been compared with those found in the Raman spectra. The calculations of structure optimization and vibrational frequencies of AsS_3 (triangular), AsS_3 (pyramid), AsS_4 (3S on one side, one on the other side of As, S_3-As-S, 3-1 model), AsS_4 (pyramid), AsS_4 (tetrahedral), AsS_7, As_2S_6 (dumb bell), As_2S_3 (bipyramid), As_2S_3 (zig-zag), As_3S_2 (bipyramid), As_3S_2 (linear), As_4S_4 (cubic), As_4S_4 (ring), As_4S (tetrahedral), As_4S (pyramid), As_4S_3 (linear) and As_6S_2 (dumb bell) have been performed. By comparing the calculated values with those found from the Raman spectra of actual glasses, it is found that AsS_4 (S_3-As-S), As_4S_4 (ring), As_2S_3 (bipyramid), As_4S_4 (cubic), As_4S_3 (linear), As_2S_3 (zig-zag), AsS_4 (T_d), As_2S_6 (dumb bell), AsS_3 (triangle) and AsS_3 (pyramid) structures are actually present in the glass. It is found that AsS_4 stabilizes as a pyramidal molecule as well as in a 3-1 model. This is possible in a double well type potential. There is more than one position for an atom for which the molecule is stable. It is also obvious that many more molecules of sulphur and arsenic exist in addition to the well known minerals, realgar and orpiment. The decolouration in the minerals is associated with the existence of several other molecules.

4.2 Methodology

The clusters of atoms have been made while the bond distances and angles have been optimized for the minimum energy. The Schrödinger equation for a given cluster of atoms is solved in the local density approximation of the density functional theory [1, 4, 5]. The force constants are obtained from the derivative of the potential without any adjustable parameters. The Accelrys computer program is run on Core 2 Duo Quadro computer operating at 2.4 GHz. The vibrational spectra for clusters of atoms are obtained from the first principles. The Amsterdam Density Functional (ADF) program was also used occasionally [28].

In the ADF programme, the single zeta wave functions (SZ), the double zeta wave functions (DZ), the double zeta wave function with polarization (DZP), triple zeta wave function with polarization (TZP) and triple zeta wave functions with double polarization (TZ2P) can be used. In the Accelrys programme, the single zeta wave functions with minimum basis set (Min), the double numeric wave function (DN), the double numerical which leaves out the p wave functions of hydrogen (DND) and the double numeric with polarization (DNP) can be used as a basis set. It is customary to add hydrogen atoms to neutralize the charge on the clusters. In the Accelrys programme, the charge on the clusters can be selected by hand. In the present calculations, all of the clusters are metallic and hence hydrogen has not been added. There is no restriction on the number of atoms except that more computer time is needed when number of atoms is large. The vibrational frequencies are calculated from the gradient of the potential. In the calculations given in this chapter, the Raman spectra are not computed but the Raman frequencies are picked up from the full vibrational spectra. Similarly, the vibrational density of states is not calculated. Indeed, when the same cluster of atoms is calculated by Min, DN, DND and DNP wave functions, different values are obtained. For example, for AsS_4 with S_4 atoms on the corners of a square with As in the centre, a small difference in the bond length have been obtain as given in Table 4.1. Comparing these values, it show that a 14% variation is possible when different wave functions are chosen. As far as comparison of calculated frequencies with experimental values is concerned, it found that the double numeric (DN) wave function gives the closest values. The uncertainty is less than 10 cm^{-1} in the frequencies. Some of the frequencies are as close as 5 cm^{-1}. The source of the deviation is in the approximations used to solve the secular determinant.

Table 4.1: The length of the As-S bond for the square model of AsS_4 with calculated using several different types of eigen vectors.

Wave function	Min	Dn	DND	DNP
As-S bond (Å)	2.327	2.278	2.160	2.162

4.3 Clusters of atoms

The clusters of atoms have been build to obtain their optimized structures, bond lengths and angles. Then the vibrational spectra can be obtained. In some cases the same molecule occurs in three dimensions as well as in a plane showing the collapse of one of the dimensions. In some cases, one ion has been exchanged to another so the effect of ion exchange can be seen. In the density functional theory, the nuclear motion equation separates out from that of the electron. The Born-Oppenheimer approximation which means that the electronic and nuclear wave functions are written in the form a product of wave functions also seems to be very satisfactory. In the following material, 17 different clusters are reported.

The cluster AsS_4 stabilizes in several different configurations. For example the 4 sulphur atoms occupy the four corners of a square with As in the centre. The AsS_4 also stabilizes with 3 sulphur atoms on one side and one S atom on the other side of As which is call S_3-As-S(3-1 model). It is possible to stabilize AsS_4 as a pyramid in which all of the four S atoms are in a square and one As is on top. AsS_4 also stabilizes with S atoms on a tetrahedron with As in the centre. Thus several different shapes for the same set of atoms are allowed. As discussed in the above section on methodology, the SZ, DZ, DZP, DZ2P, Min, DN, DND and DNP type eigen vectors are available. As far as the comparison with the experiment is concerned, the DN works the best. Therefore, this report only tabulate the eigen values of the DN for all of the clusters.

(i) AsS_3 (triangle): In this cluster, three atoms of S are on the corners of a triangle and As is in the centre. The S-As-S angle is strictly 120° so that only one distance is sufficient to define this cluster. The optimized As-S distance is found to be 2.165 Å by using double numeric (DN) wave functions. The frequencies of vibrations and their intensities are given in Table 4.2.

(ii) AsS_3 (pyramid): From the calculation [i], it is clear that AsS_3 stabilizes in a plane. However, it is also possible to find the stable configuration in a pyramidal form. In this case the S-S bond distance is found to be 2.359 Å while the As-S distance is 3.000 Å. The frequencies and their intensities are given in Table 4.2. The vibrational spectrum calculated from the first principles by using the DN wave functions is shown in Fig. 4.1.

(iii) AsS_4 (S_3-As-S, 3-1 model): This cluster has three S atoms on one side of As and one S on the other, which is call 3-1 model. The S atoms on one side form a triangle with S-S distance 3.080 Å with As-S distance of 2.241 Å, then there is one S atom on the other side with As-S distance of 2.120 Å. The frequencies and intensities of various modes are tabulated in Table 4.2. The eigen values

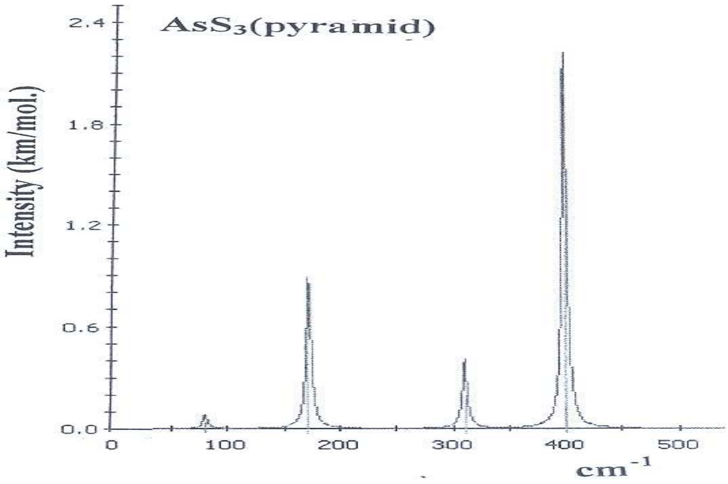

Figure 4.1: The vibrational spectrum of AsS_3 (pyramid) calculated from the first principles.

tabulated are those of the DN wave vectors. This cluster also has been solved with Min, DND and DNP wave functions. The eigen values of the DND and DNP are almost equal to each other but the minimum basis set of wave functions gives different values. Needless to say that single zeta wave function does not agree with the experimental data. The vibrational spectrum calculated from the first principles is shown in Fig. 4.2.

(iv) AsS_4 (pyramid): This is a pyramidal cluster so that all of the four S atoms are on one side forming a square and As is on top. The S-S distance is 2.671 Å and As-S distance is 2.474 Å. The calculated vibrational frequencies and intensities are given in Table 4.3.

(v) AsS_4 (T_d): It is possible to put the 4 sulphur atoms on a tetrahedron with As in the centre. This is a stable configuration. When DN wave function is used, the As-S distance is found to be 2.241 Å. The calculated vibrational frequencies are given in Table 4.3. The vibrational spectrum computed from the first principles is given in Fig. 4.3. A strong vibration at 358.3 cm^{-1} is clearly visible.

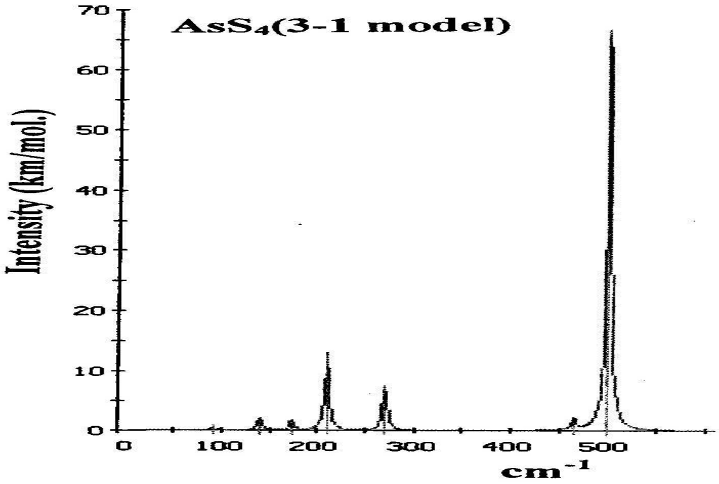

Figure 4.2: The vibrational spectrum of AsS_4 (3-1 model) calculated from the first principles.

Table 4.2: The frequencies and intensities computed from the first principles for various clusters by using DN wave functions. The degeneracy is given in the small brackets.

S. No	Cluster	Frequency cm^{-1}	Intensity km/mol
1	AsS_3(triangle)	109.07	0.30
2		110.43	0.36
3		110.89	1.32
4		387.36	0.01
5		422.75	1.86
6		424.72	1.99
7	AsS_3(pyramid)	80.81	0.04(2)
8		172.15	0.89
9		309.60	0.20(2)
10		399.60	2.23
11	AsS_4(3-1 model)	90.00	0.45
12		139.00	1.97
13		173.00	1.60
14		210.00	13.20
15		270.00	7.71
16		466.00	1.91
17		500.00	66.81

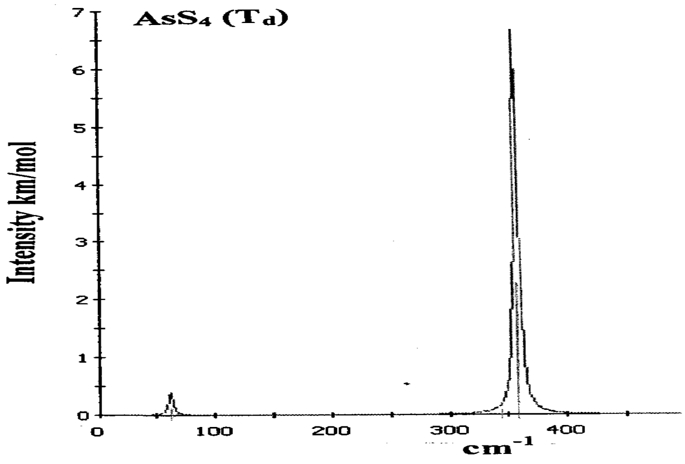

Figure 4.3: The vibrational spectrum of AsS_4 (tetrahedral) calculated from the first principles.

(vi) AsS_7: There is one As in the centre and 7 atoms of S are all around it. The As-S distance is 2.521 Å and the S-S distance is 2.314 Å. The calculated frequencies and intensities of this cluster for the DN wave functions are given in Table 4.3.

(vii) As_2S_6 (dumb bell): In this model the two As atoms are far apart. The distance between two As atoms is 3.474 Å and then three S atoms are attached to each As atom. The AsS atoms are 2.169 Å apart. Since the figure is symmetric each set of 3 atoms of S are symmetrically connected. The calculated vibrational frequencies as well as intensities are given in Table 4.3. The vibrational spectrum shown in Fig. 4.4.

(viii) As_2S_3 (bipyramid): This is a bipyramidal cluster. The S_3 form a triangle with one As is on top position while another As atom is on the bottom position. The As-S distance is 3.388 Å and S-S distance is 2.441 Å. The calculated frequencies are given in Table 4.3 and the calculated spectrum is given in Fig. 4.5.

(ix) As_2S_3 (zig-zag): The atoms are arranged in a straight line as S-As-S-As-S. Then

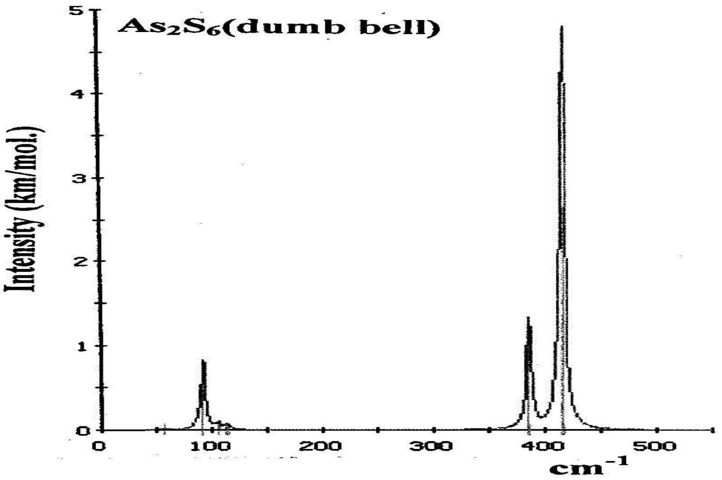

Figure 4.4: The vibrational spectrum of As_2S_6 (dumb bell) calculated from the first principles.

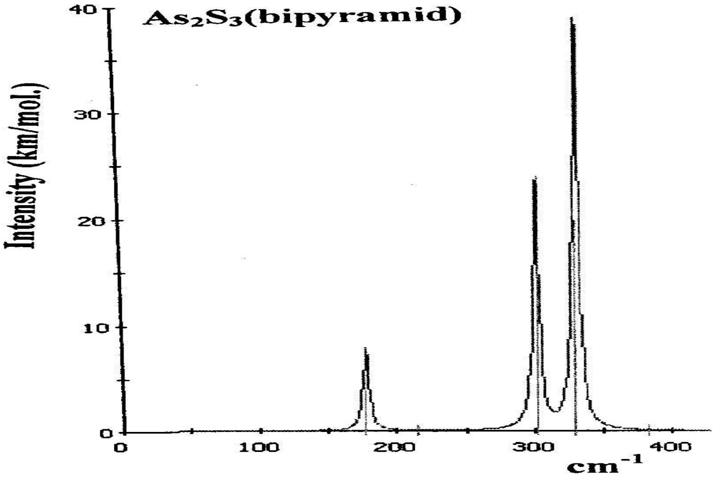

Figure 4.5: The vibrational spectrum of As_2S_3 (bipyramid) calculated from the first principles.

Table 4.3: The frequencies and intensities computed from the first principles for various clusters by using DN wave functions. The degeneracy, when different from 1, is given in small brackets.

S.No	Cluster	Frequency cm^{-1}	Intensity km/mol
1	AsS_4(pyramid)	203.90	0.88
2		288.20	20.36
3		383.10	2.61
4	AsS_4(T_d)	61.70	0.12(3)
5		358.30	2.28(3)
6	AsS_7	162.60	5.12
7		163.22	6.25
8		257.02	0.03
9		296.30	0.10
10		358.08	0.38
11	As_2S_6(dumb bell)	55.68	0.01
12		91.95	0.84
13		105.60	0.07
14		113.17	0.01
15		113.21	0.04
16		116.00	0.01(2)
17		385.50	1.28
18		415.00	2.68(2)
19		416.30	0.02(2)
20	As_2S_3(bipyramid)	177.20	3.93(2)
21		301.60	23.90
22		330.60	19.83(2)

optimization makes the zig-zag so that S atoms are in one line and all of the As atoms are pulled slightly below that line. The As-S distance is 2.390 Å and S-S distance is 2.131 Å. The vibrational frequencies calculated for the DN wave functions are given in Table 4.4. The calculated vibrational spectrum is given in Fig. 4.6.

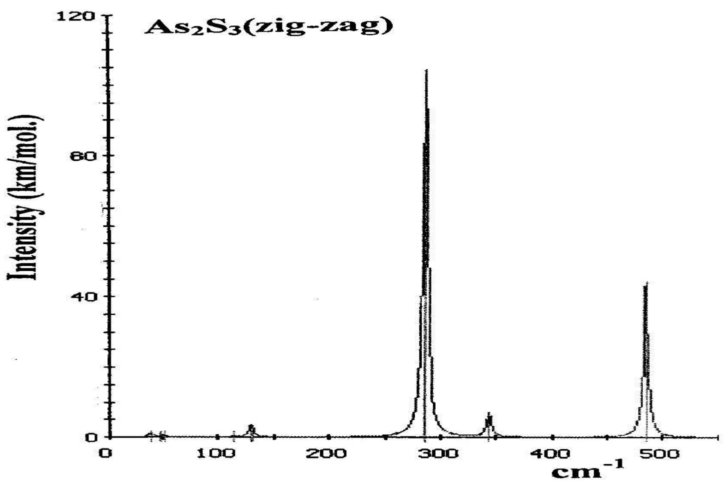

Figure 4.6: The vibrational spectrum of As_2S_3 (zig-zag) calculated from the first principles.

(x) As_3S_2 (bipyramid): In this cluster, there is a triangle of As atoms with one S atom on the top position and the other S atom on the bottom position. The As-As distance is 2.528 Å and the As-S distance is 2.714 Å. The vibrational frequencies are given in Table 4.4. The DN eigen vectors have been used for this calculation.

(xi) As_3S_2 (linear): It is possible to stabilize As-S-As-S-As in a linear cluster. In this case, the As-S distance near the end is 2.345 Å while near the centre it is 2.153 Å when DN eigen vectors are used. The vibrational frequencies of this system are given in Table 4.4.

(xii) As_4S_4 (cubic): The S_4 atoms are on the tetrahedron sites. The cubic sites left vacant by S are occupied by As atoms. The cell size is 2.529 Å so that a single distance determines the structure. The vibrational frequencies corresponding to DN wave functions are given in Table 4.4 and the calculated spectrum is given in Fig. 4.7.

(xiii) As_4S_4 (ring): A circular cluster is formed with alternate As and S atoms with As-S distance 2.208 Å. The circumference of the circle is thus 8 times this distance, i.e., 17.664 Å. The diameter of this molecule is about 5.62 Å. The vibrational frequencies of this molecule are given in Table 4.4 and the calculated spectrum is shown in Fig. 4.8.

Table 4.4: The frequencies and intensities calculated from the first principles for various clusters. The degeneracy, when different from unity, is given in the small brackets.

S.No	Cluster	Frequency cm^{-1}	Intensity km/mol
1	As_2S_3(zig-zag)	39.11	1.23
2		51.83	0.14
3		114.06	0.19
4		129.22	3.58
5		285.84	104.70
6		344.00	6.68
7		484.80	44.46
8		486.08	0.36
9	As_3S_2(bipyramid)	115.71	2.76(2)
10		242.47	41.86
11	As_3S_2(linear)	119.94	5.90(2)
12		160.45	5.60
13		468.80	38.00
14	As_4S_4(cubic)	118.60	0.96(3)
15		211.90	3.77(3)
16		279.30	1.82(3)
17	As_4S_4(ring)	113.18	2.71
18		156.15	1.55(2)
19		183.40	5.15
20		226.97	6.41
21		238.37	8.72(2)
22		346.50	4.69(2)

(xiv) As_4S (T_d): There are four As atoms on the tetrahedral sites and one S atom in

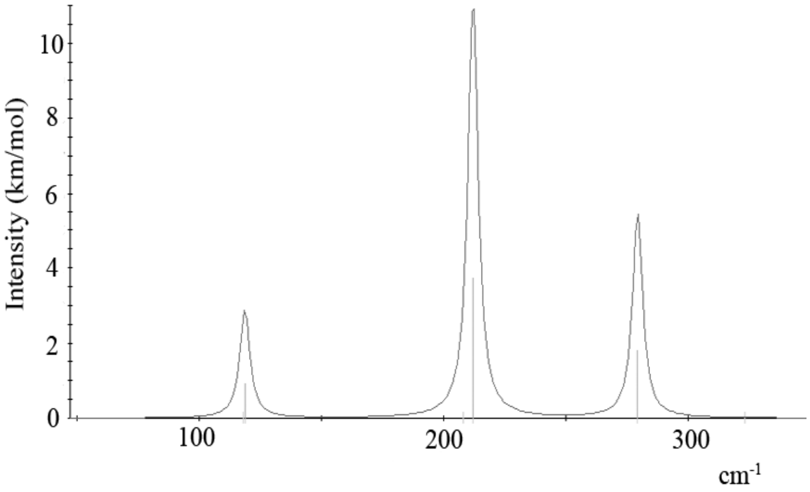

Figure 4.7: The vibrational spectrum of As_4S_4 (cubic) calculated from the first principles.

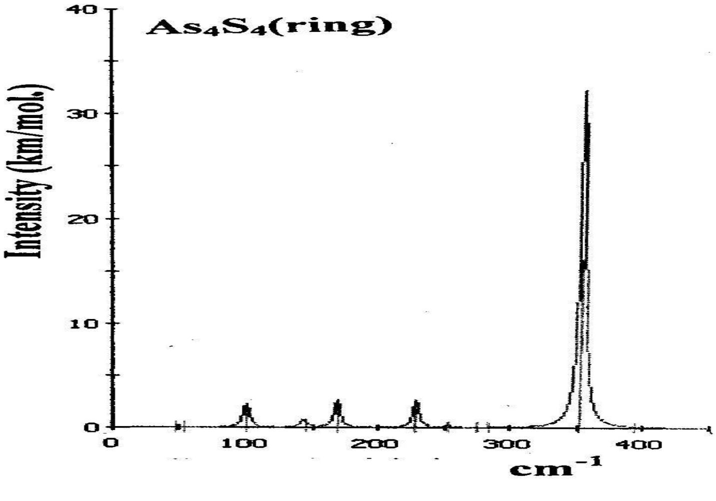

Figure 4.8: The vibrational spectrum of As_4S_4 (ring) calculated from the first principles.

the centre. The As-S bond distance is 2.298 Å and its vibrational frequencies are given in Table 4.5.

(xv) As_4S (pyramid): In this system, the four As atoms form a square with As-As distance 2.503 Å and one S is on top position with As-S distance 2.892 Å. The vibrations belong to A_1, A_2 and E irreducible representation are found. The frequencies of these oscillations along with degeneracy are given in Table 4.5.

(xvi) As_4S_3 (linear): This molecule is genuinely linear. The bond length at the end of the molecule is 2.529 Å. As one approaches from the end towards the centre, the bond becomes smaller and the values change to 2.2999 Å and then near the centre to 2.152 Å. This molecule has a strong mode at 343 cm^{-1} and a weak mode at 411.39 cm^{-1} as given in Table 4.5 and the spectrum is given in Fig. 4.9.

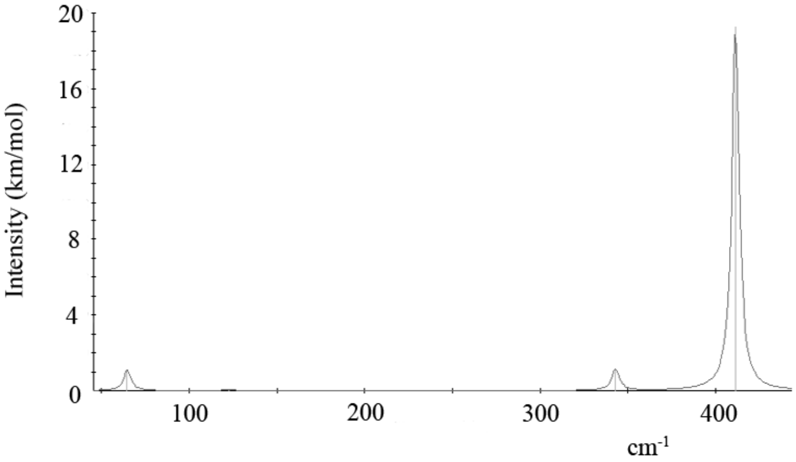

Figure 4.9: The vibrational spectrum of As_4S_3 (linear) calculated from the first principles.

(xvii) As_6S_2 (dumb bell): The two S atoms are now far apart with S-S distance of 4.031 Å. This means that there is unusual expansion of the S-S bond. Three As atoms are attached to each S. The As atoms belonging to one S are attracted to those belonging to the other S atom. The As-S distance is 2.556 Å. The vibrational frequencies of this molecule calculated by using the DN eigen vectors are given in Table 4.5.

Table 4.5: The vibrational frequencies of various clusters calculated by using DN wave functions. The degeneracy, when different from unity, is given in small brackets.

S. No	Cluster	Frequency cm^{-1}	Intensity km/mol
1	$As_4S(T_d)$	412.45	2.10
2		443.60	5.50
3		409.70	8.80
4	As_4S(pyramid)	231.09	0.18
5		242.17	0.52(2)
6		297.63	0.11
7	As_4S_3(linear)	38.60	0.01
8		64.50	1.11
9		122.60	0.04
10		343.00	1.14
11		411.40	1.93
12	As_6S_2(dumb bell)	69.30	1.13(2)
13		148.70	0.08
14		157.30	0.61(2)
15		234.80	3.88(2)
16		246.30	4.33

4.4 Discussion

Usually, when the electronically degenerate state is interacting with a lattice vibration with respect to which it is unstable, the degeneracy is removed. Therefore, some of the symmetries are not found in molecules. This phenomenon is called the “Jahn-Teller effect”. In this calculations it was found that the same set of atoms, for example, AsS_3 have two stable configurations, the S_3 in a triangle with As in the centre and a pyramid. This phenomenon of multiple symmetries is more pronounced in AsS_4 where three stable configurations are found. The AsS_4 with As_4S which is call “ion exchange” has been compared. The atomic number of As is 33 and that of S is 16. Hence As_4S is much heavier than AsS_4. Accordingly, the heavier cluster tends to be bigger than the lighter cluster for the same symmetry. The calculated and experimentally observed frequencies help in identifying the clusters actually present in the real material. (a) Realgar. The frequencies 187, 218, 272, 342 and 362 cm^{-1} experimentally found in the realgar, are identified with AsS_4 (3-1 model), AsS_4 (T_d), As_4S_4 (ring), As_2S_3 (bipyramid) and As_4S_4 (cubic). (b) Orpiment. The frequencies 308, 330, 378 and 397 cm^{-1} are found experimentally in the orpiment. According to Table 4.6, these frequencies are identified with AsS_3 (pyramid), As_2S_3 (bipyramid), As_2S_6 (dumb bell) and AsS_3 (triangular). The orpiment is therefore built from AsS_3 (pyramid). However, there can occur tunneling of As through the triangle of S_3 atoms so that AsS_3 triangles are also stable. When glass is formed, As_2S_3 (bipyramid) and As_2S_6 (dumb bell) are also predicted. The experimental data is completely blank for frequencies > 400 cm^{-1}. Whereas, the calculations do show some vibrational modes. This phenomenon of transparency is caused by the non-availability of “change in polarizability” upon shining the material with light.

4.5 Experimental Raman Spectra

The Raman spectra of As_2S_3 given by Tanaka [40] are poorly resolved. There is a peak at 20 cm^{-1} due to scattering from the particle size, which means that the particle size is equal to the wave length of radiation, $\nu = v/2d$. Here v is the velocity of sound and d is the diameter of the grain. Let us take $\nu = 20$ cm^{-1} as an exercise. This is equivalent to 20c in c.p.s. units. The diameter of the particle which scatters this radiation is $d = v/2\nu$, where $v \cong 3X10^5$ cm/s is the velocity of sound. Substituting v and ν in the expression for d found that $d = 25$ Å which is 250 nm. This is just the size of the particles present in the glass. Therefore, the 20 cm^{-1} radiation is caused by the particle size. This particle is a boson which is not related to the electronic structure of the atoms. It is also not related to the force constants. There are weak lines at 230 cm^{-1} and 500 cm^{-1} along with a strong and broad line at 350 cm^{-1}. Georgiev *et al.* [36] have made efforts to resolve the broad line into components. In the glass $\text{As}_x\text{S}_{1-x}(x = 0.38)$ there is a broad line but at $x = 0.44$ some resolution becomes apparent and lines at 185 and 220 cm^{-1} look like peaks on a broad back ground. In the Raman spectrum of the glass $\text{As}_{0.44}\text{S}_{0.56}$, the values of the frequencies can be identified easily. The actual glass is a mixture of many different compositions. In the mineral form also, it is easy to see the different compositions distinguished by different colours. The quantity of sulphur is strongly reflected by decolouration. The different colour parts of the mineral have different chemical formula. A typical Raman spectrum has been selected to know the experimental values of the vibrational frequencies. The experimental Raman spectra which are deduced from ref. [36] has been showed in Fig. 4.10. The experimental Raman frequencies clearly visible in this spectrum are, 187, 218, 272, 308, 330, 342, 362, 378 and 397 cm^{-1}.

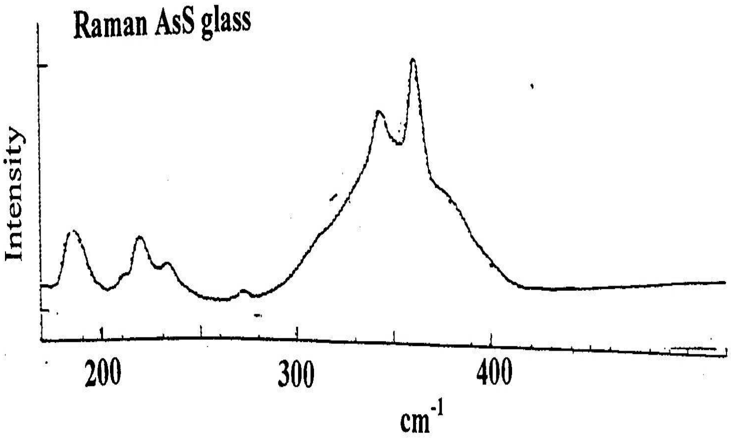

Figure 4.10: The experimental Raman spectrum of As-S glass. The measured frequencies are given in Table 4.6.

4.6 Comparison Between Theory and Experiments

The experimental as well as the values obtained from the first principle's calculations have been showed in Table 4.6. All of the experimentally found frequencies agree with those of calculated for the clusters. This means that the glass consists of random self-organized arrangements of clusters. The existence of As_4S_3 (linear) shows the linear growth which gives strength to the glass by working like a "back bone". The zig-zag As_2S_3 also shows that the structure of the back bone is not like a linear chain but more like a zig-zag arrangement of atoms. Besides, the "back bone", there are clusters which resemble rings, pyramids, bipyramids and triangles. The clusters relax with time and reorganize their orientations. This type of self-organization gives long relaxation times to the glass.

Table 4.6: Comparison of experimentally observed values of frequencies with those calculated for the given clusters.

S.No	Experimental (cm^{-1})	Calculated (cm^{-1})	Cluster
1	187	183.0	As_4S_4(ring)
		177.0	As_2S_3(bipyramid)
		173.0	AsS_4(3-1 model)
2	218	211.9	As_4S_4(cubic)
		210.0	AsS_4(3-1 model)
3	272	270.0	AsS_4(3-1 model)
		279.3	As_4S_4(cubic)
4	308	309.6	AsS_3(pyramid)
5	330	330.6	As_2S_3(bipyramid)
6	342	343.0	As_4S_3(linear)
		344.0	As_2S_3(zig-zag)
7	362	358.3	$AsS_4(T_d)$
8	378	385.5	As_2S_6(dumb bell)
		387.3	AsS_3(triangular)
9	397	399.6	AsS_3(pyramid)

4.7 Conclusions

The arsenic sulphide consists of several different compositions mixed together have been found. Although the minerals realgar (AsS) and orpiment (As_2S_3) are well known, it found that other molecules such as AsS_3 (triangular), AsS_3 (pyramid), AsS_4 (3-1 model), AsS_4 (T_d), As_4S_4 (ring), As_2S_3 (bipyramid), As_4S_4 (cubic), As_2S_3 (zig-zag), As_4S3 (linear) and As_2S_6 (dumb bell) are predicted on the basis of quantum mechanical first principle calculations. This prediction is in accord with the experimentally observed Raman spectra. The existence of these molecules is also apparent from the decolouration in the samples. The usefulness of quantum mechanics for the study of glass structures is well demonstrated. Hence, the existent of a class of “quantum glasses” has been predicted for which the vibrational frequencies are predictable by quantum mechanics. The calculations may help in decoding local structures of clusters that are produced by atomic beams. The molecular clusters are also populated in nanoscale phase separated molecular glasses.

Chapter 5

DFT Calculation of Structure and Vibrations in AsO Glass.

A large number of cluster of atoms are made by using the density functional theory. Out of the clusters, it is found that AsO_2, AsO_4 (T_d), As_2O_2 (rectangular), AsO_2 (triangle) and AsO_3 (pyramid) are really present in the vitreous As_2O_3. The dominant Raman frequencies found in the experimental data are identified by theoretical calculations.

5.1 Introduction

Recently, it was pointed out by Phillips [47, 48] that anomalous properties exist over a narrow range of composition in molecular glasses. It was also shown that long relaxation times occur in glasses [22]. In fact, some of the phonon frequencies can become soft and approach towards zero [23]. There is a phase transitions in the rigidness of glasses [24]. The random network of atoms is considered to be important for the understanding of glasses. Random network of clusters of atoms have been found present in many glasses [25, 27, 32]. Arsenic is found in several different valencies. The arsenic trioxide As_2O_3 dissolves in alkaline solutions to make arsenites. It reacts with oxidizing agents to form As_2O_5. The vibrational excitations of arsenic oxides have been reported [49–52] in vitreous and disordered phases. The polarized Raman spectra with second-order scattering are reported by Galeener *et al.* [50].

In this chapter, the calculation of vibrational frequencies of several clusters of arsenic and oxygen atoms will be report. Configuration of clusters have been optimized for which the energy of the Schrödinger equations is minimum.

These calculations are based on the kinetic energy of the electrons and the nuclei and all of the Coulomb interactions with no adjustable parameters. The calculated values from the first principles have been compared with those found from the experimental Raman spectra. The values calculated for the clusters were found to be in reasonable agreement with those measured. Therefore, it found that there were clusters in the vitreous As_2O_3. The glassy state is therefore made from the random network of clusters.

5.2 Clusters

The density functional theory in the local density approximation (LDA) has been used. The Kohn - Sham equations are solved and vibrational frequencies are deduced. The bond lengths and angles are obtained for the minimum energy [4]. The computer program DMol^3 is used. The double numeric (DN) wave functions are used in all of the calculations.

(i) AsO: This is a diatomic cluster. In the optimized configuration the distance between the two atoms is found to be 1.698 Å. There is a single vibrational frequency belonging to the bond stretching. The vibrational frequency is 881.37 cm^{-1}.

(ii) AsO_2: In this molecule for the optimized geometry, the bond angle is found to be 122.18 degrees. The As-O bond length is found to be 1.719 Å. The vibrational frequencies (intensities) are 219.8 (19.9), 753.7 (13.2) and 754.1 (1.59) cm^{-1} (km/mol).

(iii) AsO_2 (linear): It is possible to optimize this molecule in a linear form so that O-As-O angle is 180 degrees. The As-O bond length is found to be 1.734 Å. The vibrational frequency is calculated to be 753.8 cm^{-1}.

(iv) AsO_2 (triangle): It is also possible to optimize AsO_2 in the shape of a triangle. The As-O distance is 1.896 Å and O-O distance is 1.590 Å. The vibrational frequencies (intensities) are found to be 535.8 (11), 544.7 (11.8) and 855.1 (7.42) cm^{-1} (km/mol).

(v) AsO_3 (triangular): In this cluster the three oxygen atoms are at the corners of a triangle and As is in the centre. In the optimized configuration, the As-O distance is 1.662 Å and the vibrational frequencies (intensities) are 156.3 (3.5), 159.5 (3.3), 237.1 (24.7), 819.1 (2.2), 820.2 (2.1) and 826.9 (0.02) cm^{-1} (km/mol). The vibrational spectrum calculated for the cluster from the first principles is given in Fig.5.1.

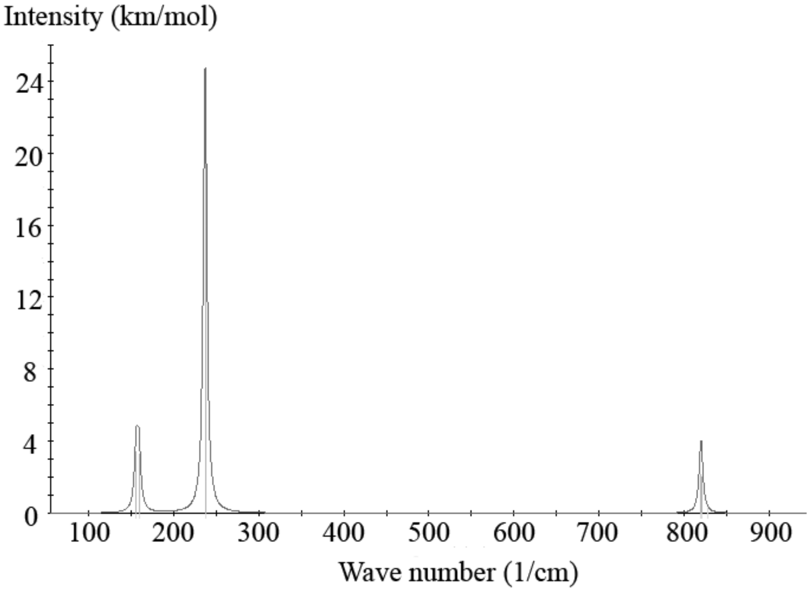

Figure 5.1: The vibrational spectrum of AsO_3 (triangular) calculated from the first principles.

(vi) AsO_3 (pyramidal): The O-O distance is 1.865 Å in the O_3 triangle. The As atom sits on top of the triangle to form a pyramidal. The As-O distance is 2.250 Å. It has strong vibrations at 280.3 (5.28), 532.1 (0.91) {2} and 701.8 (11.8) cm^{-1} (km/mol){degeneracy}. The vibrational spectrum calculated from first principles is shown in Fig.5.2.

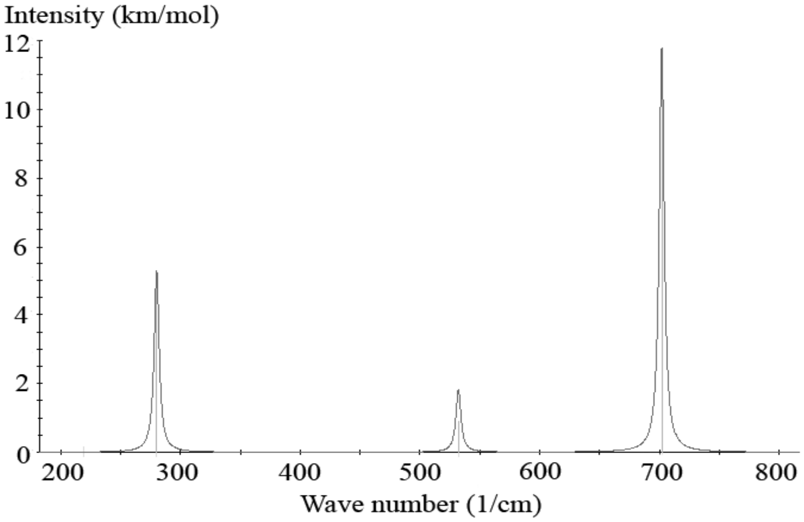

Figure 5.2: The vibrational spectrum of AsO_3 (pyramidal) calculated from the first principles.

(vii) AsO_4 (T_d): This is a tetrahedral molecule. The O-As distance is 1.759 Å. The dominant mode occurs at 335.1 cm^{-1} and it is tripely degenerate.

(viii) As_2O: This molecule has As-O-As angle of 71.36 degrees and bond length is 1.971 Å. The vibrational frequencies (intensities) are 195.4 (6.2), 305.7 (6.09), 605.8 (22.9) cm^{-1} (km/mol). The calculated spectrum for this model is shown in Fig.5.3.

(ix) As_2O (triangle): The three atoms are arranged in a triangle. The As-As distance is 2.299 Å and As-O distance is 1.971 Å. There are three vibrational frequencies (intensities) at 194.7 (6.2), 305.7 (6.1) and 605.1 (22.9) cm^{-1} (km/mol).

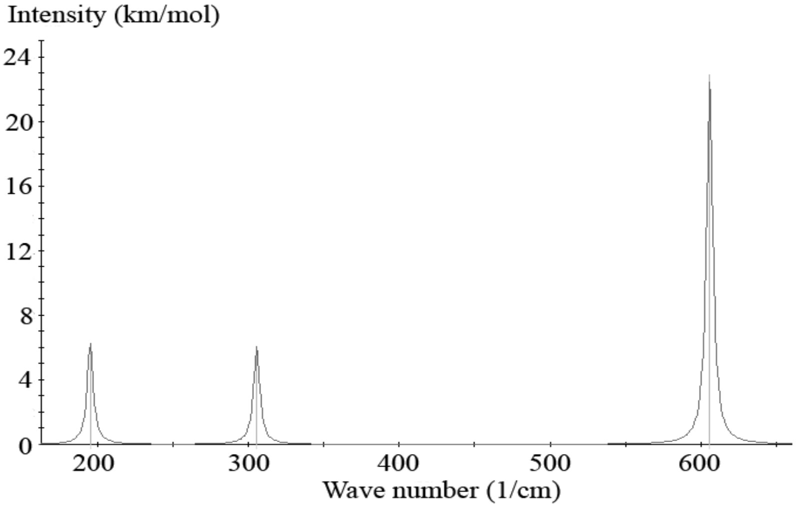

Figure 5.3: The vibrational spectrum of As_2O calculated from the first principles.

(x) As_2O (linear): It found that with O in the centre and two As on both sides to form a straight line is stable. The As - O bond distance is 1.759 Å. There is a doubly degenerate vibration at 233.2 (20.8) cm^{-1} (km/mol) {2} and a singly degenerate oscillation at 981.6 (22.2) cm^{-1} (km/mol).

(xi) As_2O_2 (rectangular): The As-O bond length is 1.871 Å and the angle of the rectangle is 100.5 degrees. There are two strong frequencies at 296.5 (39.7) and 489.7 (48.2) cm^{-1} (km/mol).

(xii) As_2O_2 (pyramidal): In this cluster the As-As distance is 2.348 Å, the O-O distance is 1.952 Å and the As-O distance is 2.157 Å. The vibrational frequencies (intensities) are 328.9 (15.3), 376.3 (1.6), 384.5 (6.3), 573.8 (52.3) and 643.4 (19.5) cm^{-1} (km/mol). The computed vibrational spectrum is shown in Fig.5.4.

(xiii) As_2O_3 (linear): In this system all the atoms are in a straight line with one oxygen atom in the centre and two oxygen atoms at both ends. The end bond length is 1.721 Å and the inner bond length is 1.968 Å. The end correction is thus clearly seen in the structure. This system has the positive vibrational frequencies

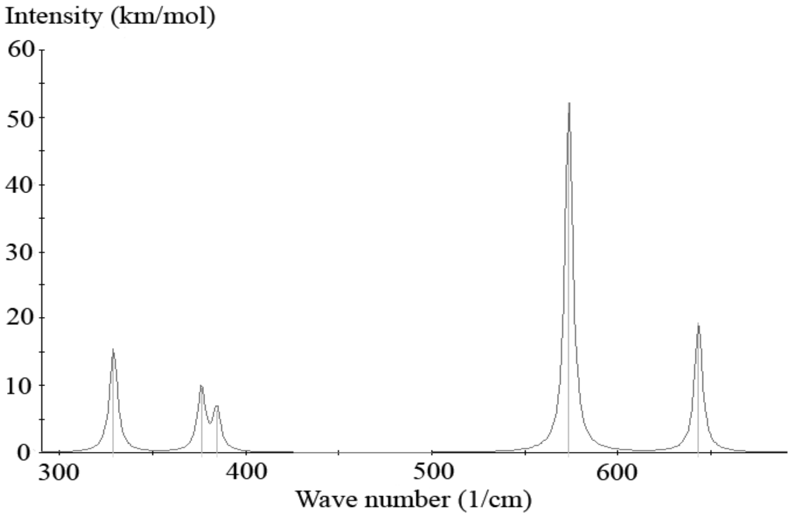

Figure 5.4: The vibrational spectrum of As_2O_2 (pyramidal) calculated from the first principles.

(intensities) {degeneracies} as 31.6 (2.66) {2}, 327.3 (159), 782.4 (240) cm^{-1} (km/mol).

(xiv) As_2O_3 (bipyramidal): In this system, first a triangle is made with three oxygen atoms and then one As is put on top of the triangle and another is put symmetrically on the other side to form a bipyramid. The O-O distance in the triangle is 2.496 Å and the O - As distance is 1.927 Å. There are two strong vibrations at 375.7 (39.7) 2, 561.1 (154), 562.6 (34.9) {2}. The later two are not well resolved.

(xv) As_2O_4 (bipyramid): The square shape contain 4 oxygen atoms has been made with one As atom on the top of the plane square and another symmetrically in the bottom of the square. The O-O distance is 2.260 Å and As-O distance is 2.036 Å. The vibrational frequencies (intensities) {degeneracies} are found to be 138.4 (97.8) {2} and 443.9 (774) {2}.

(xvi) As_3O (triangle): The three As atoms are on the corners of a triangle and one is in the centre. the As-O distance is 1.868 Å. The vibrational frequencies found are 131.8 (4.3), 671.5 (12.3) and 693.9 (10.6) cm^{-1} (km/mol).

(xvii) As_3O (pyramidal): In this model the three As form a triangle with O-O distance of 2.477 Å and one As atom is on top to form a pyramid. The As-O distance is 2.151 Å. The vibrational frequencies (intensities) are 235.9 (0.7), 300.6 (2.95) and 491.5 (17.7) cm^{-1} (km/mol).

(xviii) As_3O_2 (linear): In this cluster all of the five atoms are in a straight line with As on two ends. The bond distance near the ends is 1.753 Å and towards the centre it is 1.919 Å. There are strong oscillations at the frequencies (intensities), 23.9 (0.91) {2}, 238.8 (5.5), 291.6 (44.3) {2} and 760.2 (131).

5.3 Experimental Raman Data

The experimental Raman spectra of vitreous As_2O_3 are reported by Galeener *et al.* [50]. The experimental data shows the frequencies 220 (weak), 342, 485 (weak), 552 (weak), 700 and 850 cm^{-1}. The identification of these bands and comparison with the calculated values is shown in Table 5.1. Apparently all of the experimentally found frequencies can be identified with the help of large number of computed frequencies. It is found that the vitreous state of As_2O_3 is made of several clusters of different valencies. It is possible that the second-order Raman scattering at 2ν is also present in the data but the 6 frequencies experimentally found in the oxide of arsenic are identified as arising from our clusters.

5.4 Conclusions

The first principle calculations of vibrational frequencies in a large number of clusters containing As and O atoms have been performed. The clusters present in the actual sample have been identified by comparing the calculated values with these found in the

Table 5.1: The calculated and measured bands in vitreous As_2O_3 along with their identification.

S.No	Experimental cm^{-1}	Calculated cm^{-1}	Cluster
1	220(weak)	219.8	AsO_2
2	342	335.1	AsO_4 (T_d)
3	485(weak)	489.7	As_2O_2 (rectangular)
4	552(weak)	544.7	AsO_2 (triangle)
5	700	701.8	AsO_3 (pyramidal)
6	850	855.1	AsO_2 (triangle)

data. Therefore, a method to identify new clusters and molecules found in the minerals has been found.

Chapter 6

DFT Determination of Law of Force in Fe and P Clusters of Atoms

The density functional theory has been used to make clusters of atoms of Fe with a few atoms of P and the geometry in each case has been optimized. The vibrational spectra has been determined for each cluster with vary number of P atoms. The largest vibrational frequency has been calculated as a function of number of P atoms. It is found that the force, F = -kx is not linear but shows oscillations. The oscillations arise due to the quantum mechanical orbitals which are solutions of the Schrödinger equation. The law of force between Fe and P atoms for several clusters of atoms are able to determine.

6.1 Introduction

It has recently been pointed that the Cu-O plane become superconductivity upon doping with oxygen [53]. In recent years it is found that adding excess of Co in place Fe in AFe_2As_2 (A = Ba, Sr) neutralizes the magnetic moment of Fe so that for x > 0.25, $SrFe_{2-x}Co_xAs_2$ becomes superconductivity below 20K [54]. As it is, this problem looks quite different from that of B.C.S theory which requires pairing of the electrons in the conduction band. The transition temperature of LaFePO also increase from 5K to 7K upon Ca or F doping [55], which shows the importance of chemical doping to achieve a metallic state which upon cooling becomes superconducting [56]. There is a layer of FeP atoms with FeP_4 tetrahedra which becomes superconducting upon doping. Hence, it is of interest to determine the law of force which birch the iron atoms with phosphorous. In order to investigate this problem, the clusters of Fe and P atoms have been build and the geometrical parameters have been optimized. For the optimized configuration, the vibrational frequencies have been calculated. The largest vibrational frequency has been plotted as a function of number of P atoms, n in the cluster from which it can determine the power law $\omega \propto n^{\alpha}$. In some clusters such as FeP_n, the power law does not occur and the frequency oscillates. In this chapter, the ab initio calculation of the vibrational frequencies of clusters, FeP_n, Fe_2P_n and Fe_3P_n has been reported by using double numeric wave functions with and without spin polarization. It is found that the force, F = -kx is not linear as a function of number of P atoms.

6.2 Clusters (Double Numeric Wavefunctions)

(i) Fe-P (linear) has a bond length of 2.006 Å and a strong stretching vibrational frequency of 507 cm^{-1} when double numeric wave functions has been used in the density-functional theory.

(ii) FeP_2 (ring) shows the bond lengths Fe-P = 2.157 Å , P-P = 2.186 Å and the vibrational frequencies (intensities) are calculated to be 338.8 (4.9), 352.8 (1.94), 539.5 (3.3) cm^{-1}(km/mol).

(iii) FeP_3 (pyramidal) shows Fe-P = 2.268 Å and P-P = 2.385 Å and the frequencies (intensities) of 237.5 (1.9), 311.1 (5.4), 375.3 (5.3), 545.4 (0.18), 883.0 (206) and 921.7 (258) cm^{-1} (km/mol).

(iv) FeP_4 (pyramidal) shows Fe-P bond distance of 2.320 Å and P-P bond length of 2.340 Å. The vibrational frequencies (intensities) {degeneracies} are 269.7 (2.9){2}, 345.0 (6.7){1}, 441.5 (0.03){2} and 494.2 (1.5){1} cm^{-1} (km/mol).

(v) Fe_2P (molecules) shows a bond length of 2.144 Å and the vibrational frequencies (intensities) of 173.2(0.6), 484.8(15.5), 615.5(59) cm^{-1} (km/mol).

(vi) Fe_2P_2 (square) of Fe-P distance 2.160 Å is found. The vibrational frequencies (intensities) calculated are 185.5(8.3), 208.6(0.03), 319.7(24), 495.2(0.1) and 519.7(9.7) cm^{-1} (km/mol).

(vii) Fe_2P_2 (pyramidal). In this system the bond lengths in the optimized configuration are Fe-Fe = 2.125 Å P-P = 2.551 Å Fe-P = 2.230 Å and the vibrational frequencies (intensities) are 102.5(1.9), 259.3(5.8), 287.3(1.3), 375.1(2.0) and 458.2(12.7). It may be noted that Fe_2P_2 stabilizes in the pyramidal forms as well as a square like planar form.

(viii) Fe_2P_3 (bipyramidal). A triangle of P atoms has been made with one Fe on top and another on bottom position. In the optimized configuration, the bond distances are Fe-P = 2.209 Å and P-P = 3.267 Å. The dominant positive frequencies (intensities) {degeneracies} calculated are 237.2(24), 420.8(8){2} cm^{-1} (km/mol).

(ix) Fe_2P_4 (bipyramidal). A square of P_4 atoms has been made and one Fe has been put on top and another on the bottom position. The bond lengths are Fe-P = 2.3264 Å and P-P = 2.589 Å. The frequencies (intensities) {degeneracies} are 40.8(0.9){2}, 255.9(14.7), 366.8(0.5){2} cm^{-1} (km/mol).

(x) Fe_3P (pyramidal). A triangle of Fe atoms has been made with one P atom on top position. In the optimized configuration P-Fe distance is 2.259 Å and Fe-Fe distance is 2.204 Å. The calculated vibrational frequencies (intensities) are 223.7(5.8), 225.1(5), 309.7(0.08) and 507.1(10.3) cm^{-1} (km/mol).

(xi) Fe_3P_2 (bipyramidal). A triangle of Fe atoms has been made with one P atom on the top and another P atom on the bottom of the triangle. The optimized Fe-P bond length is 2.276 Å and P-P distance is 2.288 Å. The vibrational frequencies (intensities) {degeneracies} are 161.3(7){2}, 207(0.2){2}, 273.4(40){3}, 447.8(17) and 466.2(4) cm^{-1} (km/mol).

(xii) Fe_3P_3 (prismatic). A triangle of Fe atoms is put on top of a triangle of P atoms. The various bond lengths are Fe-Fe = 2.227 Å P-P = 2.408 Å and Fe-P = 2.408 Å and Fe-P = 2.303 Å. The vibrational frequencies (intensities) {degeneracies} are 13.2(9.5){2}, 188.7(3.9){2}, 290(4.5){2}, 310.6(2.6), 331.4(2.2), 403.9(3.1){2} and 589.3(2.4). The vibrational spectrum calculated by using DFT (LDA) for this cluster of atoms is given in Fig. 6.1.

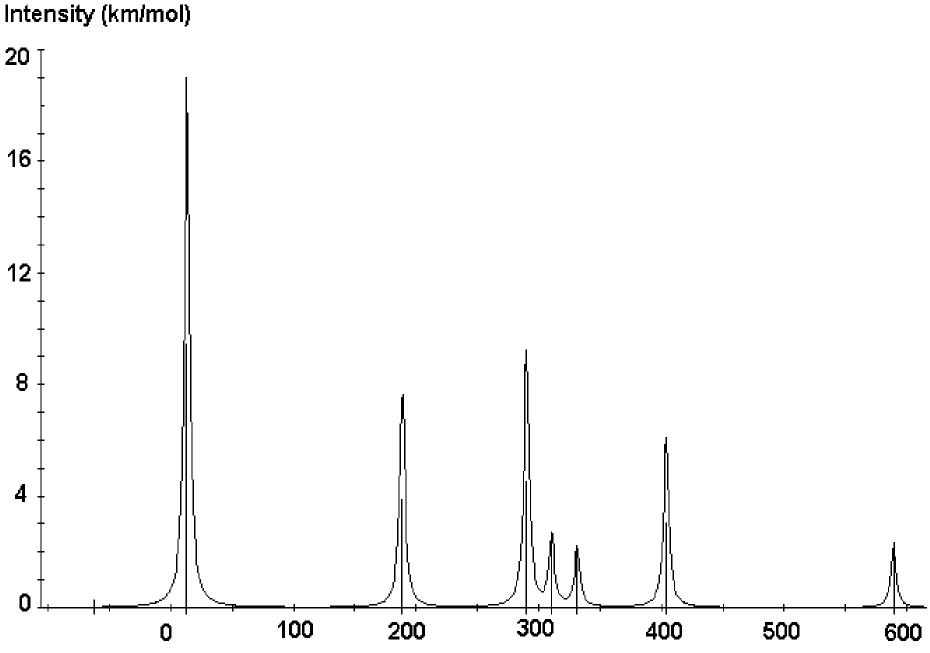

Figure 6.1: The infrared spectrum of Fe_3P_3 calculated from the first principles.

6.3 Clusters (Double Numeric Spin Polarized Wavefunctions)

In the case of magnetic atoms such as Fe, the spin polarization plays an important role. It is possible to add another atom such as Co which by aligning anti-ferromagnetically can neutralize the magnetic moment of Fe. Within a single atom also both spin alignment occur and often spin up does not have the same energy as the spin down electron. In some cases, it is possible that all of the d electrons have spin up only and then they are responsible for a large magnetic moment. The vibrational frequencies are also sensitive to the spin configurations. Therefore, the vibrational frequencies have been calculated by using spin polarized orbitals as given in this section.

(xiii) FeP. The double numeric polarized orbitals used in the density-functional theory by using LDA gave the Fe-P distance equal to 1.942 Å and a single vibrational frequency corresponding to bond stretching of 553.27 cm^{-1}.

(xiv) FeP_2 (triangular). The polarized bond lengths are found to be Fe-P = 2.117 Å and P-P = 2.041 Å and the vibrational frequencies (intensities) are calculated to be 352.8(1.5), 375.4(6.6) and 611.9(2) cm^{-1} (km/mol).

(xv) FeP_3 (triangular). The P_3 atoms form a triangle and one Fe is in the centre of the triangle. The vibrational frequencies (intensities) {degeneracies} calculated by using polarized orbitals are 14.23(1.36){2}, 608.29(6.48){2} cm^{-1} (km/mol).

(xvi) FeP_4 (T_d). In the tetrahedral configuration the polarized bond length is found to be 1.997 Å and the dominant frequencies are 129.07(2.5){3} and 474.3(31){3} cm^{-1} (km/mol).

(xvii) FeP_4 (pyramidal). The four P atoms form a square and one Fe atom is placed on top position. The bond lengths are Fe-P = 2.230 Å and P-P = 2.180 Å. The vibrational frequencies are 255.7(6.85){2}, 353.1(6.2), 430.3(2){2} and 512.8(4.8) cm^{-1} (km/mol).

(xviii) Fe_2P_2 (square). The bond length using the polarized orbitals is found to be 2.110 Å. The frequencies (intensities) are 141.1(7.8), 331.95(28) and 476.53(28) cm^{-1} (km/mol).

(xix) Fe_2P_2 (pyramidal). The polarized bond lengths are Fe-P = 2.246 Å, P-P = 2.159 Å and Fe-Fe = 2.099 Å. The vibrational frequencies (intensities) are 156.2(1.96), 291.4(1.8), 385.7(4.1), 411.7(103) and 461.5(7.5) cm^{-1} (km/mol).

(xx) Fe_2P_3 (bipyramidal). There is a triangle of P atoms and then Fe atoms are placed one on top position and the other on bottom position. The polarized Fe-P distance is 2.112 Å and P-P distance is 2.506 Å. The calculated vibrational frequencies (intensities) are 327.05(0.01), 342.4(7.4){2}, 431.8(21) cm^{-1} (km/mol).

(xxi) Fe_2P_4 (bipyramidal). There is a square of P atoms and two Fe atoms are placed one on top position and other on bottom position. The polarized bond lengths are Fe-P = 2.201 Å and P-P = 2.492 Å. The dominant frequencies (intensities){degeneracies} are 342.5(13.9), 404(4.68){2} cm^{-1} (km/mol).

6.4 Frequency Doping

From the *ab initio* computational work, the variation of the largest vibrational frequency are able to extract as a function of number of P atoms. Fig. 6.2 showed the variation of the largest frequency as a function of n for FeP_n for double numeric wave functions and in Fig. 6.3 for Fe_2P_n found for polarized wave functions. It is found that the frequency as a function of P atoms oscillates but for small doping (n<3) power law behavior is possible, $\omega \approx n^{\alpha}$.

The frequemcy of a harmonic oscillator is given by $\omega = \sqrt{\frac{k}{m}}$ where k is a force constant and m is the mass of the oscillator. Hence, the frequency of oscillations is proportional to the $m^{-\frac{1}{2}}$. This is a power law for two atoms. In the case of molecules more atoms may oscillates as in normal modes of oscillations. Hence, the variation of frequency as a function of mass in complex clusters of atoms has been calculated. Hence, the calculations of frequency as a function of number of phosphorous atoms has been performed by using the DFT quantum mechanical code. The force is $\mathbf{F} = -k\mathbf{x}$ in one dimension which can become a matrix form for more complicated molecules and clusters of atoms. Hence, the calculation of frequency which implies the force constant is important.

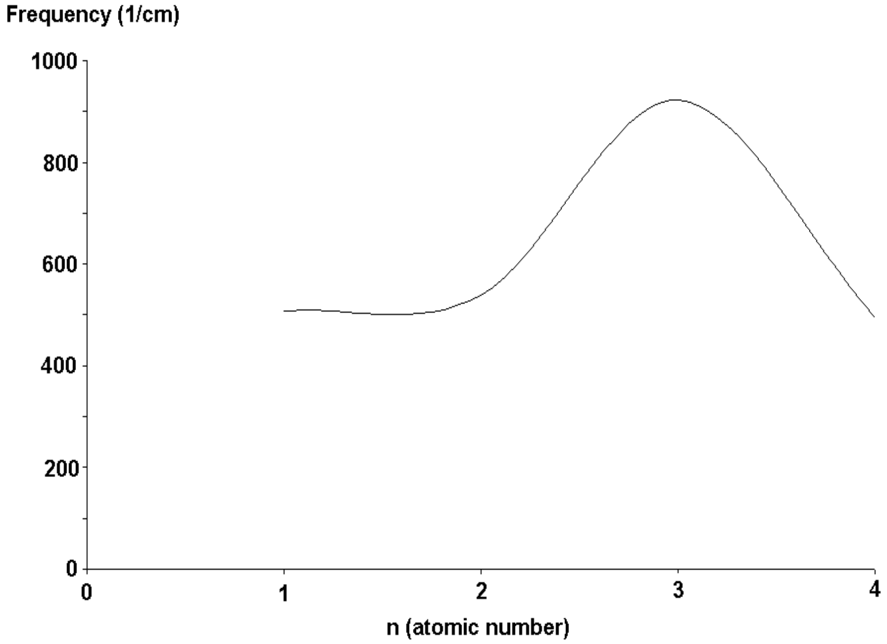

Figure 6.2: The oscillation of largest vibrational frequency of FeP$_n$ as a function of n.

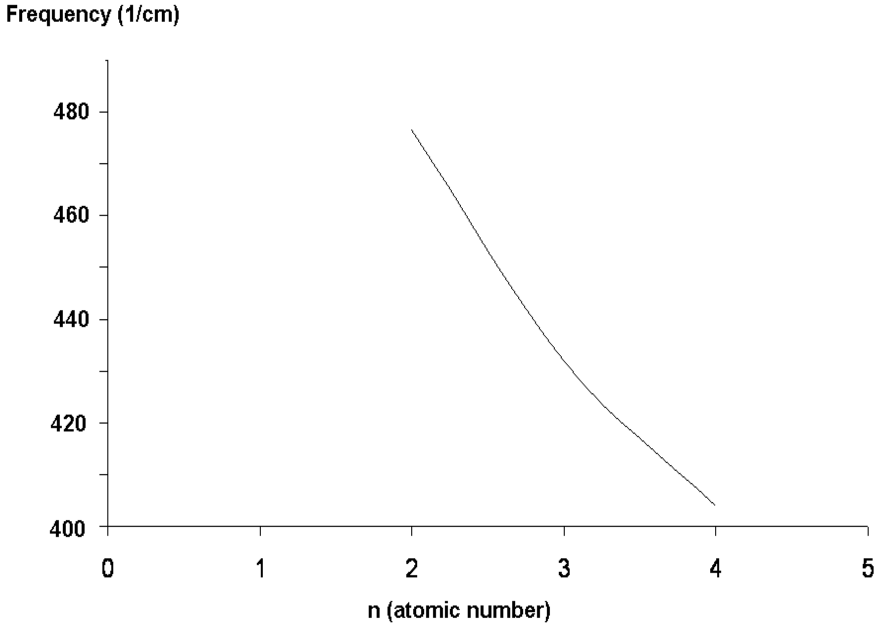

Figure 6.3: The variation of largest frequency of Fe_2P_n as a function of n calculated by using polarized orbitals.

6.5 Conclusions

LaFePO is one of the fewest of the recently discovered materials. It becomes superconducting upon doping with Ca or F. It has unusual magnetization as a function of magnetic field. Hence it is important to learn the law of force which exists between Fe and P atoms. It found that in FeP_n the law of force is not linear but in Fe_2P_n for small n, a power law is possible. According to the law of force, F = -kx = -n ω^2x, the frequency is a constant. It found that ω oscillates upon doping Fe atoms with phosphorous.

Chapter 7

DFT Calculation of Vibrational Frequencies in Clusters of Fe and As Atoms

The density-functional theory (DFT) is used to simulate clusters of the formula Fe_mAs_n. The bond lengths and angles has been optimized to determine the stable structure for integer values of m and n. The vibrational frequencies have been calculated for all of the clusters and hence determine the largest frequency each cluster as a function of number of As atoms. For $FeAs_n$, it found that the lowest frequency of 220.5 cm^{-1} occurs for n = 1. As n increase the frequency shows a maximum. In Fe_2As_n, Fe_3As_n and Fe_4As_n, the largest frequency shows oscillations as a function of n.

7.1 Introduction

Recently, it has been reported that compounds containing FeAs atoms become superconducting upon doping [57, 58]. Usually, the compounds containing Fe atoms will not be superconducting or even if they superconduct, their transition temperatures are expected to be very small. The field inside a superconductor is zero and they exhibit perfect diamagnetism. The presence of a large magnetic moment of Fe is not commensurate with perfect diamagnetism. Usually there are two critical fields. Above the lower critical field there are vortices of magnetic lines forces so that it is called a type-II superconductor. The present materials of FeAs doped with electrons or holes are neither type-I nor type-II superconductor. They are a class themselves. The field inside a superconductor is given by H + 4πm which is zero so that the susceptibility is x = -1/4π. In the FeAs doped superconductors the value of -1/4π is not obtained. The transition temperature of a superconductor depends on the phonon frequency. Hence, investigation of phonon frequencies in these materials may help in the understanding of the transition temperature.

In this chapter, the density-functional theory has been used to stimulate clusters of Fe and As atoms and determine their vibrational frequencies. The largest vibrational frequency of a cluster of Fe_mAs_n atoms has been determines so that the largest frequency as a function of As atoms can be find and calculate its variation as a function of number of As atoms. It found that such a vibrational frequency oscillates as a function of As atoms indicating the presence of oscillations in the force which determines the transition temperature of the superconductor.

7.2 Clusters

The density-functional theory has been used to optimize the structures in the local-density approximation (LDA). The vibrational frequencies are determined for the optimized clusters. The double numeric wave functions are used in all of the calculations.

(i) FeAs. The cluster of Fe-As as a diatomic molecule has been made. It has a bond length of 2.379 Å and a single vibrational frequency corresponding to bond stretching. The calculated frequency is 220.5 cm^{-1}.

(ii) $FeAs_2$ (linear). In this case the optimized bond length is 2.394 Å and the vibrational frequencies (intensities) {degeneracies} are 14.97 (1.96) {2}, 266.18 (0.01).

(iii) $FeAs_2$ (triangular). In this cluster the Fe-As distance is 2.248 Å and As-As distance is 2.365 Å. The vibrational frequencies are 236.29 (1.69), 247.28 (1.16) and 358.68 (2.61) cm^{-1} (km/mol). The spectrum calculated from the first principles is shown in Fig. 7.1.

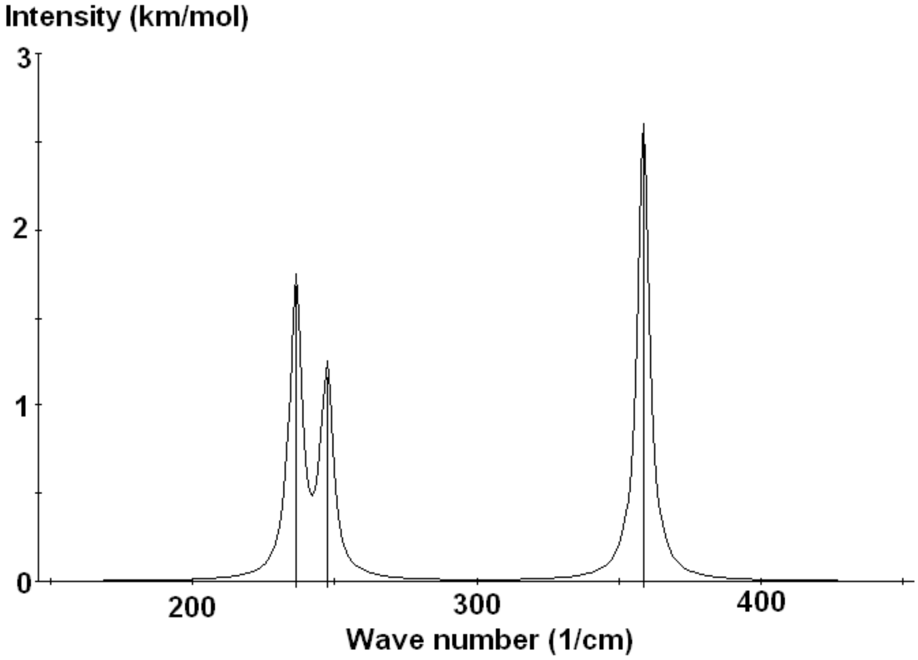

Figure 7.1: The vibrational spectrum of $FeAs_2$ triagonal with DN wave function.

(iv) $FeAs_3$ (triangular). This is a triangular molecule with one Fe atom in the centre of the triangle. The Fe-As distance is 2.081 Å and the vibrational frequencies (intensities) are 282.6 (0.01), 490.7 (1.02) and 491.78 (1.05) cm^{-1} (km/mol).

(v) $FeAs_3$ (pyramidal). The three As atoms form a triangle and one Fe sits on top position. The As-As distance is 2.596 Å and the Fe-Fe distance is 2.336 Å. The vibrational frequencies found are 124.74 (0.02), 134.15 (0.1), 189.04 (3.98), 214.56 (2.47), 216.13 (2.18) and 350.08 (0.95) cm^{-1} (km/mol). The calculated vibrational spectrum is shown in Fig. 7.2.

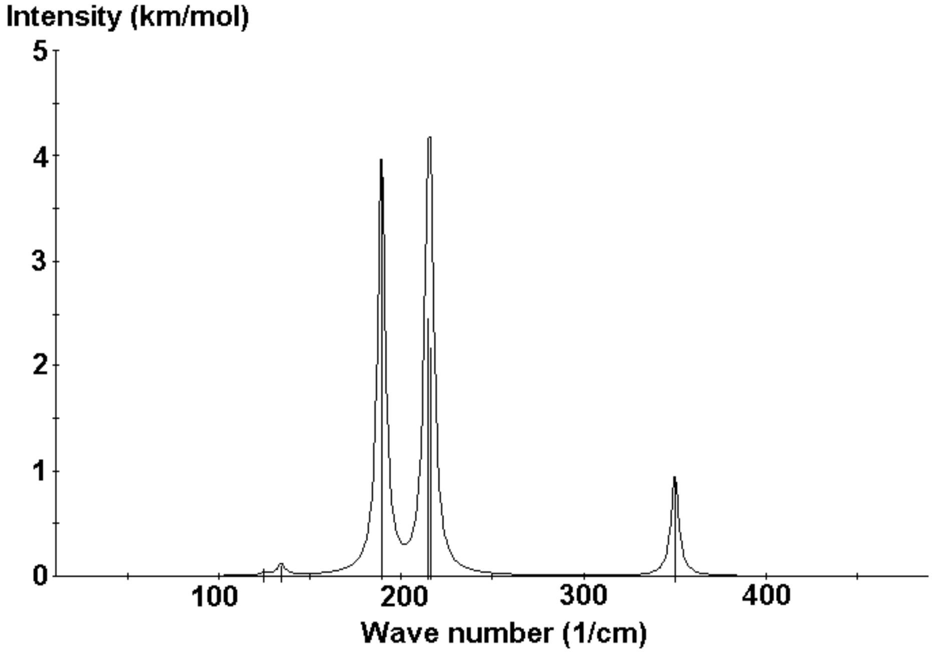

Figure 7.2: The vibrational spectrum of $FeAs_3$ pyramidal calculated from the first principles.

(vi) $FeAs_4$. In this cluster, the four As atoms sit on the four corners of a square and one Fe atom at the centre of the square. The Fe-As bond length is 2.164 Å and the vibrational frequencies are 87.98 (1.16) and 261.16 (9.63) cm^{-1} (km/mol).

(vii) $FeAs_4$ (T_d). In the tetrahedral arrangement of atoms, the bond length is 2.394 Å and the vibrational frequencies are 27.57 (0.03) {3}, 226.06 (0.01) {3}.

(viii) $FeAs_4$ (pyramidal). The four As atoms form a square with As-As distance of 2.504 Å and Fe-As distance of 2.400 Å. The calculated vibrational frequencies are 187.38 (3.43){2}, 230.57 (0.53), 239.29 (2.39){2} and 308.79 (3.59) cm^{-1} (km/mol). The vibrational spectrum calculated from the first principles is shown in Fig. 7.3.

In the clusters of $FeAs_n$ (n = 1 - 4) it is observed that largest frequency occurs for n = 3. Hence, the plot of the largest frequency as a function of n not linear but peaked

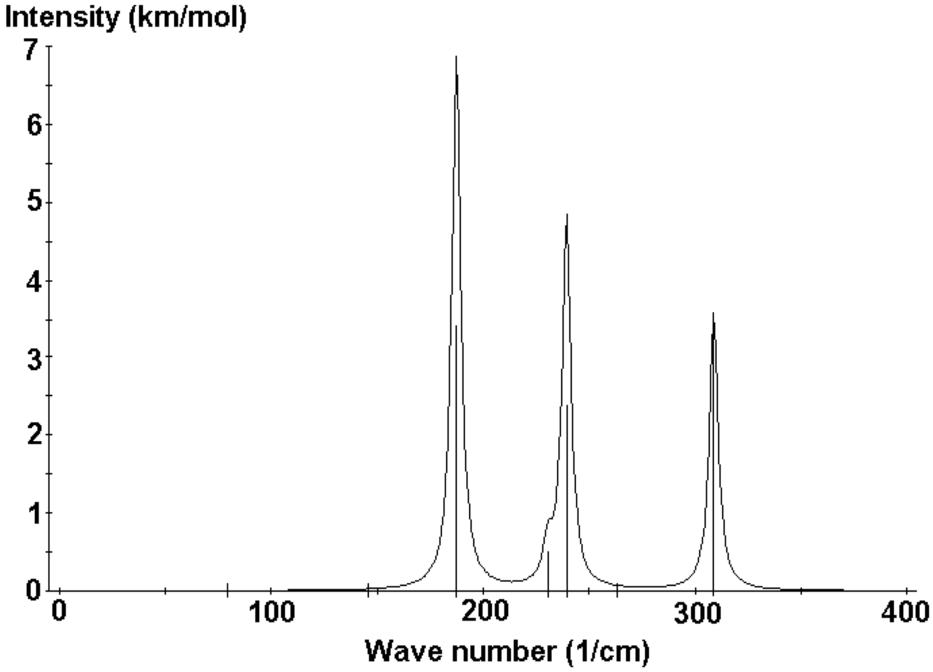

Figure 7.3: The vibrational spectrum of $FeAs_4$ pyramidal with DN wave function.

at $n = 3$. Since the vibrational frequencies are related to the force constant $\omega = \sqrt{\frac{k}{m}}$, the force constant oscillates as a function of concentration of As. Now, the vibrational frequencies of clusters containing two atoms of Fe have been calculated and shown below.

(ix) Fe_2As (linear). In this case, the Fe-As bond length is 2.374 Å and the vibrational frequency is 263.99 cm^{-1}.

(x) Fe_2As_2 (triangular). In this molecule, Fe-Fe distance is 2.461 Å and Fe-As distance is 2.438 Å. The vibrational frequencies are 259.4 (0.25) and 232.04 (0.63) cm^{-1} (km/mol).

(xi) Fe_2As_2 (rectangular). The Fe-As bond length is 2.249 Å and the vibrational frequencies are 101.12 (4.28), 238.92 (8.7), 361.5 (10.5).

(xii) Fe_2As_3 (bipyramidal). The three As atoms form a triangle and two Fe atoms sit on each side of the triangle. The As-As distance is 3.413 Å and Fe-As distance is 2.291 Å. The vibrational frequencies (intensities) degeneracies are 38.2 (0.42){2}, 197.08 (0.01), 202.39 (11.5) and 316.4 (2.8) {2}.

(xiii) Fe_2As_4 (bipyramidal). The As atoms form a square and two Fe atoms sit on top and bottom positions. The As-As distance is 2.822 Å and Fe-As distance is 2.354 Å. The calculated vibrational frequencies are 77.04 (0.71) {2}, 241.68 (5.28) and 293.36 (2.4) {2}. The vibrational spectrum calculated from the first principle is shown in Fig. 7.4.

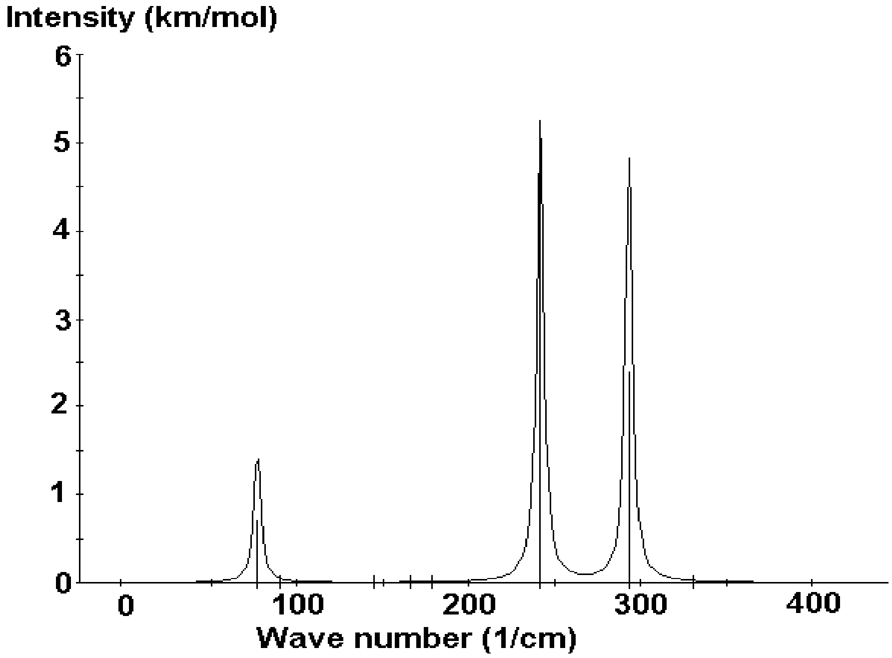

Figure 7.4: The vibrational spectrum of Fe_2As_4 bypyramid calculated from the first principles.

7.3 Results

From the above calculations, the largest vibrational frequency oscillates as a function of number of As atoms in $FeAs_n$ and Fe_2As_n has been found. The oscillations vibrational frequencies indicate oscillations in the transitions temperature of a superconductor upon doping. Usually, the B.C.S. theory of superconductivity series upon the electron-phonon interaction in the conduction band where the strength depends on the translational symmetry [56, 59]. In the present case, the superconductivity arises upon doping which lacks in translational symmetry. Hence, the phonon-induced B.C.S. theory is not taken into account but the chances that theory showed will be based on doping.

Chapter 8

DFT Calculations of Vibrational Frequencies of Carbon-Nitrogen Clusters: Raman Spectra of Carbon Nitrides

8.1 Introduction

Diamond is the hardest of the materials known. The cubic boron nitride is also known to be a hard material [60, 61]. It is expected that carbon nitride C_3N_4 should also be a very hand material [62]. There is a lot of effort to make the carbon nitrides and obtain their Raman spectra but the reaction products are difficult to isolate. Many different structures are formed which contribute to the Raman spectra. Hence, it is a difficult task to identify the clusters present in the material. The infrared and Raman spectra of amorphous carbon nitrides have been reported by Ferrari *et al.* [63]. Cote and Cohen [64] have shown that the sp^2 bonding is favourable to sp^3 bonding which implies that rhombohedral phase is more stable than the zinc-blende and rocksalt phases. The x-ray absorption and photoemission of carbon nitrides has been discussed by Zheng *et al.* [65]. The p bonding in hard films is discussed by Jimenez *et al.* [66]. The six-fold ring structure is given by Abrasonis *et al.* [67]. The ab initio calculations of Merchant *et al.* [68] show the effect of the electronic configurations on the density of the clusters. The carbon nitrides also occur in graphitic structures, the stability of which has been discussed by Lowther [69].

This chapter report the calculation of vibrational frequencies of clusters containing carbon and nitrogen atoms. The structural parameters as well as vibrational frequencies have been reported and these calculated values have been compared with those measured by the Raman spectra of amorphous carbon nitrides. The density-functional theory in the local-density approximation (DFT-LDA) has been used. The experience with this type of calculations shows that the calculated values should be very close to the experimental values [25, 27, 32]. The vibrational frequencies of Ge based glasses as well as those of AsSe clusters are indeed in agreement with the experimental data [70].

8.2 The Methodology

The density-functional theory is used to obtain the solution of the Schrödinger equation. The electron density is used to differentiate the Schrödinger equation so that Kohn-Sham equations are obtained [4, 5]. These equations are solved in the local-density approximation (LDA). It is also possible to obtain the result in the generalized gradient approximation (GGA) but these results are very close to that of LDA . Hence, it is not necessary to obtain the results in both approximations. Two programs are available for this purpose. The Amsterdam density-functional theory (ADF) uses the double zeta wave functions. The DMol^3 package of Accelerys Software Inc, San Diego, California also uses a variety of wave functions out of which the double numeric (DN) wave function works the best. Hence, the DMol^3 with double numeric wave functions has been used. The calculation of vibrational frequencies is also explained by Lopez-Duran *et al.* [71].

All possible clusters starting from the simplest one which has only two atoms have been made. For this cluster, the electronic energy is calculated as a function of distance between atoms. The calculation stops when the energy is a minimum and the distance between atoms is noted. The minimum energy configuration is considered to be stable. For distances, other than those for which the energy is a minimum are considered to be instable and discarded. In a second step, the vibrational frequencies are calculated for the stable structures. The electronic energy calculation is used to optimize the structure and then the vibrational frequencies are calculated. Naturally the electronic energy is held constant to calculate the vibrational frequencies which are independent of the electronic energy. The number of atoms has been increased by one, considering all of the possibilities such as CN_2 and C_2N. The optimization of the electronic energy determines the structure and the vibrational frequencies are always obtained for the optimized structure. Various clusters of atoms have been build until the number of atoms in a cluster becomes eight. The experimental Raman frequencies indicate that the number of atoms in a cluster of atoms is quite small. When the number of atoms becomes large, none of the calculated frequencies correspond to the experimental data. This is because the large number of atoms require large distances which reduces the Coulomb interactions as 1/r. Hence most of the experimental data uses only small molecules. In large molecules also, the vibrations corresponds to nearest neighbors only or to atoms confined within a unit cell. All of the possible clusters have been built and only the stable ones have been retained. These all possible configurations are also obtained with due consideration of the symmetries. Usually, the stable structures are symmetric. The large asymmetric structures tend to be instable. The accuracy of the calculation has been set to much less than 1 cm^{-1} such as 10^{-5} cm^{-1} but only one digit after the decimal point is retained for tabulation.

8.3 Carbon-Nitrogen Clusters.

(i) CN. The diatomic molecule CN has been optimized for the minimum energy of the Schrödinger equation. This calculation gives the CN bond length of 1.187 Å and the vibrational frequency is calculated to be 2049.8 cm^{-1}.

(ii) CN_2 (linear). In this molecule, the carbon atom is kept in the centre and two nitrogen atoms are located on each side of C so that N - C - N are aligned in a straight line. The bond length is found to be 1.245 Å. The calculated vibrational frequencies (intensities){degeneracies} are 407.3 (19.3) {2}, 1571.1 (90.2) cm^{-1} (km/mol).

(iii) CN_3 (triangular). In this cluster, three atoms of N sit on three corners of a triangle and C sits in the centre of the triangle. The CN bond length is found to be 1.370 Å and the vibrational frequencies are given in Table 8.1.

(iv) CN_3 (pyramidal). The three N atoms form a triangle and one C atom sits on top position. The N - N bond length is 1.645 Å and CN bond distance is 1.458 Å. The calculated vibrational frequencies are given in Table 8.1.

(v) CN_4 (pyramidal). The four N atoms form a square and one C atom sits on the top position. The CN bond length is 1.777 Å and N - N bond distance is 1.477 Å. The calculated frequencies are given in Table 8.1.

(vi) CN_4 (square). The four N atoms are on the corners of a square and one C is located in the centre of the square. The CN bond length is 1.419 Å and the vibrational frequencies are given in Table 8.1.

(vii) CN_4 (T_d). In the tetrahedral coordination the bond length is 1.390 Å and the frequencies are given in Table 8.1.

Table 8.1: The vibrational frequencies of various clusters calculated from the first principles

S.No.	Cluster	Frequency (cm^{-1})	Intensity (km/mol)	Degeneracy
1	CN_3 (triangular)	509.6	8.0	2
2	CN_3 (triangular)	587.2	12.8	1
3	CN_3 (triangular)	932.5	65.5	2
4	CN_3 (pyramidal)	561.2	1.2	2
5	CN_3 (pyramidal)	901.0	2.2	2
6	CN_3 (pyramidal)	1257.5	1.8	1
7	CN_4 (pyramidal)	736.1	1.7	2
8	CN_4 (pyramidal)	779.3	101.2	1
9	CN_4 (pyramidal)	988.7	3.7	1
10	CN_4 (square)	280.2	11.1	1
11	CN_4 (square)	781.7	23.7	2
12	CN_4 (T_d)	130.2	1.0	3
13	CN_4 (T_d)	4420.9	5.0	3

(viii) C_2N (linear). The C_2N is linear with one N in the centre. The C - N bond length is 1.264 Å. The vibrational frequencies are given in Table 8.2.

(ix) C_2N (triangular). In this cluster the CN distance is 1.340 Å and the N - N distance is 1.615 Å. The vibrational frequencies for this configuration are given in Table 8.2.

(x) C_2N_2 (rectangular). The atoms are alternately arranged with the bond length 1.414 Å. The vibrational frequencies are given in Table 8.2.

(xi) C_2N_3 (bipyramid). The three N atoms form a triangle and one C atom sits on the top position and another C in the bottom position. The C - N bond length is 1.498 Å and the N - N bond length is 2.163 Å. The calculated vibrational frequencies are given in Table 8.2.

(xii) C_2N_3 (linear). This is a linear molecule with N atoms at the centre and the ends. The CN bond length near the end is 1.207 Å and towards the centre is 1.250

Å. The vibrational frequencies are given in Table 8.2. The frequency of 1544 cm^{-1} found in C_2N_3 (linear) is very close to the value 1512.3 cm^{-1} found in the C_2N (linear) showing that this value is characteristic of linear property of the molecule. In the amorphous structure such a linear frequency can be interpreted to be a back bone which gives strength or hardness to the glassy sample.

(xiii) C_2N_4 (bipyramid). The four nitrogen atoms form a square and one C is located on top and the other on bottom position. The CN bond length is 1.784 Å and C - N bond length is 1.753 Å. The calculated frequencies are given in Table 8.2.

Table 8.2: The vibrational frequencies of various clusters calculated from the first principles

S.No.	Cluster	Frequency (cm^{-1})	Intensity (km/mol)	Degeneracy
1	C_2N (linear)	237.7	6.8	2
2	C_2N (linear)	1512.3	89.5	1
3	C_2N (triangular)	474.2	2.6	1
4	C_2N (triangular)	616.0	68.7	1
5	C_2N (triangular)	1436.4	45.3	1
6	C_2N_2 (rectangular)	409.1	13.5	1
7	C_2N_2 (rectangular)	582.3	19.0	1
8	C_2N_2 (rectangular)	1296.4	44.9	1
9	C_2N_3 (bipyramidal)	481.7	26.0	1
10	C_2N_3 (bipyramidal)	852.7	0.3	2
11	C_2N_3 (linear)	100.1	2.36	2
12	C_2N_3 (linear)	458.5	34.7	2
13	C_2N_3 (linear)	1544.4	13.3	1
14	C_2N_3 (linear)	2004.9	1.8	1
15	C_2N_4 (bipyramidal)	474.3	10.8	2
16	C_2N_4 (bipyramidal)	641.3	136.1	1

(xiv) C_3N (pyramidal). The three C atoms form a triangle with CN bond distance 1.638 Å and C - C bond length is 1.467 Å. The calculated values of the frequencies are given in Table 8.3.

(xv) C_3N (triangular). The three C atoms form a triangle and one N sits on the centre. In this case the C - N bond length is 1.395 Å. The calculated vibrational frequencies are given in Table 8.3.

(xvi) C_3N_2 (bipyramidal). The three C atoms form a triangle and one N is on top position and the other in the bottom position. The C - N distance is 1.543 Å and the N - N distance is 1.893 Å. The various vibrational frequencies calculated from the first principles are given in Table 8.3.

(xvii) C_3N_2 (linear). This is a linear molecule with carbon atoms at the ends and one C at the centre. The bond length at the end point is 1.241 Å and near the centre it is 1.252 Å. There is a strong vibration at 293.4 cm^{-1} which is doubly degenerate and there is vibration at 1473.1 cm^{-1} which is characteristic of linear "back bone". The calculated frequencies are given in Table 8.3.

(xviii) C_3N_3 (ring). This is a hexagonal ring with alternate sites occupied by C and N atoms with unusual resonating bond. The vibrational frequencies are given in Table 8.3.

(xix) C_3N_4 (linear). This is a linear molecule with N atoms at the ends. The bond lengths are smallest at the ends and largest near the centre. The bonds near the ends are 1.184 Å long while at the centre it is 1.205 Å. The middle bond has a length of 1.284 Å. In this way there is expansion of the bond near the centre. The calculated vibrational frequencies are given in Table 8.4.

(xx) C_4N (T_d). This is a tetrahedral molecule with CN bond length of 1.1469 Å. The calculated vibrational frequencies are given in Table 8.4.

(xxi) C_4N (square). The C atoms are located at the corners of a square and N is at the centre. The CN bond length is 1.447 Å. The strong vibrational frequencies are given in Table 8.4.

Table 8.3: The vibrational frequencies calculated from the first principles.

S.No.	Cluster	Frequency (cm^{-1})	Intensity (km/mol)	Degeneracy
1	C_3N (pyramidal)	309.0	142.0	2
2	C_3N (pyramidal)	582.0	24.0	1
3	C_3N (pyramidal)	1087.4	96.9	1
4	C_3N (triangular)	168.4	0.15	2
5	C_3N (triangular)	240.5	18.8	1
6	C_3N (triangular)	775.1	4.0	2
7	C_3N_2 (bipyramidal)	45.6	2.8	2
8	C_3N_2 (bipyramidal)	738.9	26.6	2
9	C_3N_2 (bipyramidal)	879.2	3.3	1
10	C_3N_2 (linear)	293.4	2.5	2
11	C_3N_2 (linear)	1473.1	0.04	1
12	C_3N_2 (linear)	1976.7	48.1	1
13	C_3N_3 (ring)	443.8	0.02	2
14	C_3N_3 (ring)	634.3	3.89	1
15	C_3N_3 (ring)	944.5	127.6	2
16	C_3N_3 (ring)	1041.1	180.8	2

Table 8.4: The vibrational frequencies calculated from the first principles.

S.No.	Cluster	Frequency (cm^{-1})	Intensity (km/mol)	Degeneracy
1	C_3N_4 (linear)	71.9	3.6	2
2	C_3N_4 (linear)	437.4	52.9	2
3	C_3N_4 (linear)	470.2	12.8	2
4	C_3N_4 (linear)	1100.2	1.4	1
5	C_3N_4 (linear)	2223.4	45.1	1
6	C_3N_4 (linear)	2529.6	2500.3	1
7	C_4N (T_d)	468.2	31.8	1
8	C_4N (T_d)	487.3	37.3	1
9	C_4N (T_d)	500.6	41.4	1
10	C_4N (square)	534.1	0.3	1
11	C_4N (square)	889.2	58.8	1

(xxii) C_4N (pyramidal). The four C atoms form a square and one N is on the top position. The C-C bond length is 1.502 Å and the CN bond distance is 1.718 Å. The calculated vibrational frequencies are given in Table 8.5.

(xxiii) C_4N_2 (bipyramidal). The four C atoms form a square with C - C distance 1.803 Å and there are two N atoms one on top position and the other on the bottom position with C - N distance 1.690 Å. The calculated vibrational frequencies are given in Table 8.5.

(xxiv) C_4N_2 (dumb bell). The two N atoms form a N - N bond with bond length 1.238 Å. Then 2 C atoms are attached to each N so it becomes C_2N - NC_2. The CN bond length is 1.441 Å. The vibrational frequencies calculated for this molecule are given in Table 8.5.

Table 8.5: The vibrational frequencies calculated from the first principles for several clusters of atoms.

S.No.	Cluster	Frequency (cm^{-1})	Intensity (km/mol)	Degeneracy
1	C_4N (pyramidal)	298.8	5.8	2
2	C_4N (pyramidal)	784.0	28.7	2
3	C_4N (pyramidal)	791.5	0.04	1
4	C_4N (pyramidal)	1121.3	0.29	1
5	C_4N_2 (bipyramidal)	567.0	1.0	1
6	C_4N_2 (bipyramidal)	667.3	150.5	1
7	C_4N_2 (dumb bell)	166.7	6.8	1
8	C_4N_2 (dumb bell)	192.8	7.3	1
9	C_4N_2 (dumb bell)	456.8	0.4	1
10	C_4N_2 (dumb bell)	461.1	0.4	1
11	C_4N_2 (dumb bell)	734.2	0.8	1
12	C_4N_2 (dumb bell)	743.7	0.7	1
13	C_4N_2 (dumb bell)	882.8	0.01	1
14	C_4N_2 (dumb bell)	962.2	10.27	1
15	C_4N_2 (dumb bell)	1270.5	0.12	1
16	C_4N_2 (dumb bell)	1640.2	0.05	1

(xxv) C_4N_4 (ring). There are 4 N and 4 C atoms alternately to form a ring. The CN bond length is 1.256 Å. All of the calculated frequencies are given in Table 8.6.

Table 8.6: The vibrational frequencies calculated from the first principles for several clusters of atoms.

S.No.	Cluster	Frequency (cm^{-1})	Intensity (km/mol)	Degeneracy
1	C_4N_4 (ring)	136.9	5.5	1
2	C_4N_4 (ring)	167.7	4.4	1
3	C_4N_4 (ring)	210.6	0.02	1
4	C_4N_4 (ring)	232.7	0.02	1
5	C_4N_4 (ring)	394.1	3.6	2
6	C_4N_4 (ring)	475.3	0.6	2
7	C_4N_4 (ring)	489.5	0.05	2
8	C_4N_4 (ring)	585.1	93.8	1
9	C_4N_4 (ring)	778.4	0.2	1
10	C_4N_4 (ring)	921.9	0.9	1
11	C_4N_4 (ring)	1005.2	114.9	1
12	C_4N_4 (ring)	1121.8	162.6	1
13	C_4N_4 (ring)	1361.7	20.7	1
14	C_4N_4 (ring)	1419.2	0.01	1
15	C_4N_4 (ring)	1445.9	103.0	1
16	C_4N_4 (ring)	1951.1	164.6	1

(xxvi) C_4N_4 (cube). All of the atoms are arranged on the eight corners of a cube alternately. The C - N bond length is 1.549 Å. There are only two oscillations, each triply degenerate. These frequencies are 661.5 cm^{-1} and 854.6 cm^{-1} as given in Table 8.7.

(xxvii) C_3N_4 (distorted cube). In this model 4 atoms, 2 C and 2 N are first arranged in a square and then 2 N atoms are put below the 2 C atoms and one C atom is put below one N atom so that the 7 atoms are arranged as if one atom is missing from the cube of 8 sites. The CN bonds are of two lengths one 1.461 Å and another 1.488 Å. One of the N atoms is connected to all of the 3 C atoms so its bond length becomes bigger. Larger coordination thus increases the bond length and the end N has smaller bond. The vibrational frequencies of this model are given in Table 8.7.

Table 8.7: The vibrational frequencies calculated from the first principles.

S.No.	Cluster	Frequency (cm^{-1})	Intensity (km/mol)	Degeneracy
1	C_4N_4 (cubic)	661.5	14.7	3
2	C_4N_4 (cubic)	854.6	24.7	3
3	C_3N_4 (distorted cube)	488.8	4.8	1
4	C_3N_4 (distorted cube)	518.3	3.1	2
5	C_3N_4 (distorted cube)	612.6	0.2	2
6	C_3N_4 (distorted cube)	681.8	1.3	1
7	C_3N_4 (distorted cube)	719.5	10.0	2
8	C_3N_4 (distorted cube)	863.5	3.0	2
9	C_3N_4 (distorted cube)	994.9	0.2	2
10	C_3N_4 (distorted cube)	995.7	3.0	1
11	C_3N_4 (distorted cube)	1012.3	27.0	1

8.4 Experimental data

The experimental Raman spectra of amorphous carbon nitrides have been published by Ferrari *et al.* [63]. For the excitation frequency of 514.5 nm, there is a shoulder near 1380 cm^{-1} and a strong peak near 1560 cm^{-1}. The spectra depend on the excitation. Another small peak appears at 720 cm^{-1} when excitation is at 244 nm. Hence, the Raman frequencies found experimentally are 720 cm^{-1}, 1380 cm^{-1}, 1560 cm^{-1}, 1580 cm^{-1} and 2260 cm^{-1}. When the excitation frequency is 514.5 nm sputtered material gives 760 cm^{-1}, 1380 cm^{-1} and 2230 cm^{-1}. The experimental values along with those calculated in the present calculation showed in Table 8.8. It is clear that many different clusters are found in the amorphous material. The fact that at least three frequencies are assigned to linear molecules, shows the existence of “back bone” type structure which gives the strength to the glassy state.

Actually, all of the calculated values should be identified in the experimental data. However, the infrared spectra are usually noisy and poorly resolved. It requires to

Table 8.8: Identification of clusters by comparison of measured frequency values with those calculated

S.No.	Experimental (cm^{-1})	Calculated (cm^{-1})	Cluster
1	720	719.5	C_3N_4 (distorted cube)
2	1380	1361.7	C_4N_4 (ring)
3	1560	1571.1	CN_2 (linear)
4	1580	1571.1	CN_2 (linear)
5	2220	2223.4	C_3N_4 (linear)

All frequencies which are Raman active have not been included because of the poor resolution in the observed Raman spectra

use a large number of lines to simulate the observed infrared. Since, the number of vibrational frequencies is large, the resolution in the infrared is wiped out and the structure is masked due to large line widths. In the case of Raman spectra also all of the Raman active modes are not resolved due to poor resolution in the experimental spectra. Hence only sharp lines are noted and broad lines are left out.

8.5 Discussions

An effort is made to show all of the clusters by stick-ball models in Figs. 8.1, 8.2, 8.3. It makes it easy to visualize the models. However, it may be noted that when all of the variety of clusters are present, the material will become amorphous and will not exhibit the periodic boundary conditions. Since the clusters have varying sizes and shapes, they do not form a single crystal. The zero-intensity lines has not been described. The intensity coordinate is in arbitrary units which is described as km/mol. It fixes the relative intensities very accurately. As an example, CN_2 shows three frequencies, not 4. One frequency is due to the uniform stretching or contracting the full length of NCN. The CN bond frequency is doubly degenerate and hence there are two equal values for the CN bond. The NN bond is very far away and hence does not come in this calculation. Some times a frequency has a zero intensity which is not tabulated. When the system has a translational symmetry as in a crystal, it call the “density of vibrational states”. In the case of clusters which is the translational symmetry does not occur, it call “vibrational spectrum”. In the case of electrons is call “density of states” (DOS) and for crystals, is “vibrational density of states” (vDOS) but in molecules is call the vibrational spectrum. The infrared spectra are very rich. In the case of amorphous carbon nitride, the infrared spectra are very poorly resolved or not resolved at all and there are impurity modes. Hence at the present time, such data can not be compared with the calculated frequencies. Actually, this calculation gives all of the infrared bands but the experimental data is not resolved. The Raman spectra arise only if there is a change in the polarizability upon shining with light but the IR does not have such a requirement. There are several isomers in this calculation. These are the clusters with the same number of atoms but arranged differently so that the symmetries are different. Usually, the symmetries which are absent are considered to be broken due to the electron-vibrational interaction. If there is a vibration with respect to which a degenerate electronic state is not stable, the molecules get distorted which is called the Jahn-Teller effect. For example, the cluster (iii) CN_3 has the same number of atoms as the cluster (iv) CN_3. These isomers indicate that the CN bond is smaller in the planar configuration than in the pyramidal configuration. There is a potential with two wells so that the two molecules are located in different wells. Hence, both clusters are stable. Similarly, CN_4 is found in three different symmetries (v), (vi) and (vii). The CN bond is shortest in the tetrahedral symmetry and longest in the pyramidal molecule. The C_2N is also found in two symmetries, (viii) and (ix). The linear CNC has a CN bond length of 1.264 Å while the triangular molecule has CN bond length of 1.340 Å.

The molecule C_2N_3 is also stable in two configurations, (xi) and (xii). The linear molecule NCNCN is having shorter CN bond length than the bipyramidal. In the case

(i) CN

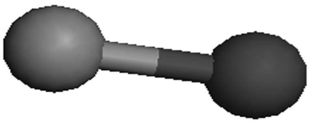

(ii) CN_2 Linear

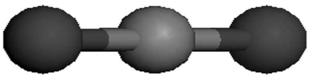

(iii) CN_3 Triangular

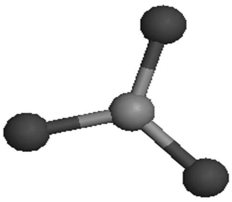

(iv) CN_3 Pyramidal

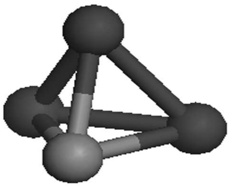

(v) CN_4 Pyramidal

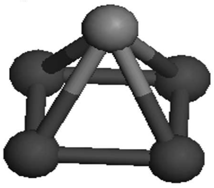

(vi) CN_4 Square

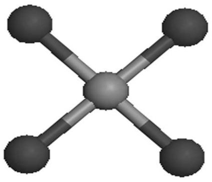

(vii) CN_4 T_d

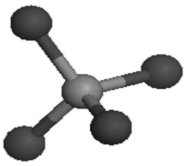

(viii) C_2N Linear

(ix) C_2N Triangular

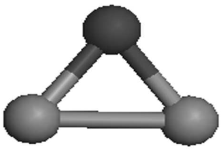

(x) C_2N_2 Rectangular

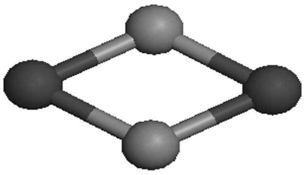

Figure 8.1: The qualitative geometry of clusters (i) to (x) shown by stick-ball models without electronic structure.

of C_3N two stable configurations are given by (xiv) and (xv). The planar molecule with C_3 forming a triangle with one N in the centre has smaller CN bond length than the pyramidal molecule. The molecule C_3N_2 also occurs in two configurations. In this case also the linear molecule has shorter bond length than the bipyramidal. In the case of C_4N_2 the dumb bell configuration has smaller CN bonds than the bipyramidal. Basically, the isomers, with the same number of atoms,occur in double well potentials and both of the configurations are stable. The stability of the clusters, the binding energies and the effect of approximations is further indicated by the energy values given in Table 8.9. The local density approximation (LDA) values are slightly different from those obtained from the generalized gradient approximation (GGA). It is believed that GGA values are better approximation to the actual cluster than those of LDA. The binding energy strongly depends on the number of atoms and for isomers on the symmetry of the cluster.

8.6 Conclusions

There is considerable effect of ion exchange on the vibrational frequencies. For example, comparison of CN_3 (pyramidal) with C_3N (pyramidal) shows that CN_3 has 561.2 cm^{-1} whereas C_3N has 309 cm^{-1} as the smallest frequency so that the effect of force constant is much stronger than the effect of the mass. The vibrational frequencies of several clusters of carbon and nitrogen atoms have been calculated. Several calculated frequencies agree with the measured values. It has been pointed out by Liu and Cohen [72] that prototype structure may be metastable. It was reported by Hu *et al.* [73] that as the nitrogen concentration changes from 11 to 17 percent, the density changes from 3.3 g/cm^3 to 2.1 g/cm^3. In this cluster calculation it is very clear that the bond distances depend on the structure. The population of the vibrations depends on temperature. Hence there is a small effect of temperature on the bond formation. The effect of extra boron atoms on the boron-carbon-nitrogen bonds has been examined by

(xi) C_2N_3 Bipyramid

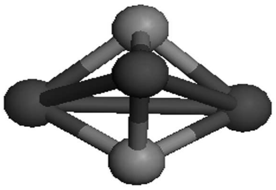

(xii) C_2N_3 Linear

(xiii) C_2N_4 Bipyramid

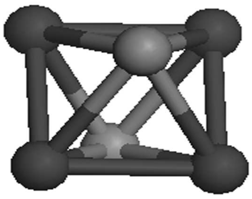

(xiv) C_3N Pyramidal

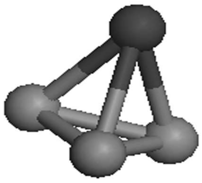

(xv) C_3N Triangular

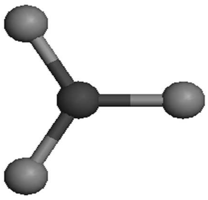

(xvi) C_3N_2 Bipyramidal

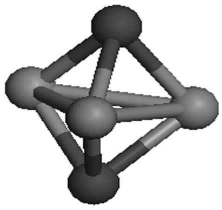

(xvii) C_3N_2 Linear

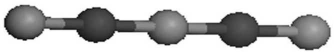

(viii) C_3N_3 Linear

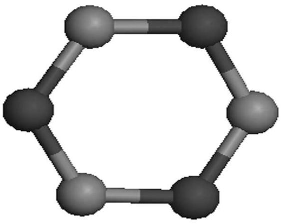

(xix) C_3N_4 Linear

(xx) C_4N T_d

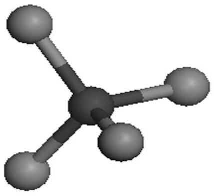

Figure 8.2: The qualitative geometry of clusters (xi) to (xx) shown by stick-ball models without electronic structure.

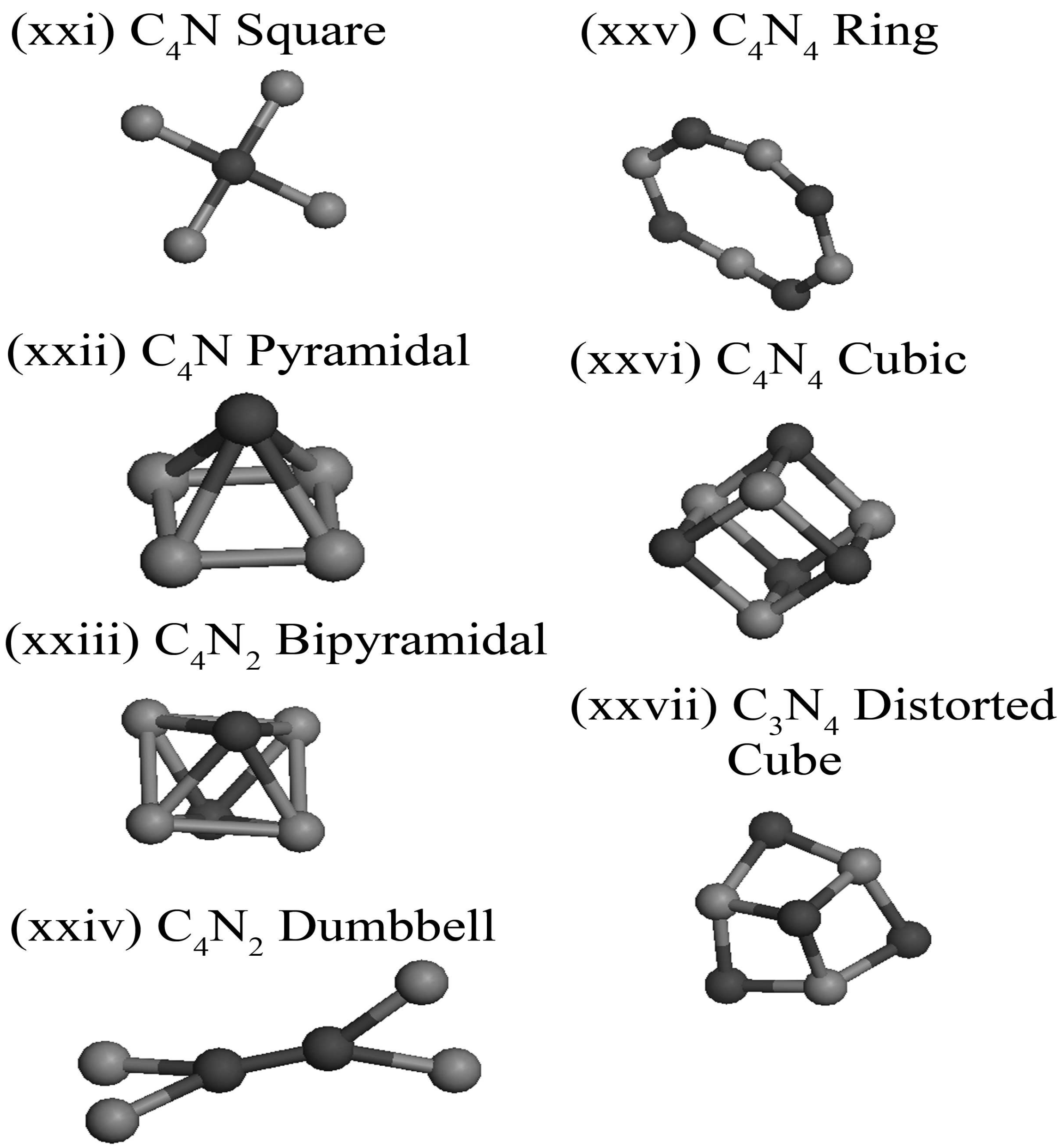

(xxi) C_4N Square

(xxii) C_4N Pyramidal

(xxiii) C_4N_2 Bipyramidal

(xxiv) C_4N_2 Dumbbell

(xxv) C_4N_4 Ring

(xxvi) C_4N_4 Cubic

(xxvii) C_3N_4 Distorted Cube

Figure 8.3: The qualitative geometry of clusters (xxi) to (xxvii) shown by stick-ball models without electronic structure.

Table 8.9: The zero-point vibrational energy and the binding energy of a cluster

S.No.	Cluster	Zero point vibrational energy (eV)		Binding energy (eV)	
		LDA	GGA	LDA	GGA
1	CN	0.1271	0.1253	8.4889	7.6700
2	CN_2 Linear	0.2227	0.2133	14.0713	12.6098
3	CN_3 Triangular	0.2732	0.2651	14.3830	12.5825
4	CN_3 Pyramidal	0.3020	0.2945	13.1572	10.7857
5	CN_4 Pyramidal	0.3533	0.3428	17.2567	14.0698
6	CN_4 Square	0.2531	0.3345	13.1520	10.3472
7	CN_4 T_d	0.8935	0.2050	13.6548	11.7459
8	C_2N Linear	0.1971	0.2075	14.1565	12.9131
9	C_2N Triangular	0.1566	0.1495	12.7557	11.3248
10	C_2N_2 Rectangular	0.2741	0.2658	17.9783	15.5362
11	C_2N_3 Bipyramid	0.3318	0.3283	19.7156	16.4972
12	C_2N_3 Linear	0.5252	0.4827	27.7429	24.4425
13	C_2N_4 Bipyramid	0.1970	0.2086	16.7952	13.2403
14	C_3N Pyramidal	0.1418	0.1658	14.4209	12.1873
15	C_3N Triangular	0.1895	0.1906	14.9572	13.1571
16	C_3N_2 Bipyramid	0.2985	0.2979	21.0665	18.1002
17	C_3N_2 Linear	0.4526	0.4239	26.8867	23.8476
18	C_3N_3 Ring	0.5115	0.4739	31.9007	27.6289
19	C_3N_4 Linear	0.8381	0.7756	41.6774	36.6537
20	C_4N T_d	0.1413	0.2933	15.8692	13.3594
21	C_4N Square	0.1982	0.1500	17.3608	14.7165
22	C_4N Pyramidal	0.2528	0.2378	22.7600	19.7943
23	C_4N_2 Bipyramid	0.3572	0.3567	23.3756	19.9261
24	C_4N_2 Dumb bell	0.5039	0.4815	27.1663	23.3923
25	C_4N_4 Ring	0.9104	0.8282	43.2208	40.9440
26	C_4N_4 Cube	0.6620	0.6571	36.6185	30.7557
27	C_3N_4 Distorted Cube	0.6800	0.6495	31.9706	26.8455

Yuge [74]. Many of this clusters are found to be stable with several different relative concentrations of carbon and nitrogen. The stability of a molecule with slightly different concentration than C:N=3:4 has also been discussed by Mattesini and Mater [75]. The linear bonds contribute to the strength of the glassy state and these are influenced by doping [76].

Chapter 9

Graphene Infrared Spectroscopy: DFT Vibrational Frequencies

The band structure asymmetry in terms of positive energy solution not being equal to the negative energy solution for the electron has been found. The experimental work shows the gap resonance and the linear Stark effect upon application of the electric field. The vibrational frequencies of various models of graphene have been calculated using the density functional theory (DFT). The bond length in a single hexagonal carbon ring is 1.376 Å and its vibrational frequency is 1062.27 cm^{-1}. In a monolayer of 32 atoms, there are a large number of vibrations starting from 42.24 cm^{-1} to about 1551.32 cm^{-1}. In another type of graphene model of 30 atoms, the frequencies calculated vary from 23.12 cm^{-1} to 1546.26 cm^{-1}. In the case of the two layers of 30 atoms each, the vibrational frequencies vary from 32.55 cm^{-1} to 1548.23 cm^{-1}.

9.1 Introduction

In a recent study [77], the electronic band structure of a monolayer of graphene has been found. It showed that the bands do not cross with a small gap of about 27 meV. The band structure of multilayer of graphene has been calculated from which it found that the calculations as well as the experimental data agree with nonrelativistic theory. This chapter reports the calculation of the vibrational frequencies of graphene. The periodic boundary conditions are automatically done by the computer programme. However, in clusters or glasses the "periodic boundary conditions" are not necessary. In the periodic boundary condition, the atoms are not oscillating due to the rigidity of the system so the vibration mode cannot be observed. The vibration modes can be observed using a cluster method. The clusters of material will be minimized to the ground state energy before the vibrational frequency can be calculated.

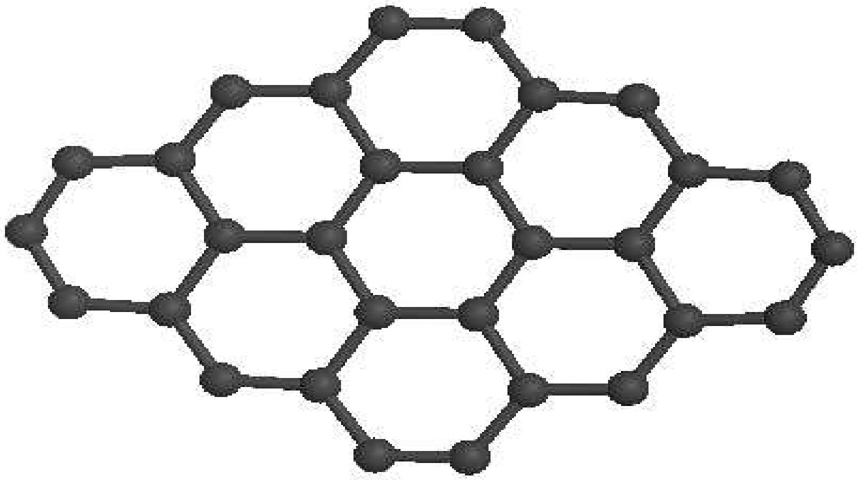

Figure 9.1: A model of 30 atoms of carbon for 1 layer of graphene called type A.

9.2 Results

A single hexagonal ring of carbon atoms has a C - C bond length of 1.376 Å and its vibrational frequency is 1062.27 cm^{-1}. A model of 30 atoms of carbon has been made called A type as shown in Fig. 9.1. The vibrational spectrum for this model is shown in Fig. 9.2. The calculated vibrational frequencies are given in Table 9.1. A model with 32 atoms whichs is called B has been built and shown in Fig. 9.3. The calculated vibrational spectrum is shown in Fig. 9.4. The two layers of the AA type are shown in Fig. 9.5 and their frequencies are shown in Table 9.3 and Table 9.4. The vibrational spectrum of AA type is shown in Fig. 9.6.

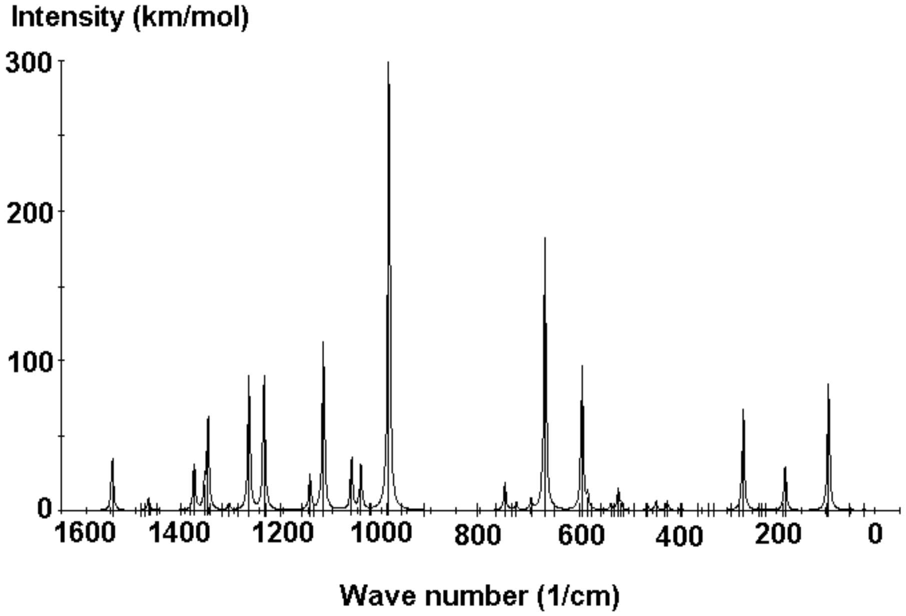

Figure 9.2: The vibrational frequencies of 1 layer of graphene type A.

9.3 Conclusions

It is found that the energy of 18 meV is of electronic origin. Similarly, the gap of nearly 3100 cm^{-1} occurs in a system of 12 layers of atoms. The experimental study [78] of infrared in graphene is therefore concerned with electronic band structure. It is nice to calculate the vibrational frequencies which show that 18 meV gap can occur in the electronic bands as well as in vibrational spectra. The resonance effect are expected if the same energy occurs in the electrons as well as in phonons. Considering the mass of the carbon atom, the frequency of 3100 cm^{-1} does not occur in the vibrational spectra of graphene.

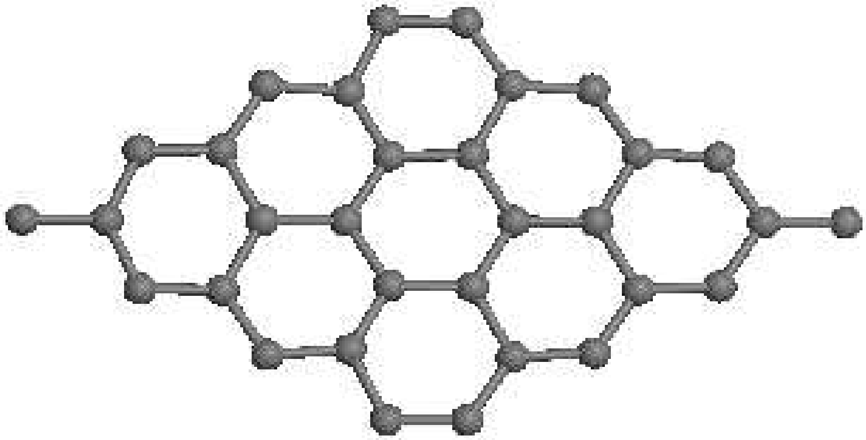

Figure 9.3: A model of 32 atoms of carbon for 1 layer of graphene type B.

Table 9.1: The calculated vibrational frequencies of 1 graphene layer of type A

Frequency cm^{-1}	Intensity (km/mol)
23.12	1.01
51.36	2.26
94.51	84.70
95.31	0.56
182.37	28.70
188.16	1.88
220.77	0.97
236.42	1.46
267.45	68.16
275.54	0.24
293.20	0.18
337.22	0.04
390.63	0.01
391.02	0.07
393.48	1.53
421.36	6.07
426.58	0.05
443.50	0.15
444.21	6.05
461.32	3.47
488.48	0.02
488.74	0.07
514.68	0.09
514.69	3.81
520.91	14.47
535.82	4.26
555.46	0.38
556.51	0.39
582.64	9.15
594.19	95.63
649.79	0.02
650.76	0.36
669.34	182.86
670.02	0.07
697.49	6.80
727.63	4.71
736.73	0.22
750.59	19.27
770.28	0.00
807.86	0.03
960.28	0.01
985.95	299.51
989.62	1.53
1024.44	0.14
1042.70	29.84
1061.38	34.69
1118.65	113.39
1145.84	23.53
1163.27	0.03
1204.22	0.07
1234.24	0.44
1239.07	89.13
1269.68	90.38
1310.15	3.97
1349.03	0.06
1352.46	60.92
1359.32	17.78
1380.46	30.61
1406.51	0.04
1456.05	0.27
1472.24	0.01
1473.00	8.28
1546.26	34.74

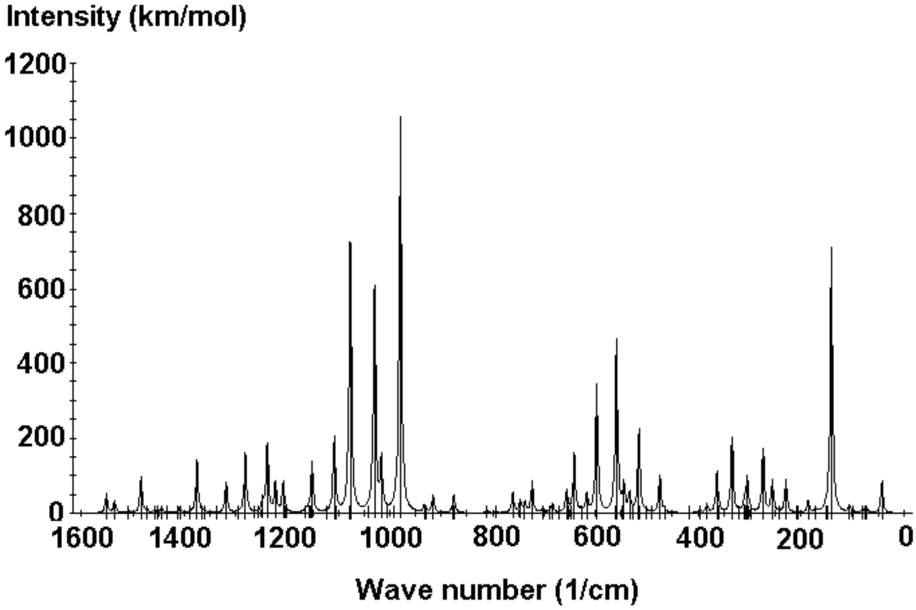

Figure 9.4: The vibrational frequencies of 1 layer of graphene type B.

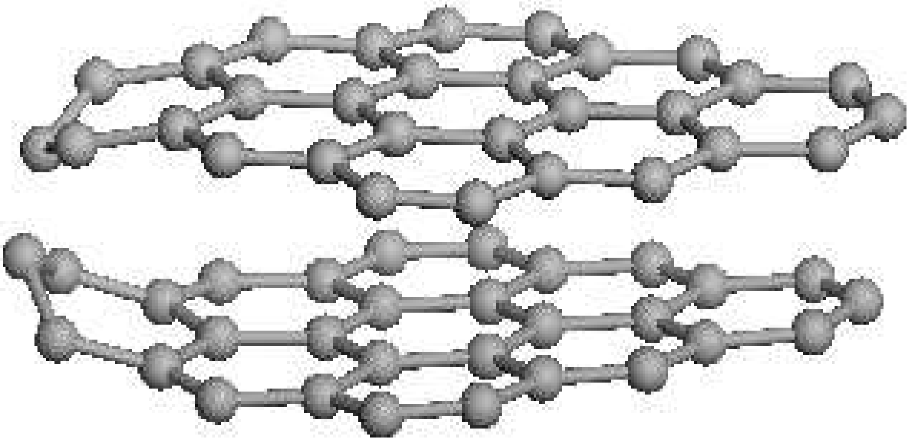

Figure 9.5: Graphene 2 layers, type AA, view from the side.

Table 9.2: The calculated vibrational frequencies of 1 graphene layer of type B

Frequency cm^{-1}	Intensity (km/mol)	Frequency cm^{-1}	Intensity (km/mol)	Frequency cm^{-1}	Intensity (km/mol)
42.24	83.71	533.53	3.28	1042.71	2.72
72.05	9.79	544.32	66.81	1076.83	725.60
74.07	3.80	544.52	1.63	1078.40	15.89
80.13	8.23	548.41	4.11	1105.16	17.39
99.73	2.78	558.19	51.85	1108.16	191.69
105.67	19.35	559.02	412.79	1123.52	0.55
140.70	713.95	560.79	7.13	1151.08	129.95
148.74	1.34	596.65	79.18	1154.56	11.18
150.90	2.38	597.34	263.66	1157.02	0.24
171.32	7.61	598.53	1.37	1163.21	12.00
185.96	31.40	616.62	47.22	1201.99	0.61
205.98	2.31	626.59	5.53	1202.42	0.08
208.29	2.03	627.50	2.57	1207.16	82.96
229.16	87.19	640.99	156.42	1222.34	78.48
242.78	1.45	647.92	2.64	1238.43	181.80
255.37	84.86	651.93	0.74	1247.65	32.22
273.59	171.29	655.84	56.98	1256.80	0.58
297.01	1.71	670.88	0.36	1262.98	1.34
302.83	18.00	683.25	21.05	1280.96	160.97
304.84	80.25	688.54	7.35	1294.34	2.48
306.49	2.76	701.92	6.77	1318.36	79.80
309.93	25.59	702.98	3.54	1337.00	3.12
319.68	4.80	723.09	83.06	1360.88	5.74
333.88	202.17	737.35	25.63	1366.50	1.34
358.74	0.16	745.84	34.14	1375.04	143.30
360.17	3.40	760.44	54.72	1387.80	0.84
363.32	109.49	793.37	1.93	1408.39	16.78
382.66	21.96	810.97	6.35	1411.33	0.07
396.03	7.22	874.40	22.58	1432.48	0.20
418.45	0.19	876.04	28.17	1432.60	3.70
465.21	7.73	915.57	45.39	1444.07	13.60
474.18	96.98	930.32	9.41	1450.76	2.72
489.73	0.57	933.10	12.73	1457.57	7.68
500.78	6.05	979.48	1060.16	1472.42	7.43
513.17	9.63	993.31	0.03	1483.82	98.13
515.28	212.62	1006.21	0.02	1508.41	6.05
526.86	0.03	1016.15	133.01	1535.28	32.96
533.25	42.76	1029.69	611.55	1551.32	50.55

Table 9.3: The calculated vibrational frequencies of 2 graphene layers of type AA for frequency range between 0 - 650 cm^{-1}

Frequency cm^{-1}	Intensity (km/mol)
32.55	260.56
36.81	73.46
54.66	768.90
66.33	99.30
82.51	16.77
103.59	72.76
107.83	100.24
114.67	153.75
119.37	747.62
126.07	359.38
128.05	80.70
141.40	22.28
143.28	43.50
163.46	19.80
193.32	79.86
195.89	627.88
208.24	2.77
218.17	38.04
226.59	17.02
233.86	626.24
238.78	12.56
244.31	73.38
245.61	218.30
268.77	113.44
269.96	140.78
274.85	301.19
275.99	12.12
281.55	38.68
282.91	196.05
294.18	65.00
298.49	37.50
320.34	146.78
325.92	42.81
332.10	49.97
339.79	45.14
342.71	616.00
351.59	206.73
367.53	238.17
387.82	191.36
389.87	13.52
390.46	45.55
393.56	256.65
397.53	38.41
399.61	7.80
417.37	11.71
426.21	13.60
430.02	4.49
431.36	3.47
435.27	88.15
446.84	62.78
454.06	14.09
455.04	1.65
457.12	51.00
463.25	150.63
479.76	56.46
489.25	141.95
489.66	119.17
493.56	82.87
495.38	423.70
505.82	49.00
507.35	41.12
508.52	174.72
512.28	165.54
516.98	22.67
521.21	98.19
523.30	54.20
524.37	89.45
526.19	188.28
528.91	27.49
533.56	271.59
536.46	8.47
547.52	216.02
550.78	4.44
566.11	276.43
567.45	173.97
575.00	33.05
578.79	301.27
581.73	59.60
583.24	463.48
586.04	419.10
587.64	17.16
592.72	95.42
608.34	203.20
610.58	124.70
634.58	141.62
640.92	7.46

Table 9.4: The calculated vibrational frequencies of 2 graphene layers of type AA for frequency range between 650 - 1550 cm^{-1}

Frequency cm^{-1}	Intensity (km/mol)
654.43	56.16
663.74	37.35
664.90	22.78
670.20	93.95
672.27	27.47
675.02	453.18
690.68	457.97
692.88	73.91
727.71	149.04
728.65	3.50
733.29	13.34
744.38	536.88
748.65	839.46
751.36	41.63
769.63	13.42
776.41	190.97
798.08	39.98
811.19	6.62
875.98	150.97
916.43	418.09
917.86	105.31
956.70	52.97
959.98	434.30
974.07	55.97
976.21	0.48
994.95	61.29
1005.52	157.05
1016.12	27.38
1018.41	18.86
1027.84	284.81
1040.40	61.91
1043.81	127.35
1056.84	271.83
1062.36	58.33
1063.63	295.47
1113.67	16.76
1122.50	17.85
1126.66	86.74
1130.55	48.28
1149.34	192.17
1150.14	66.58
1161.44	13.80
1162.19	166.38
1164.60	135.64
1168.28	47.39
1192.91	3.93
1200.86	11.47
1202.93	17.94
1206.74	81.92
1235.04	619.84
1238.50	0.29
1262.36	59.85
1265.49	48.59
1267.82	164.45
1275.82	109.55
1291.93	68.65
1296.46	168.29
1312.28	27.75
1314.67	131.63
1337.32	348.11
1344.89	31.23
1347.09	190.34
1357.66	388.47
1358.54	214.42
1360.84	93.33
1362.89	583.19
1363.35	274.15
1372.52	3.62
1377.66	60.45
1387.56	271.78
1390.26	266.34
1409.60	179.15
1450.43	69.82
1453.91	41.31
1466.97	15.01
1467.39	139.48
1469.71	79.11
1470.22	208.99
1477.80	17.41
1479.98	3.71
1485.23	62.76
1485.66	481.42
1540.34	197.99
1542.98	309.07
1546.15	95.67
1548.23	79.26

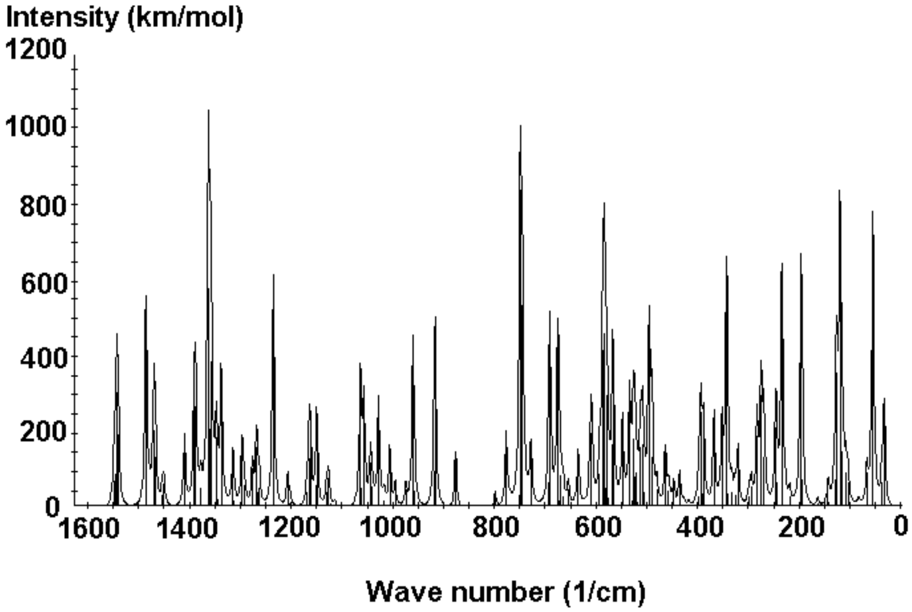

Figure 9.6: The vibrational frequencies of 2 layers of graphene, type AA.

Chapter 10

Oscillations in The Force Upon Doping Cuprates

10.1 Introduction

The present view of the understanding of superconductivity is recently provided by Alex Müller [53]. Needless to say that there have been more than 80000 papers since the original discovery of indications of high transition temperatures of superconductors [79]. According to the view point of Müller, CuO_2 planes exist and when doped with holes, the phenomenon of "high-temperature superconductivity" occurs. In the original B.C.S theory, the pairing of the electrons in the conduction band occurs via the electron-phonon interaction but the transition temperatures are less than 23 K [56]. Since, large transition temperatures are observed $T_c \sim 148$ K, it is of concern to determine the mechanism of superconductivity. At one time, it was thought that if a Hubbard type hoping term is added to the B.C.S. theory, it will provide the correct theory of superconductivity [56, 80]. It will be of interest if on theoretical grounds it can be proved that superconductivity is a result of hole doping. The force which is largely responsible for the lattice vibrations is, (F)=-(k)(x) which is in the form of a matrix due to anisotropic force constant. The potential from this force is determined from, F=-$\partial V/\partial$x with similar expressions for $\partial/\partial y$ and $\partial/\partial z$. The integrated force is due to the potential V=$\frac{1}{2}kx^2$ which is again in the form of a matrix due to anisotropy. It will be of importance if the effect of hole doping on the force can be found which is relevant for the understanding of the vibrations in superconductors. The density functional theory has been used to make models of clusters of atoms which have minimum energy. Therefore, the clusters of atoms can be built and their vibrational frequencies can be determined. The transition temperature of a superconductor depends on the inverse square root of the atomic mass. Hence, the maximum vibrational frequency of a cluster determines the transition temperature.

In this chapter, the models of CuO_n, Cu_2O_n, Cu_3O_n and Cu_4O_n(n=1 to 6) have been made. In the case of each cluster, the vibrational frequencies have been calculated. The largest vibrational frequency has been plotted as a function of number of oxygen atoms. It found that for a small increase in the number of oxygen atoms near a Cu atom, the vibrational frequency increases. For further increase in the number of oxygen atoms, the maximum vibrational frequency shows oscillations as a function of number of oxygen atoms. The vibrational frequency is proportional to the square root of the force constant, $\omega = \sqrt{k/m}$. When normal modes are considered, the force constant will be represented by a matrix. Therefore the increase in vibrational frequency shows that the force constant increases upon increasing the number of oxygen atoms and hence the magnitude of the force increases upon initial doping with oxygen. It is found that with increasing the number of oxygen atoms, the force oscillates. These oscillations are important for the understanding of superconductivity.

10.2 The Methodology

One atom of Cu has been considered, on which the various numbers of oxygen atoms have been added and minimize the energy of the Schrödinger equation for all of the electrons which determines the bond lengths and the positions of various atoms. After the minimum energy configuration is obtained, the vibrational frequencies have been found. This programme has been tested and the calculated vibrational frequencies have been compared with the experimental data of Raman spectra with reasonable degree of confidence. At least in the cases of three different glasses, GeSi, GeSP and GeSe, these calculated values are in reasonable agreement with the data [25,27,32]. The calculation is based on the density functional theory in the local density approximation and double numerical wave functions are used [4,5]. The complete electronic configurations of Cu and O atoms are taken into account. The atomic number of Cu is 29 and that of O is 8 which shows the size of the secular determinant. The Schrödinger equation is differentiated with respect to the electron density to obtain the Kohn-Sham equation which is solved. An example of obtaining the vibrational frequencies by this method is given by Lopez-Duran *et al.* [71]. The whole system of electrons and nuclei is considered correctly. The programme provides the local density approximation (LDA) as well as the generalized gradient approximation (GGA) values but they are quite close to each other. It is kindly provided by Accelrys Software Inc., San Diego, California. The specific programme used is called DMol^3, the details of which are available. The variety of wave functions have been used and found by experience [25, 27, 32] that double numeric is the closest to the experimental data.

10.3 Clusters of CuO$_n$

(i) The clusters of CuO molecule has been made with only two atoms, one of Cu and one of O. The bond length for which the energy is minimum is 1.716 Å. The vibrational frequency of the stretching frequency is found to be 706.5 cm^{-1}. The intensity is of reasonable magnitude and the mode is non-degenerate as given in Table 10.1.

(ii) A linear molecule O-Cu-O has been made using only the first principles potential without any adjustable parameters and minimize the energy of the Schrödinger equation. The bond length corresponding to the minimum energy configuration is found to be 1.672 Å and the vibrational frequencies are given in Table 10.1. In addition to the usual mode, there is one more strong vibration at relatively lower frequency.

(iii) The CuO_2(triangular) structure has been made. After optimization for the minimum energy, it is found that Cu-O bond length is 1.921 Å and the O-O distance is 1.478 Å. The vibrational frequencies of this molecule are given in Table 10.1.

(iv) CuO_3(pyramidal). The three oxygen atoms have been arrange in a triangle and put one Cu atom on top so that a pyramid is formed. In the optimized structure, the Cu-O distance is found to be 1.750 Å and the O-O distance is 3.032 Å. The vibrational frequencies are given in Table 10.1. There are two doubly degenerate modes and one in non-degenerate.

(v) $CuO_4(T_d)$. In this system, the four oxygen atoms are connected to a central Cu atom so that the symmetry is tetrahedral. In the optimized structure Cu-O bond length is found to be 1.799 Å and the vibrational frequencies are given in Table 10.1.

(vi) CuO_4(pyramidal). A square with four oxygen atoms has firstly made and then one Cu atom has been putted on the top position. In the optimized structure O-O distance is 1.760 Å and Cu-O distance is 2.025 Å. The vibrational frequencies are given in Table 10.1.

(vii) CuO_5(pyramidal). A five sided figure from five oxygen atoms has been made and one Cu atom has been putted on top position. By using double numeric polarized wave functions, the configuration for which the energy is a minimum, shows O-O bond length of 1.051 Å and the Cu-O distance is 2.469 Å. The vibrational frequencies calculated from the density functional theory by using local-density approximation are given in Table 10.1.

(viii) CuO_6(bipyramidal). The three oxygen atoms forming a triangle are on the right hand side of one Cu atom and the remaining three oxygen atoms are on the left. The O-O distance in the minimized configuration is 1.654 Å and the Cu-O distance is 2.134 Å. The calculated vibrational frequencies are given in Table 10.1.

Table 10.1: The vibrational frequencies of CuO_n (n=1-6) along with intensities and degeneracies.

S.No.	Cluster	Frequency (cm^{-1})	Intensity km/mol	Degeneracy
1	CuO	706.5	2.6	1
2	CuO_2(linear)	133.6	20.0	2
3	CuO_2(linear)	845.9	1.2	1
4	CuO_2(triangular)	226.6	5.4	1
5	CuO_2(triangular)	390.1	11.6	1
6	CuO_2(triangular)	892.5	122.8	1
7	CuO_3(pyramidal)	49.8	1.2	2
8	CuO_3(pyramidal)	161.0	19.1	1
9	CuO_3(pyramidal)	649.8	6.9	2
10	$CuO_4(T_d)$	116.5	5.1	3
11	$CuO_4(T_d)$	550.7	3.6	3
12	CuO_4(pyramidal)	246.2	3.7	1
13	CuO_4(pyramidal)	270.9	2.9	2
14	CuO_4(pyramidal)	706.2	4.4	1
15	CuO_5(pyramidal)	251.6	93.0	2
16	CuO_5(pyramidal)	625.7	350.0	1
17	CuO_6(bipyramidal)	82.0	5.6	2
18	CuO_6(bipyramidal)	247.4	66.3	1
19	CuO_6(bipyramidal)	778.9	96.6	1

(ix) CuO_7. In this cluster seven oxygen atoms are on the surface of a sphere and Cu is located in the central position. In the optimized configuration Cu-O distance is 1.934 Å and the vibrational frequencies are given in Table 10.2.

(x) CuO_8. The double numeric polarized wave functions gave Cu-O distance as 2.194 Å. The Cu atom is in the centre and four oxygen atoms are on one side and the remaining four on the other side. All of the oxygen atoms are on the surface of a sphere. The vibrational frequencies for this system are given in Table 10.2.

(xi) CuO_9. In this cluster one Cu atom is in the centre and all of the oxygen atoms are on the surface of a sphere. In the optimized configuration Cu-O distance is 2.020 Å and the frequencies are given in Table 10.2.

(xii) CuO_{10}. In this cluster the Cu-O distance is 2.335 Å and O-O distance is 1.984 Å. In the optimized configuration,the vibrational frequencies are given in Table 10.2.

(xiii) Cu_2O (triangular). A molecule of three atoms with one oxygen and two Cu atoms has been made. The Cu-Cu bond length is found to be 2.407 Å and the Cu-O distance is 1.771 Å. The vibrational frequencies calculated for this system are given in Table 10.3.

(xiv) Cu_2O_2 (rectangular). The alternate atoms are Cu and O to form a closed molecule with Cu-O distance of 1.810 Å. The calculated vibrational frequencies are given in Table 10.3 and the spectrum calculated from the first principles is given in Fig. 10.1.

(xv) Cu_2O_4 (bipyramidal). The four oxygen atoms are first placed in a square and then one Cu atom is put on one side and another Cu atom on the other side of the O_4 plane. The O-O distance is 2.238 Å and Cu-O distance is found to be 1.950 Å. The vibrational frequencies calculated for this system are given in Table 10.3.

(xvi) Cu_2O_4 (dumb bell). The Cu-Cu distance is 2.277 Å. Two oxygen atoms are attached to each Cu atom with Cu-O distance of 1.823 Å. The spectrum calcu-

Table 10.2: The vibrational frequencies of CuO_n (n=7-10) along with intensities and degeneracies.

S.No.	Cluster	Frequency (cm^{-1})	Intensity km/mol	Degeneracy
1	CuO_7	48.4	0.3	1
2	CuO_7	52.1	0.1	1
3	CuO_7	401.1	0.01	1
4	CuO_7	447.9	7.05	1
5	CuO_7	450.3	7.07	1
6	CuO_7	486.8	0.01	1
7	CuO_7	609.4	0.10	1
8	CuO_8	209.5	13.3	1
9	CuO_8	733.0	373.0	1
10	CuO_9	51.1	0.01	1
11	CuO_9	87.8	1.4	2
12	CuO_9	94.8	0.97	2
13	CuO_9	125.1	0.26	1
14	CuO_9	149.2	2.35	1
15	CuO_9	300.0	2.12	2
16	CuO_9	342.1	0.14	1
17	CuO_9	441.4	23.0	2
18	CuO_9	446.5	8.14	1
19	CuO_9	448.6	0.03	1
20	CuO_{10}	172.5	0.38	2
21	CuO_{10}	269.6	2.71	1
22	CuO_{10}	435.6	5.38	1
23	CuO_{10}	467.1	23.1	2

lated from the first principles is shown in Fig. 10.2. The vibrational frequencies calculated for this system are given in Table 10.3.

(xvii) Cu_2O_5 (bipyramidal). A pentagon with oxygen atoms has been made. The O-O bond length is 2.003 Å and two Cu atoms are placed on the two sides of the pentagon to form a bipyramidal figure. The Cu-O distance in 2.057 Å. The calculated vibrational frequencies are given in Table 10.4.

(xviii) Cu_2O_6 (bipyramidal). A hexagon with oxygen atoms has been made and then place two Cu atoms, one on each side of the hexagon to form a bipyramidal figure.

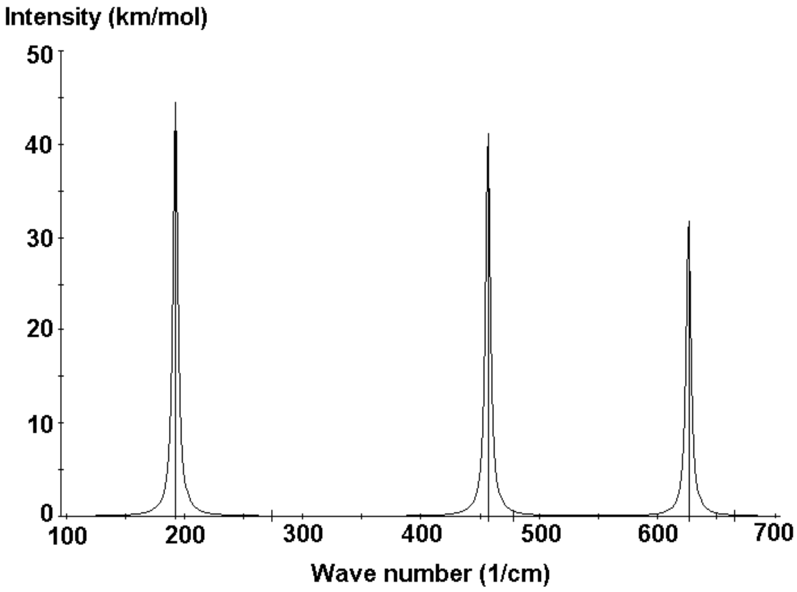

Figure 10.1: The vibrational spectrum of Cu_2O_2(rectangular) calculated from the first principles.

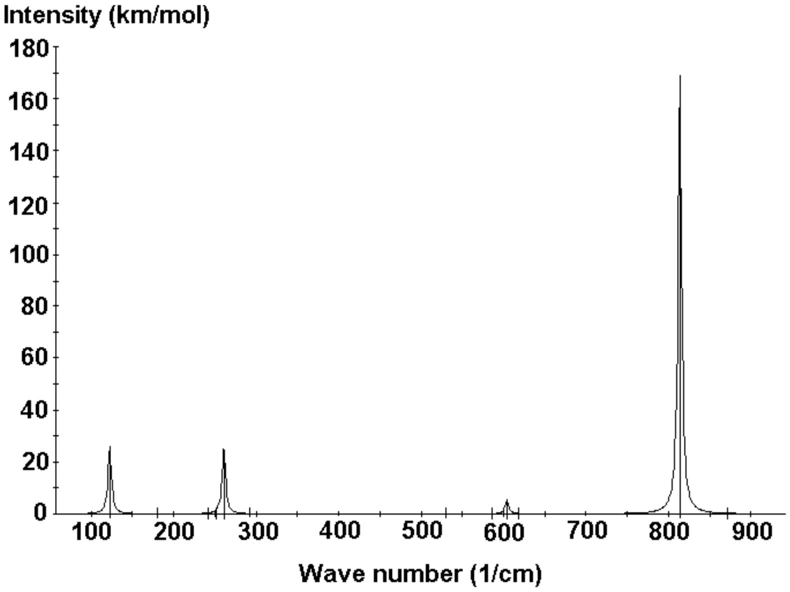

Figure 10.2: The vibrational spectrum of Cu_2O_4(dumb bell) calculated from the first principles.

Table 10.3: The vibrational frequencies of Cu_2O_n (n=1-4) along with intensities and degeneracies.

S.No.	Cluster	Frequency (cm^{-1})	Intensity km/mol	Degeneracy
1	Cu_2O(triangular)	156.1	1.2	1
2	Cu_2O(triangular)	565.5	30.2	1
3	Cu_2O(triangular)	668.9	22.7	1
4	Cu_2O_2(rectangular)	192.2	44.5	1
5	Cu_2O_2(rectangular)	456.7	41.3	1
6	Cu_2O_2(rectangular)	626.6	31.9	1
7	Cu_2O_4(bipyramidal)	108.6	32.5	1
8	Cu_2O_4(bipyramidal)	135.7	0.7	2
9	Cu_2O_4(bipyramidal)	234.1	0.01	2
10	Cu_2O_4(bipyramidal)	492.8	8.6	2
11	Cu_2O_4(dumb bell)	122.7	25.8	1
12	Cu_2O_4(dumb bell)	260.8	24.9	1
13	Cu_2O_4(dumb bell)	585.5	0.03	1
14	Cu_2O_4(dumb bell)	604.0	5.48	1
15	Cu_2O_4(dumb bell)	813.7	168.8	1
16	Cu_2O_3(bipyramidal)	112.6	3.2	2
17	Cu_2O_3(bipyramidal)	267.2	0.01	2
18	Cu_2O_3(bipyramidal)	316.7	11.6	2
19	Cu_2O_3(bipyramidal)	414.8	14.1	1

The O-O distance in the optimized configuration is 1.821 Å and the Cu-O bond length is 2.164 Å. The calculated vibrational frequencies are given in Table 10.4.

(xix) Cu_2O_6 (dumb bell). Two Cu atoms which are separated by 2.974 Å has been made. Then three O atoms are attached to each Cu atom in the three fold symmetry. The Cu-O bond length is found to be 1.842 Å. The calculated vibrational frequencies are given in Table 10.4.

Table 10.4: The vibrational frequencies of Cu_2O_n (n=5-7) along with intensities and degeneracies.

S.No.	Cluster	Frequency (cm^{-1})	Intensity km/mol	Degeneracy
1	Cu_2O_5(bipyramidal)	166.4	0.02	1
2	Cu_2O_5(bipyramidal)	171.6	0.02	1
3	Cu_2O_5(bipyramidal)	255.5	28.7	1
4	Cu_2O_5(bipyramidal)	360.8	9.7	1
5	Cu_2O_5(bipyramidal)	362.4	9.6	1
6	Cu_2O_6(bipyramidal)	137.7	28.2	1
7	Cu_2O_6(bipyramidal)	226.9	0.01	1
8	Cu_2O_6(bipyramidal)	500.9	24.2	1
9	Cu_2O_6(bipyramidal)	501.0	23.6	1
10	Cu_2O_6(dumb bell)	130.8	11.4	2
11	Cu_2O_6(dumb bell)	172.1	48.3	1
12	Cu_2O_6(dumb bell)	321.7	2.4	2
13	Cu_2O_6(dumb bell)	516.5	0.3	2
14	Cu_2O_6(dumb bell)	524.9	17.1	1
15	Cu_2O_7(bipyramidal)	395.4	0.01	1
16	Cu_2O_7(bipyramidal)	503.1	17.8	2
17	Cu_2O_7(bipyramidal)	515.3	0.01	1

(xx) Cu_3O(pyramidal). Three copper atoms form a triangle with Cu-Cu distance of 2.407 Å and one O atom sits on the top position with Cu-O distance of 1.882 Å. The vibrational frequencies of clusters containing three Cu atoms are given in Table 10.5.

(xxi) Cu_3O_2(bipyramidal). First a triangle is made by using three copper atoms and then one oxygen atom is put on top and another Cu atom is placed symmetrically on the other side of the triangle to form a bipyramid. In the optimized structure the Cu-Cu distance is 2.374 Å and Cu-O distance is 1.945 Å. The vibrational frequencies are given in Table 10.5.

(xxii) Cu_3O_2(linear). A linear molecule with one Cu atom in the centre has been made. Near the ends, the Cu-O bond is 1.721 Å long whereas near the centre, the O-Cu distance is 1.729 Å. The DFT naturally distinguishes the bonds which are near the ends of the molecule compared with the same atoms near the centre. In the molecular physics all of the Cu-O bonds should be of equal length but the more accurate study clearly distinguishes more modes than old molecular physics in which all of the Cu-O bonds must be of equal length. The vibrational frequencies are given in Table 10.5.

(xxiii) Cu_3O_3(bitriangular). The oxygen atoms form one triangle and Cu atoms form another. The two triangles are superimposed on each other. The Cu-O bonds have length 1.795 Å. The vibrational frequencies are given in Table 10.5.

(xxiv) Cu_3O_4(linear). All of the seven atoms are in a straight line. As expected the Cu-O distance at the end is less than in the centre. The bond distances are 1.699, 1.720 and 1.712 Å. The vibrational frequencies are given in Table 10.5.

(xxv) Cu_3O_5(extrabipyramidal). The three Cu atoms form a triangle with Cu-Cu distance of 2.617 Å. Two O atoms sit one on top and the other on bottom of the triangle to form a bipyramid. The Cu-O distance in the pyramids is 1.892 Å. The remaining three O atoms are attached, one to each Cu atom. Outside the pyramids the Cu-O distance is 1.698 Å. The vibrational spectrum calculated from the first principles is given in Fig. 10.3. The vibrational frequencies of clusters containing three Cu atoms and 5 O atoms are given in Table 10.6.

Table 10.5: The vibrational frequencies of Cu_3O_n (n=1-4) along with intensities and degeneracies.

S.No.	Cluster	Frequency (cm^{-1})	Intensity km/mol	Degeneracy
1	Cu_3O(pyramidal)	119.8	0.13	2
2	Cu_3O(pyramidal)	184.6	0.71	1
3	Cu_3O(pyramidal)	370.3	0.01	2
4	Cu_3O(pyramidal)	558.6	15.88	1
5	Cu_3O_2(bipyramidal)	163.2	2.2	2
6	Cu_3O_2(bipyramidal)	309.6	23.2	2
7	Cu_3O_2(bipyramidal)	492.6	41.7	1
8	Cu_3O_2(linear)	54.9	3.4	2
9	Cu_3O_2(linear)	396.3	7.2	1
10	Cu_3O_2(linear)	972.0	66.6	1
11	Cu_3O_3(bitriangular)	104.0	16.5	2
12	Cu_3O_3(bitriangular)	121.7	0.01	1
13	Cu_3O_3(bitriangular)	135.7	53.1	1
14	Cu_3O_3(bitriangular)	189.6	0.08	1
15	Cu_3O_3(bitriangular)	496.4	7.3	1
16	Cu_3O_3(bitriangular)	497.9	8.4	1
17	Cu_3O_3(bitriangular)	596.2	0.09	1
18	Cu_3O_3(bitriangular)	602.5	0.02	1
19	Cu_3O_3(bitriangular)	655.2	35.4	1
20	Cu_3O_3(bitriangular)	656.3	38.6	1
21	Cu_3O_4(linear)	32.2	1.4	2
22	Cu_3O_4(linear)	122.8	5.7	2
23	Cu_3O_4(linear)	287.0	41.6	2
24	Cu_3O_4(linear)	387.2	1.5	1
25	Cu_3O_4(linear)	756.3	10.7	1
26	Cu_3O_4(linear)	1016.5	50.2	1

(xxvi) Cu_3O_5(asymmetric). In this model there are three Cu atoms. One oxygen atom is attached to the central Cu atom and two oxygen atoms to each Cu atoms at the ends of the molecule. The central Cu-O bond distance is 1.712 Å. The Cu-O distance at the ends is 1.755 Å and Cu-Cu distance is 2.557 Å.

(xxvii) Cu_3O_6(triangular). The three Cu atoms are in a triangle and two oxygen atoms are attached to each Cu atom. The Cu-Cu distance is 2.280 Å. The Cu-O distance for the central Cu atom is 1.944 Å whereas for the Cu-O bonds at the two ends, the Cu-O distance is 1.841 Å. Usually, all of the three Cu atoms will be symmetric but there is a charge effect similar to the ionization which opens up the Cu-Cu-Cu to form an angle. Therefore, there is a central Cu atom and two Cu atoms are on the ends. The vibrational frequencies are given in Table 10.7.

(xxviii) Cu_4O(pyramidal). The four Cu atoms form a square with one O atom on top position. The Cu-Cu distance is 2.451 Å and O-Cu distance is 1.908 Å. The vibrational frequencies are given in Table 10.8.

(xxix) Cu_4O (T_d). This molecule has a tetrahedral arrangement of atoms with one oxygen atom in the centre. The Cu-O distance is 1.845 Å. The vibrational frequencies are given in Table 10.8.

(xxx) Cu_4O_2(dumb bell). There are two oxygen atoms with a relatively large separation of 4.182 Å. Two Cu atoms are attached to each oxygen atom with Cu-O distance of 1.783 Å. The vibrational spectrum calculated from the first principles is shown in Fig. 10.4. The vibrational frequencies are given in Table 10.8.

(xxxi) Cu_4O_3(linear). All of the seven atoms are arranged alternatively with Cu atoms on both ends. The Cu-O bond length near the centre is 1.77 Å and 2.153 Å near the ends. The vibrational frequencies are given in Table 10.8.

(xxxii) Cu_4O_4(cube). The eight atoms are alternately on the eight corners of a simple

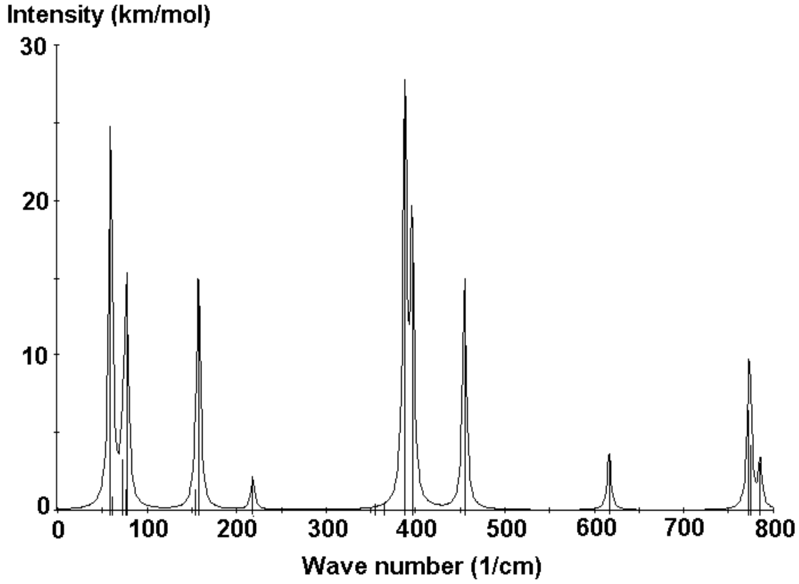

Figure 10.3: The vibrational spectrum of Cu_3O_5(extrabipyramidal) calculated from the first principles.

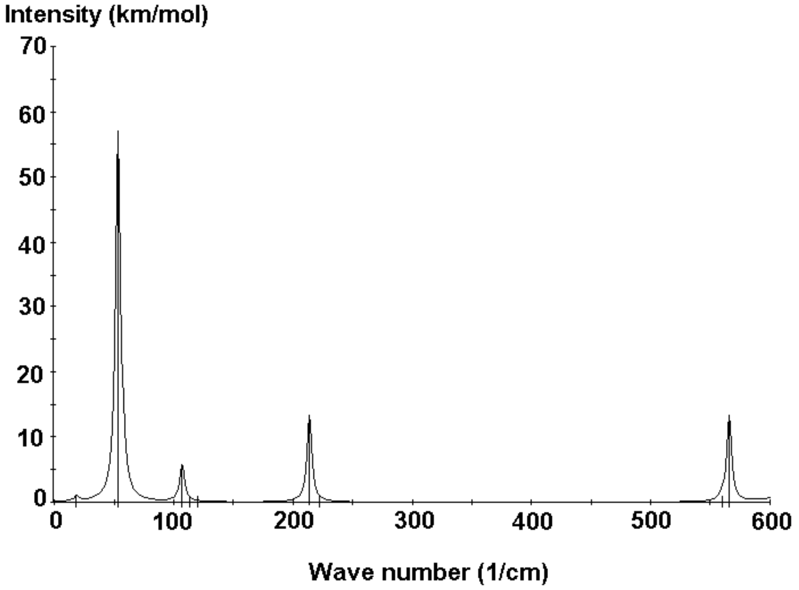

Figure 10.4: The vibrational spectrum of Cu_4O_2(dumb bell) calculated from the first principles.

Table 10.6: The vibrational frequencies of Cu$_3O_n$ (n=5) along with intensities and degeneracies.

S.No.	Cluster	Frequency (cm^{-1})	Intensity km/mol	Degeneracy
1	Cu_3O_5(extrabipyramidal)	58.9	23.6	1
2	Cu_3O_5(extrabipyramidal)	60.4	0.9	1
3	Cu_3O_5(extrabipyramidal)	72.3	3.3	1
4	Cu_3O_5(extrabipyramidal)	76.2	1.4	1
5	Cu_3O_5(extrabipyramidal)	77.0	12.9	1
6	Cu_3O_5(extrabipyramidal)	153.2	1.3	1
7	Cu_3O_5(extrabipyramidal)	157.6	13.4	2
8	Cu_3O_5(extrabipyramidal)	218.0	2.08	1
9	Cu_3O_5(extrabipyramidal)	354.7	0.01	1
10	Cu_3O_5(extrabipyramidal)	365.1	0.01	1
11	Cu_3O_5(extrabipyramidal)	388.1	26.4	1
12	Cu_3O_5(extrabipyramidal)	396.3	17.5	1
13	Cu_3O_5(extrabipyramidal)	454.8	14.9	1
14	Cu_3O_5(extrabipyramidal)	616.5	3.7	1
15	Cu_3O_5(extrabipyramidal)	772.8	6.4	1
16	Cu_3O_5(extrabipyramidal)	774.4	4.2	1
17	Cu_3O_5(extrabipyramidal)	785.5	3.1	1
18	Cu_3O_5(asymmetric)	101.9	6.6	1
19	Cu_3O_5(asymmetric)	117.1	4.3	2
20	Cu_3O_5(asymmetric)	143.5	0.01	1
21	Cu_3O_5(asymmetric)	202.2	30.8	1
22	Cu_3O_5(asymmetric)	212.8	5.1	1
23	Cu_3O_5(asymmetric)	280.0	11.3	1
24	Cu_3O_5(asymmetric)	526.1	19.6	1
25	Cu_3O_5(asymmetric)	572.7	0.16	1
26	Cu_3O_5(asymmetric)	628.4	35.1	1
27	Cu_3O_5(asymmetric)	685.2	5.6	1
28	Cu_3O_5(asymmetric)	686.9	30.7	1
29	Cu_3O_5(asymmetric)	694.8	5.3	1
30	Cu_3O_5(asymmetric)	891.7	140.8	1

cube. The Cu-O bond length is 1.946 Å. The vibrational frequencies are given in Table 10.9.

(xxxiii) Cu_4O_5(linear). All of the nine atoms are in a straight line. The Cu-O distances are 1.698, 1.713 and 1.716 Å. When there is a variety in the bond lengths, naturally there is a variety in the vibrational frequencies. When small and bigger bond occur, the vibrational frequencies are different. The vibrational frequencies are given in Table 10.9.

(xxxiv) Cu_4O_6. The four atoms of Cu and four atoms of oxygen form a square. The four O atoms are on the 4 corners of a square and then four Cu atoms are on the side centres. The remaining two oxygen atoms are on top and bottom positions forming a double pyramid. The Cu-O bond lengths are 1.777 and 2.453 Å, respectively. The vibrational frequencies are given in Table 10.9.

10.4 Jahn-Teller effect

Some of the clusters are not stable in isolation. Therefore, only those for which the bond lengths and structures are optimized have been described. It may be noted from (ii) and (iii) that the same number of atoms occur in two different configurations indicating that two different configurations are stable so that there must exist a double well potential [81]. This is due to the strong vibronic coupling interacting with degenerate states which are not stable because of the interaction energy. Thus, the Jahn-Teller effect removes some of the symmetries which are not found in stable crystals. The clusters give information about the vibrations which upon cooling contribute to the formation of Cooper pairs. The B.C.S. theory in the present form is written in terms of simple integrals which assume isotropic electron-phonon interaction. Performing the integrals numerically improves the transition temperatures but the expression, $\hbar\omega \exp(-1/N(0)V)$, for the transition temperature, with ω as the phonon frequency,

$N(0)$ as the electron density of states at the Fermi level and V the coupling constant of the electron-phonon interaction, makes the T_c very small. Hence the work should be done in the region where the exponential factor is almost 1. The anisotropy of the interaction has not been included in the calculation of the transition temperature.

10.5 Vibrational frequencies

The vibrational frequencies of various clusters of Cu-O are given in Tables 10.1-10.9. For one Cu atom, the values are given in Table 10.1 and 10.2. The highest frequency has been looked in analogy with a cutoff model and plot this frequency as a function of number of atoms. This simulates the doping of the Cu atom with oxygen. When number of O atom increases from one O to two O atoms, the frequency increases but when the frequency has been plotted as a function of number of O atoms from 1-10, there are oscillations as shown in Fig. 10.5. The frequency of a harmonic oscillator is $\omega = \sqrt{k/m}$, which in the clusters appears as normal modes. Since, the mass is more likely to be a constant, the variation in the frequency as a function of doping indicates that the force constant is oscillating. The potential is related to the force as F=-grad V. For a one-dimensional harmonic oscillator, V=(1/2)kx^2. Therefore, the expression F=-kx, indicates that the oscillations of the force constant are equivalent to oscillations in the force. In the actual crystal F, k and x are matrices. From the data in Fig. 10.5, it is found that the force oscillates upon doping one Cu atom with a variable number of oxygen atoms.

Next, the calculation of the highest vibrational frequency of Cu_2O_n with n = 1 to 7 has been performed. It is found that for n = 4, the vibrational frequency has a peak and there is symmetry near this point as shown in Fig. 10.6. The oscillations in the force as a function of doping are clearly visible. The phonons in the system have oscillations due to the oscillating force. Hence, it is expected that the electron-phonon interaction will also be affected by these oscillations.

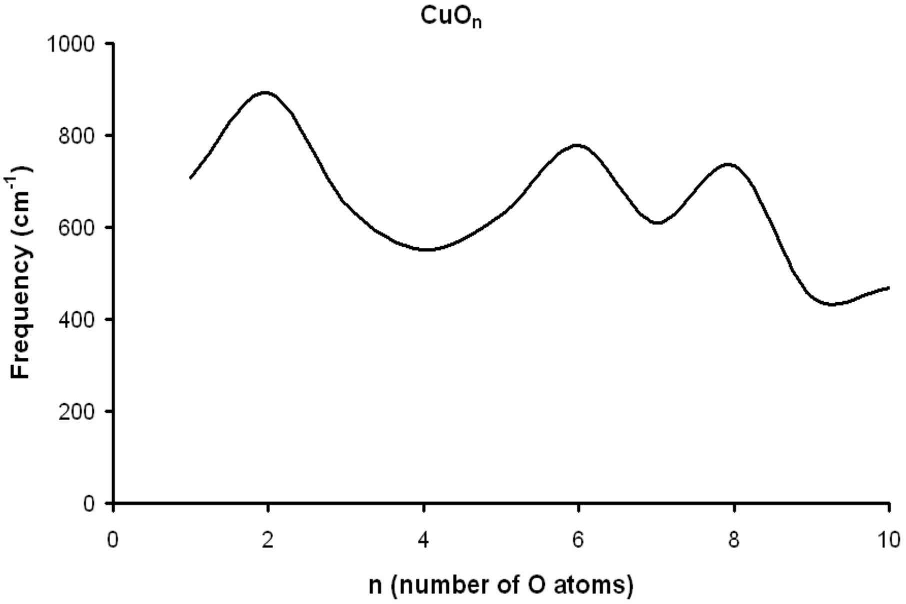

Figure 10.5: A plot of the largest vibrational frequency as a function of number of oxygen atoms in the cluster with only one Cu atom as calculated from the first principles. For n going from 1 to 2 the frequency increases, otherwise, it oscillates.

Next, the highest phonon frequency of Cu_3O_n has been plotted for n = 1 to 6 as shown in Fig. 10.7. As the number of oxygen atoms increases from 1 to 2, there is an increase in the phonon frequency. When the number of oxygen atoms increases to 7, there are oscillations in the frequency as a function of number of oxygen atoms. This means that the electron-phonon interaction which depends on the phonon frequency may also oscillate as a function of doping. The transition temperature qualitatively depends on the phonon frequency and hence on the $\sqrt{k/m}$. Therefore, oscillations in the force constant may lead to oscillations in the transition temperature. Next, the phonon frequency of Cu_4O_n has been calculated. In this system also, there is clearly an increase in the phonon frequency as a function of doping from n=1-3.

Later for $n \geq 4$, there are oscillations as shown in Fig. 10.8. Therefore, it conclude that the transition temperature of a superconductor oscillates upon doping with oxygen

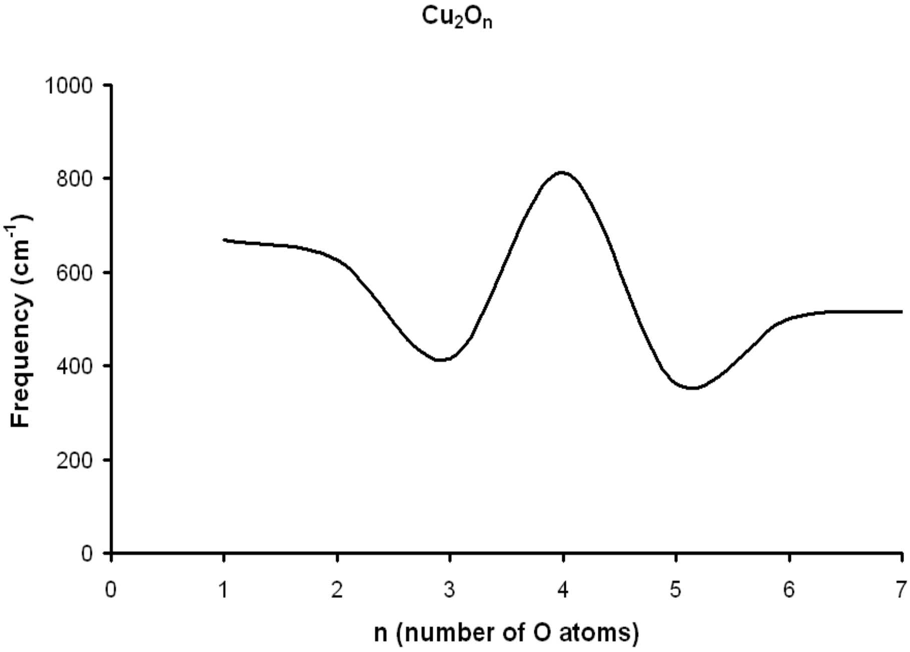

Figure 10.6: A plot of the largest frequency as a function of number of oxygen atoms with only two Cu atoms calculated from the first principles, showing a peak at n=4 and oscillations around it.

and hence often a large transition temperature is found.

10.6 Discussions.

The group theoretical study of CuO has been performed by Guha *et al.* [82] and the vibrational frequencies found in pure CuO single crystals are of the same order of magnitude as found in the present work but the basic idea of the present work is to dope the CuO with oxygen. Another Raman study [83] of CuO thin films also identifies Cu_2O as well as CuO. However, in the case of clusters, valencies other than 1 and 2 are quite possible which have minimum energy configurations. The thermodynamic stability of copper oxide surfaces has been discussed by Soon *et al.* [84]. It is also found that nanostructures occur which support the idea of cluster formation [85]. The copper

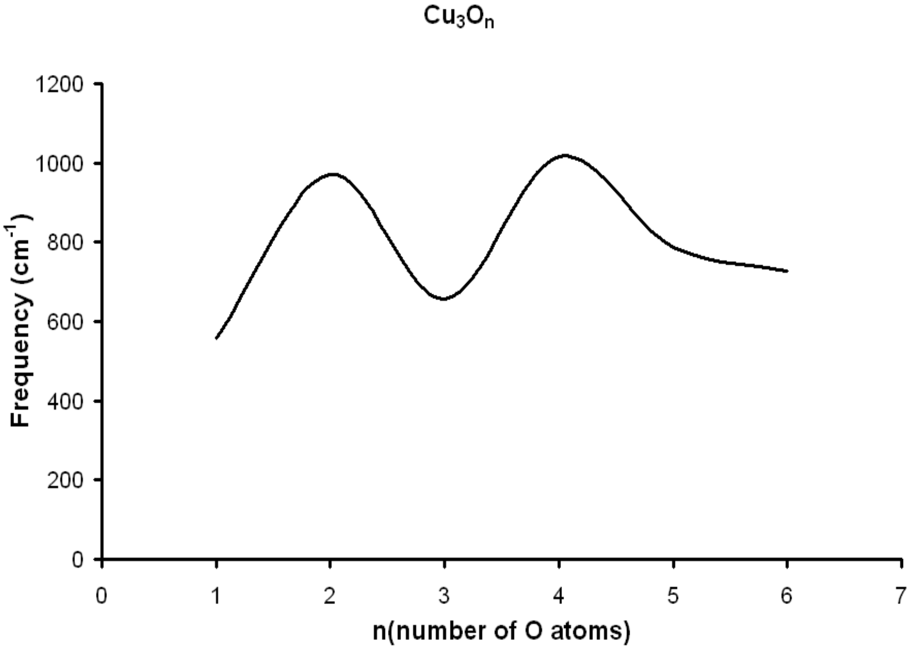

Figure 10.7: A plot of the largest frequency as a function of number of oxygen atoms with only three Cu atoms showing increase in the frequency for n going from 1 to 2 and oscillations upon further doping.

oxide is an important component of the superconductors [86–89], which show increase in the transition temperatures upon doping. Some of these materials have a normal phase and superconductivity occurs only upon doping. Therefore, this calculation of doping of copper oxide by excessive oxygen simulates the conditions in which the superconductivity emerges.

10.7 Conclusions.

The first principles calculation of vibrational frequencies as a function of doping Cu with oxygen atoms has been performed. The highest phonon frequency first increases upon doping and then upon further doping shows oscillations. From these calculations, it is found that the transition temperatures first increase upon doping CuO with oxygen

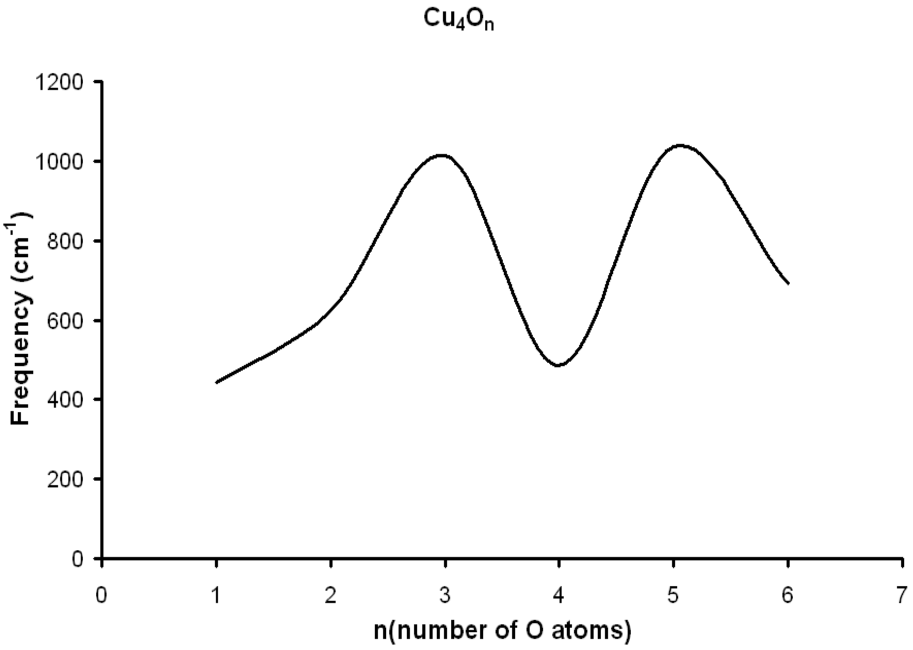

Figure 10.8: A plot of the largest vibrational frequency of four Cu atoms upon doping with oxygen atoms showing increase in the frequency with increasing number of oxygen atoms. For $n > 3$, there are oscillations. Since the transition temperature of a superconductor depends on the vibrational frequency, the transition temperature upon doping is expected to be increase.

atoms and later upon further doping shows oscillations. Hence for a given structure the transition temperature can be increased by hole doping. In the B.C.S. theory the oscillations occur in the x but not in k. In the present work, it is found that the force, F=-kx, oscillates due to oscillations in k. The electron-phonon interaction is obtained by assuming that only δx has phonon operators but $\partial V/\partial x$ should be evaluated at the equilibrium, where V is the Coulomb potential. It means that the coupling constant of the electron-phonon interaction oscillates and enhances the transition temperature of a superconductor .

Table 10.7: The vibrational frequencies of Cu_3O_n (n=6) along with intensities and degeneracies.

S.No.	Cluster	Frequency (cm^{-1})	Intensity km/mol	Degeneracy
14	Cu_3O_6(triangular)	99.8	0.01	1
15	Cu_3O_6(triangular)	175.9	1.8	1
16	Cu_3O_6(triangular)	181.7	7.0	1
17	Cu_3O_6(triangular)	184.5	26.8	1
18	Cu_3O_6(triangular)	208.1	1.2	1
19	Cu_3O_6(triangular)	259.8	2.3	1
20	Cu_3O_6(triangular)	384.3	1.5	1
21	Cu_3O_6(triangular)	452.8	0.2	1
22	Cu_3O_6(triangular)	453.2	0.04	1
23	Cu_3O_6(triangular)	480.6	103.3	1
24	Cu_3O_6(triangular)	563.8	0.6	1
25	Cu_3O_6(triangular)	569.5	65.7	1
26	Cu_3O_6(triangular)	574.7	24.7	1
27	Cu_3O_6(triangular)	680.0	126.8	1
28	Cu_3O_6(triangular)	727.1	0.01	1

Table 10.8: The vibrational frequencies of Cu_4O_n (n=1-3) along with intensities and degeneracies.

S.No.	Cluster	Frequency (cm^{-1})	Intensity km/mol	Degeneracy
1	Cu_4O(pyramidal)	111.2	1.6	1
2	Cu_4O(pyramidal)	128.3	2.2	2
3	Cu_4O(pyramidal)	406.3	9.4	1
4	Cu_4O(pyramidal)	441.9	24.5	2
5	$Cu_4O(T_d)$	524.2	5.6	3
6	Cu_4O_2(bipyramidal)	168.2	0.9	2
7	Cu_4O_2(bipyramidal)	265.1	2.2	2
8	Cu_4O_2(bipyramidal)	370.8	50.8	1
9	Cu_4O_2(dumb bell)	18.4	0.8	1
10	Cu_4O_2(dumb bell)	53.5	57.1	1
11	Cu_4O_2(dumb bell)	107.0	5.7	1
12	Cu_4O_2(dumb bell)	213.8	13.4	1
13	Cu_4O_2(dumb bell)	565.7	13.2	1
14	Cu_4O_2(dumb bell)	625.1	64.3	1
15	Cu_4O_3(linear)	26.2	2.0	2
16	Cu_4O_3(linear)	266.8	23.2	2
17	Cu_4O_3(linear)	324.0	2.1	1
18	Cu_4O_3(linear)	930.8	317.1	1
19	Cu_4O_3(linear)	1014.3	19.9	1

Table 10.9: The vibrational frequencies of $\mathrm{Cu_4O}_n$ (n=4-6) along with intensities and degeneracies.

S.No.	Cluster	Frequency (cm^{-1})	Intensity km/mol	Degeneracy
1	$\mathrm{Cu_4O_4}$	153.1	2.27	3
2	$\mathrm{Cu_4O_4}$	340.5	21.9	3
3	$\mathrm{Cu_4O_4}$	486.5	26.1	3
4	$\mathrm{Cu_4O_5}$	18.0	0.85	1
5	$\mathrm{Cu_4O_5}$	41.6	0.01	1
6	$\mathrm{Cu_4O_5}$	75.0	2.90	1
7	$\mathrm{Cu_4O_5}$	117.6	0.03	1
8	$\mathrm{Cu_4O_5}$	195.6	9.2	2
9	$\mathrm{Cu_4O_5}$	305.4	0.21	1
10	$\mathrm{Cu_4O_5}$	319.8	45.5	2
11	$\mathrm{Cu_4O_5}$	750.8	27.6	1
12	$\mathrm{Cu_4O_5}$	945.6	117.5	1
13	$\mathrm{Cu_4O_5}$	997.0	0.02	1
14	$\mathrm{Cu_4O_5}$	1035.9	34.9	1
15	$Cu_4\mathrm{O}_6$	186.1	1.26	2
16	$Cu_4\mathrm{O}_6$	227.9	5.9	2
17	$Cu_4\mathrm{O}_6$	230.9	2.7	2
18	$Cu_4\mathrm{O}_6$	281.6	48.5	1
19	$Cu_4\mathrm{O}_6$	547.1	3.4	2
20	$Cu_4\mathrm{O}_6$	649.6	0.06	1
21	$Cu_4\mathrm{O}_6$	692.5	48.3	2

Chapter 11

Vibrations in Selenium Glass

The density functional theory has been used for calculating the vibrational frequencies of clusters of atoms. The bond distances and angles have been obtained for which the energy of the Schrödinger equation is minimum. It is found that the bond distance between two Se atoms to be 232.1 picometer when double zeta wave function is used. The frequency of oscillations is calculated to be 325.3 cm^{-1} but the intensity is zero so that Se_2 molecule is in very small number. When polarized double zeta wave function (DZP) is used, the bond length of Se_2 is found to be 223.1 pm and the frequency is 367.4 cm^{-1}. Similarly, for double zeta wave functions (DZ), Se_3 linear molecule has a frequency of 247.18 cm^{-1} and bond length of 248.6 pm. For the (DZP), the bond length of Se_3 is 238.3 pm and the vibrational frequency is 260.1 cm^{-1}. For triangular Se_3 (DZ), gives 253.8 pm and 217.3 cm^{-1}. For triangular Se_3 (DZP), gives 241.3 pm and 248.38 cm^{-1}. The experimental Raman spectra give 250 cm^{-1} for a selenium glass. By comparing the experimental frequencies with those calculated, it found that linear Se_3 is present in the glass. This indicates the possibility of linear growth in the glass.

11.1 Introduction

The study of glasses is important for the understanding of its strength and for the knowledge of their elastic properties. In some glasses, the phenomenon of self-organization can be learned [22]. In some glasses, there are soft phonons [23], the frequencies of which go to zero. In the Raman spectra, the frequency of the soft phonon becomes so small that it merges with the Rayleigh line . The experimental measurements of the Raman spectra have been carried out by Boolchand [24, 91]. In recent years, the vibrational frequencies have been calculated from the first principles [25, 27]. In glasses of the GeSI, the calculated values [25] of the vibrational frequencies are in good agreement with those found experimentally from the Raman spectra. In the case of GePS glass [27] also the calculated values are close to the experimental values obtained from the Raman spectra. The calculated values are so good that it confirms our faith in quantum mechanics. Therefore, an effort has been made to determine the vibrational frequencies in selenium, Se metal. Many different models have been made by using the density functional theory and calculated the vibrational frequencies in each case. The smallest molecule Se_2 is not formed at all and there are a minimum number of atoms before which the system can stabilize.

The calculation of vibrational frequencies of clusters of Se atoms have been reported. It is found that Se_3 is the smallest cluster for which the stability is obtained and the vibrational frequencies are calculated. The calculation is performed by having double zeta wave functions with and without polarization. Many different clusters have been studied. The molecules Se_2, Se_3, Se_3-linear, Se_3-ring, Se_4-linear, Se_4-pyramid, Se_4-square, Se_5-linear, Se_5-pyramidal and Se_5-ring have been optimized and their bond lengths are obtained for the minimum energy. The vibrational frequencies have been calculated in each case. The calculated frequencies are compared with those found in the experimentally measured Raman spectra of Se glass. This comparison shows that Se_3 is present in the glass and Se_2 is not stable due to its zero intensity.

11.2 Calculated Frequencies

The density functional theory is used to make a model of several atoms. The energy of the Schrödinger equation is minimized to obtain the bond lengths and angles in the cluster models. The vibrational frequencies are obtained for the optimized clusters and several clusters have been made with a variety of wave functions. The double zeta wave functions are used with and without the polarization. Some of the calculated Se clusters are described below.

(i) Se_2-linear cluster: The Se_2 molecule is made and optimized for the minimum energy. The optimized bond length is found to be 232.1 picometer. In this case, the intensity of the vibrational spectrum is almost zero, indicating that the number of molecules formed is very small. The vibrational frequency is found to be 325.3 cm^{-1} but zero intensity shows that it is unlikely to be observed. The double zeta wave function (DZ) is then replaced by the polarized wave function. The double zeta wave function with polarization (DZP) changed the bond distance to 223.1 pm and the vibrational frequency to 367.4 cm^{-1} but the intensity continued to be negligibly small $\sim$ 0.000000 km/mol. The intensity of vibrations of the A_1 mode of NH_3 in the DZP becomes very small such as 0.7 in LDA compared with 57.8 for the doubly degenerate mode as discussed by Fan and Zeigler [90]. From this calculation, the intensity of the linear diatomic Se_2 molecule is indeed zero so it can be assume that these molecules do not exist in the metal, except in the negligibly small quantity. This raises an interesting question, namely that, then what is vibrating in the pure selenium glass?

(ii) Se_3-ring: The three atoms of Se are arranged in a triangular form. The DZ wave function gives 253.8 pm as the bond distance with degenerate two values of the vibrational frequency of 217.2 cm^{-1} each. The DZP wave function for this triangular molecule gives 241.3 pm for the bond distance and 248.38 cm^{-1} for the vibrational frequency with intensity 0.0639 km/mol. A strong vibrational spectrum is obtained as shown in Fig. 11.1.

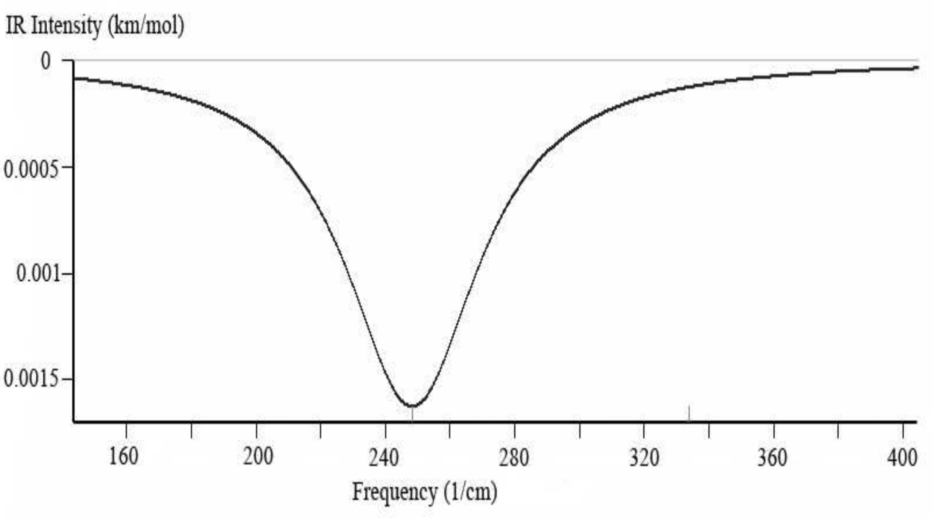

Figure 11.1: The vibrational spectrum of Se_3 ring calculated from first principles.

(iii) Se_3-linear: The DZ wave function gave the bond length 248.6 pm and the vibrational frequencies 247.2 cm^{-1} for the optimized linear arrangement of three atoms with strong intensity $\sim$ 35.7 km/mol. The DZP for this system gives 238.3 pm for the bond length, 260.1 cm^{-1} for the frequency and 68.6 km/mol for the intensity.

(iv) Se_4-linear: The DZ wave function for four atoms of Se in a linear configuration gives the bond length of 233.1 pm and a vibrational frequency of 313.5 cm^{-1} with strong intensity of 33.0 km/mol, while the DZP wave function gave the bond length of 233.0 pm with frequency 313.79 cm^{-1}.

(v) Se_4-pyramidal: The three atoms sit on a triangle and the fourth atom on the top position so that a pyramidal molecule is formed. The DZ wave function gave 287.4 pm for the bond length and three values of the vibrational frequency of 1183.7 cm^{-1}. The DZP gave 271.3 pm for the bond length and 50.9 cm^{-1} for the

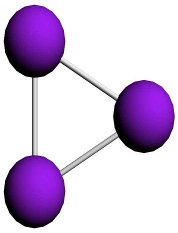

Figure 11.2: The picture of Se_3 ring structure.

frequency. Therefore, the effect of polarization in this model is very strong.

(vi) Se_4-square: The set of 4 atoms on the corners of a square when optimized for the minimum energy using the density-functional theory with DZ wave function gave 257.3 pm for the bond length and 229.07 cm^{-1} for a doubly degenerate vibration. When DZP is used the optimized bond length became 254.0 pm and the frequency got shifted to 261.7 cm^{-1} with intensity 1.13 km/mol. A strong vibrational spectrum is obtained as shown in Fig. 11.3.

(vii) Se_5-linear: Five atoms of Se arranged linearly give 258.1 pm for the bond length and weak vibrations, with DZ wave function, at 31.7 cm^{-1} (two values of intensity 0.089 km/mol each) and 147.9 cm^{-1} (two values of intensity 0.039 km/mol each). There is one more vibration at 225.7 cm^{-1} (intensity 24.3 km/mol) and strong vibration at 256.8 cm^{-1} (intensity 97.4 km/mol). Considering the intensities, the strong vibration is located at 256.8 cm^{-1}. The DZP wave function gives 229.5 pm for the bond length and weak oscillations at 39.69 cm^{-1} (two values 0.0008 km/mol each), 194.8 cm^{-1} (intensity 19.38 km/mol) and strong vibration

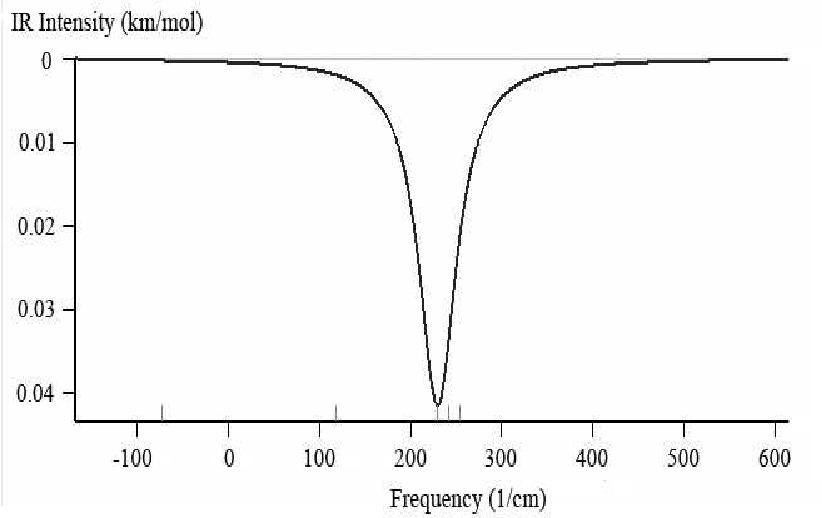

Figure 11.3: The vibrational spectrum of Se_4 (square) calculated from the first principles.

at 303.4 cm^{-1} (intensity 25.4 km/mol). A strong vibrational spectrum is obtained as shown in Fig. 11.4.

(viii) Se_5-pyramidal: There are 4 atoms in the base and one on top. The DZ wave functions give 274.0 pm for the bond length and 113.7 cm^{-1} (intensity 16.3 km/mol), with strong oscillation at 242.09 cm^{-1} (intensity 0.418 km/mol). The polarized wave function DZP gave 274.0 pm for the bond length and 131.37 cm^{-1} (0.003 km/mol) for a weak vibration and 235.0 cm^{-1} (12.06 km/mol) for a doubly degenerate strong vibration.

(ix) Se_5-ring: The ring model with five atoms by using DZ wave function gives 252.1 pm for the bond length and the ring frequency is 232.4 cm^{-1} (2.7 km/mol). The polarized wave function gave the bond length of 241.4 pm and the ring frequency of 259.8 cm^{-1} (1.01 km/mol). A vibrational spectrum is obtained as shown in Fig. 11.5 and the structure as shown in Fig 11.6.

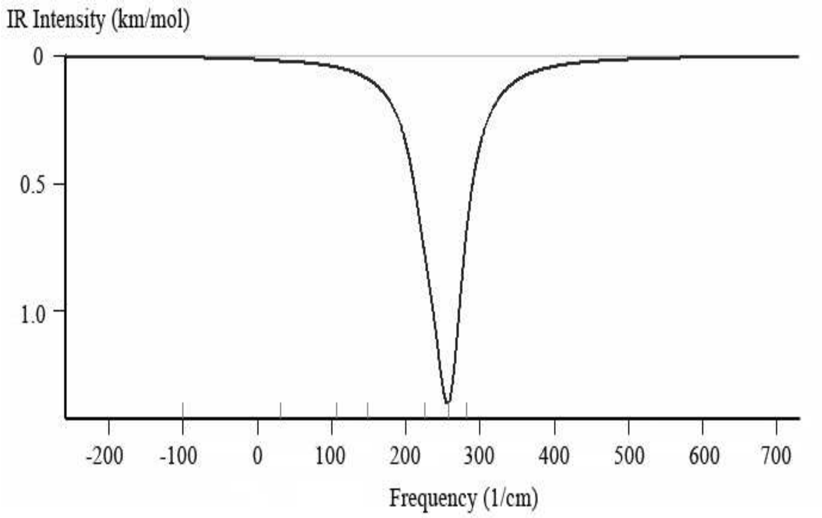

Figure 11.4: The vibrational spectrum of Se_5 (linear) calculated from the first principles.

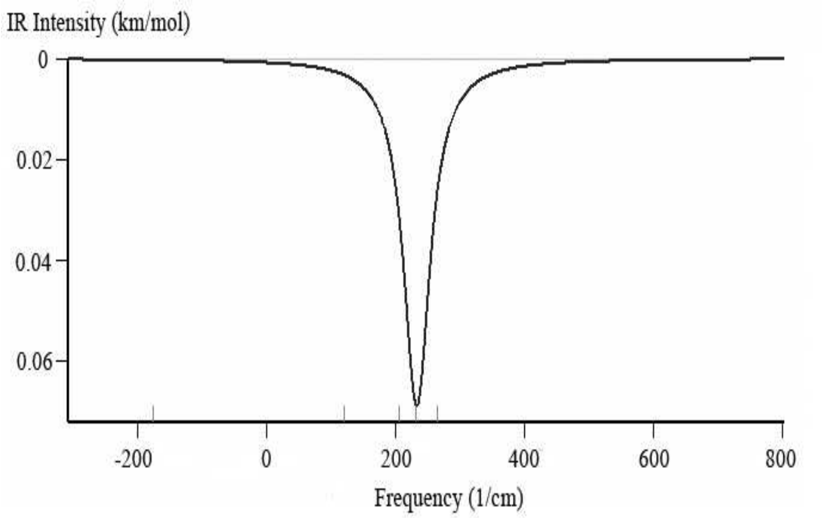

Figure 11.5: The vibrational spectrum of Se_5 ring with DZ wave function calculated from the first principles.

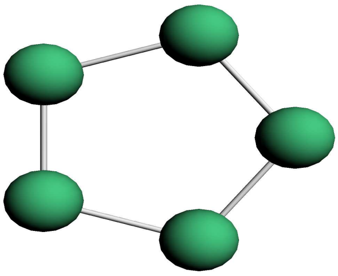

Figure 11.6: The picture of Se_5 ring structure.

11.3 Raman Spectra

The most detailed experiment studies of the Raman spectra in glasses have been performed by Boolchand [91]. The spectra of Ge_xSe_{1-x} with varying concentration lead to the discovery of rigidity transition. The cluster of Ge-Se and its vibrational frequencies have been computed [27]. During this study it was clear that Se-Se bond is not well understood. According to the experimental study, Se-Se stretch mode of Se_n - chain (chain mode) occurs at about 250 cm^{-1}. The calculations of Se clusters show that this experimental value occurs in Se_3 and the Se_2 are not formed due to metallic character of the glass as shown in Table 11.1.

Table 11.1: The experimental Se vibrational mode compared with calculations

Experimental cm^{-1}(SZ)	Calculated cm^{-1}	Model
250	247.2	Se_3-linear
	248.3	Se_3-ring

The Se_3 cluster with linear shape has 4 vibrational modes while the ring shape of Se_3 cluster has 3 vibrational modes. In the Cartesian coordinates, a molecule has $3n$ degrees of freedom while n is number of atom consist in the molecule. A linear molecule has 2 degrees of rotational and 3 degrees of translational so total of vibrational mode is $3n - 5$. For nonlinear shape, total of vibrational mode is $3n - 6$ with different in degree of rotational which is 3 degrees. That mean the diatomic molecule has only one vibrational modes, $3 \times 2 - 5 = 1$. A selenium diatomic molecule showed zero intensity for the vibrational frequency, 325.3 cm^{-1}. This vibration did not produce any changing in the dipole moment of the molecule Se_2 because of the symmetrical vibration. It showed that Se_2 has a very small energy due to the small number of atoms. Hence, the vibrations of Se_2 diatomic cannot be observed in the vibrational frequency.

11.4 Conclusions

The ab initio calculations of vibrational frequencies in several different models of selenium have been performed. From these calculations, the Se_3 molecules has been found performed in the Se glass. The calculated values are close to those measured in Se glass. The comparison of the calculated values with the Raman spectra proved that Se_2 is not formed in the metal and the Raman spectra are due to Se_3.

Chapter 12

Conclusions

The vibrational frequencies of clusters have been calculated by using the density functional theory (DFT). The values calculated by this method agree with the experimental results. The DFT has been described in chapter 1 including Hohenberg-Kohn theorems, Kohn-Shams equation, local density approximation and self consistent fields. These equations are solved by using the ADF and DMol^3 softwares.

Chapter 2 discusses the ab initio calculation of AgGeSe glass. The clusters of pure silver, clusters of AgGe and clusters of AgSe have been made to calculate the vibrational frequencies. The calculated vibrational frequencies have been compared with the experimental data and found that Ag_2Ge is formed in the glass. Amongst the pure silver clusters, Ag_3 is the smallest cluster formed.

Chapter 3 gives the vibrational frequencies of arsenic selenide (AsSe) glass. The clusters of As and Se have been optimized to the minimum energy then calculated to get the vibrational frequencies. The values calculated for a linear system are in accord with the experimental values. The linear bonds of As_2Se has been identified and present in the AsSe glass. These bonds appearing in As_2Se (linear), are important for the strength of the glassy state.

Chapter 4 continues with arsenic sulphide (AsS) glass. From this calculation, it is found that AsS consists of several different compositions mixed together. It is found that AsS_3 (triangular), AsS_3 (pyramid), AsS_4 (3-1 model), AsS_4 (Td), As_4S_4 (ring), As_2S_3 (bipyramid), As_4S_4 (cubic), As_2S_3 (zig-zag), As_4S_3 (linear), As_2S_6 (dumb bell) are predicted on the basis of quantum mechanical first principle calculations including the well known minerals like realgar (AsS) and orpiment (As_2Se_3). This prediction agrees with the experimental Raman spectra. The existence of these molecules is also apparent from the decoloration in the samples of the minerals. The usefulness of quantum mechanics for the study of glass structures is therefore well demonstrated.

In chapter 5, the first principle calculations of the vibrational frequencies have been performed in a large number of clusters containing arsenic oxides (AsO). The clusters present in the actual sample have been identified by comparing the calculated values with those found in the data. The frequencies of AsO_2, AsO_4 (T_d), As_2O_2 (rectangular), AsO_2 (triangle), AsO_3 (pyramidal) and AsO_2 (triangle) agree with the experimental values. A method to identify new clusters and molecules found in the minerals has been found. It is found that the vitreous state of As_2O_3 is made of several clusters of different valencies.

In chapter 6, the law force in iron-phosphorous (FeP) clusters of atoms has been determined. The LaFePO becomes superconducting upon doping with calcium (Ca) or fluorine (F). It is found that in FeP_n the law of force is not linear but in Fe_2P_n for small n, a power law is possible. According to the law of force, F = -kx = -n $\omega^2 x$, the frequency is a constant. The ω found oscillates upon doping Fe atoms with phosphorous.

In chapter 7, a superconducting material FeAs has been calculated to get the vibrational frequencies and found the largest vibrational frequency oscillates as a function of number of As atoms in $FeAs_n$ and Fe_2As_n. The vibrational frequencies indicate oscillations in the transitions temperature of a superconductor upon doping. Usually, the B.C.S. theory of superconductivity relies upon the electron-phonon interaction in the conduction band where the strength depends on the translational symmetry. In the present case, the superconductivity arises upon doping which lacks in translational symmetry. Hence, the phonon-induced B.C.S. theory is not taken into account but the chances that theory showed will be based on doping. The doping and the conductivity are not consistent so that a Hubbard type additional term is needed.

In chapter 8, there is considerable effect of ion exchange on the vibrational frequencies. For example, comparison of CN_3 (pyramidal) with C_3N (pyramidal) shows that CN_3 has 561.2 cm^{-1} whereas C_3N has 309 cm^{-1} as the smallest frequency so that the effect of force constant is much stronger than the effect of the mass. Several calculated frequencies agree with the measured values. In this calculation it is very clear that the bond distances depend on the structure. The population of the vibrations depends on temperature. Hence there is a small effect of temperature on the bond formation.

In chapter 9, the calculation of vibrational frequencies of graphene has been made. It is found that the energy of 18 meV is of electronic origin. Similarly, the gap of nearly 3100 cm^{-1} occurs in a system of 12 layers of atoms. If the same energy occurs in the electrons as well as in phonons, the resonance effect are expected. Considering the mass of the carbon atom, the frequency of 3100 cm^{-1} does not occur in the vibrational spectra of graphene.

In chapter 10, the first principles calculation of vibrational frequencies as a function of doping Cu with oxygen atoms has been performed. The highest phonon frequency first increases upon doping and then upon further doping shows oscillations. From these calculations, it is found that the transition temperatures first increase upon doping CuO with oxygen atoms and later upon further doping shows oscillations. Hence for a given structure the transition temperature can be increased by hole doping. In the B.C.S. theory the oscillations occur in the x but not in k. In the present work, it is found that the force, F=-kx, oscillates due to oscillations in k. The electron-phonon interaction is obtained by assuming that only δx has phonon operators but $\partial V/\partial x$ should be evaluated at the equilibrium, where V is the Coulomb potential. It means that the coupling constant of the electron-phonon interaction oscillates and enhances the transition temperature of a superconductor.

In chapter 11, the vibrational frequencies of selenium glass have been calculated. The calculated value of vibrational frequencies show that Se_3 molecules are formed in Se glass. The experimental value of the vibrational frequency in Se glass is 250 cm^{-1}. The calculated value for the Se_3 molecule is 247.2 cm^{-1} for the linear shape and 248.3 cm^{-1} for the ring shape.

For the conclusion, the objectives of this research have been achieved. The clusters of molecules have been made for the first time and these calculation are not already made by others. The vibrational frequencies in five glassy materials and five others materials including, iron-based material, graphene, carbon nitride and copper oxide have been calculated. All of these materials have been choose because of the availability of the Raman spectra done by experiment while the calculation have not been done by others. The calculated values have been compared with the experimental data. These calculations use first principles with local density approximation (LDA) of the DFT which gives good agreement with the experiment data. For carbon nitride, generalized gradient approximation (GGA) has been used as well as LDA to performed the calculations. The accuracy set in the computer programme is 0.001 cm^{-1}. This method can be applied to any other material to understand the structure of molecules.